European air quality maps of
PM and ozone for 2012
and their uncertainty

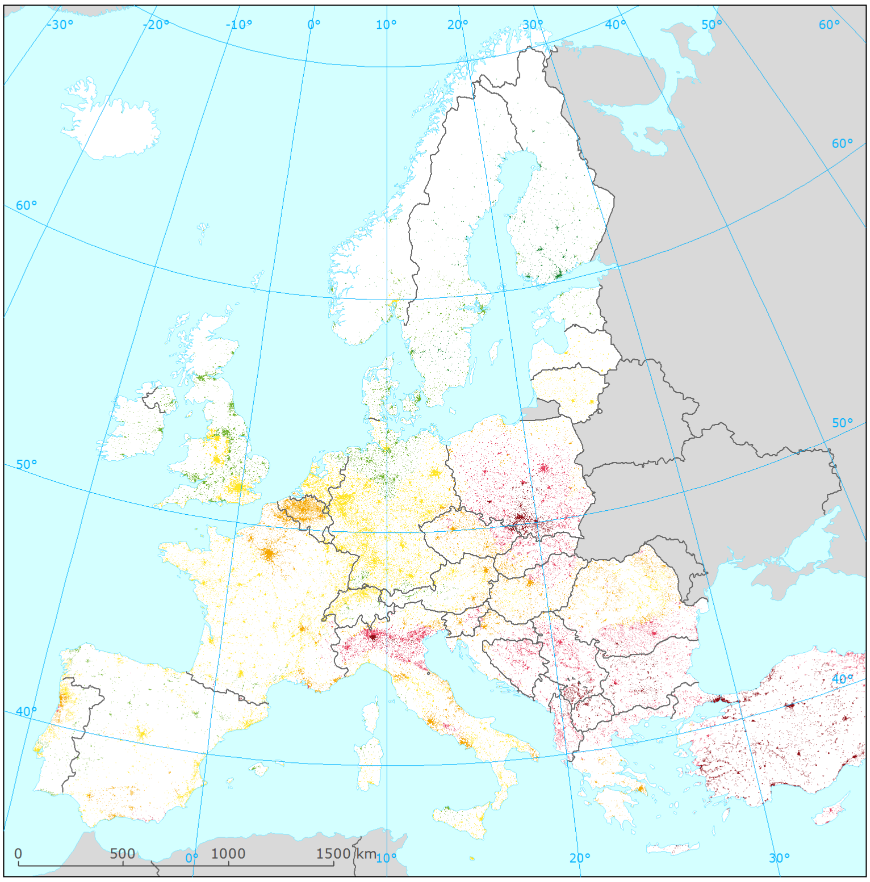

ETC/ACM Technical Paper 2014/4
January 2015

Jan Horálek, Peter de Smet, Pavel Kurfürst,
Frank de Leeuw, Nina Benešová

European Topic Centre
on Air Pollution and
Climate Change Mitigation

The European Topic Centre on Air Pollution and Climate Change Mitigation (ETC/ACM)
is a consortium of European institutes under contract of the European Environment Agency
RIVM UBA-V ÖKO AEAT EMISIA CHMI NILU INERIS PBL CSIC

Front-page picture:
Urban background concentration map of PM_{10} indicator 36^{th} highest daily average value for the year 2012. Spatially interpolated concentration field in the urban areas. Units: $\mu g.m^{-3}$. (Figure A1.2 of this paper.)

Author affiliation:
Jan Horálek, Pavel Kurfürst, Nina Benešová: Czech Hydrometeorological Institute (CHMI), Prague, Czech Republic
Peter de Smet, Frank de Leeuw: National Institute for Public Health and the Environment (RIVM), Bilthoven, The Netherlands

Refer to this document as:
Horálek J, De Smet P, Kurfürst P, De Leeuw F, Benešová N (2015). European air quality maps of PM and ozone for 2012 and their uncertainty. ETC/ACM Technical paper 2014/4 http://acm.eionet.europa.eu/reports/ETCACM_TP_2014_4_spatAQmaps_2012

DISCLAIMER

ETC/ACM Technical Paper 2014/4
European Topic Centre on Air and Climate Change Mitigation
PO Box 303
3720 AH Bilthoven
The Netherlands
Phone +31 30 2743562
Fax +31 30 2744433
Email etcacm@rivm.nl
Website http://acm.eionet.europa.eu

Contents

1 Introduction

This paper provides an update of European air quality concentrations, probabilities of exceeding relevant thresholds and population exposure estimates for another consecutive year, 2012. The analysis is based on interpolation of annual statistics of observational data from 2012, reported by EEA member and cooperating countries in 2013. The paper presents mapping results and includes an uncertainty analysis of the interpolated maps, adopting the latest methodological developments of Horálek et al. (2007, 2008, 2010, 2013, 2014a) and De Smet et al. (2009, 2010, 2011, 2012).

We again consider in this paper PM_{10} and ozone as being the most relevant pollutants for annual updating. Additionally and for the second time, $PM_{2.5}$ is presented as a third important policy-relevant pollutant and health-impact indicator based on the mapping methodology developed by Denby et al. (2011b, 2011c).

The analysis method for the year 2012 was similar to that for the previous years. In this paper, we summarise the updates applied to the 2012 data.

The mapping method used is a linear regression model followed by kriging of the residuals produced from that model (residual kriging). In the linear regression model, the measured data are taken as a dependent variable, while a dispersion model's output and other supplementary data (altitude, meteorology) as independent variables.

The maps of health related indicators of PM_{10}, $PM_{2.5}$ and ozone are created for the rural and urban background areas separately on a grid at 10x10 km resolution. Subsequently to this, the rural and urban background maps are merged into one combined air quality indicator map using a population density grid at 1x1 km resolution. We also derive the population exposure estimates on basis of this 1 x 1 km grid resolution, as it accounts better for the smaller urbanisations in the European context that are not resolved at the 10 x 10 km grid resolution. At the European scale, we present the final combined maps at 1x1 km grid resolution on aggregated maps at 10x10 km grid resolution. The maps of vegetation related ozone indicators are on a grid at 2x2 km resolution, based on rural background measurements and serve as input to EEA core indicator CSI005.

Next to the annual indicator maps, we present in tables the population exposure to PM_{10}, $PM_{2.5}$ and ozone and the exposure of vegetation to ozone. Tables of population exposure are prepared using combined final maps and the population density map of 1x1 km grid resolution. The tables of the exposure of vegetation are prepared with a 2x2 km grid resolution based on the Corine Land Cover 2006 (CLC2006).

For all the maps, we include a quantitative estimate of their interpolation uncertainty, using cross-validation parameters and scatter-plots. In addition, the paper contains the maps with probability estimates of limit/target value exceedances.

Chapter 2 describes briefly the used methodology. Chapter 3 documents the updated input data. Chapters 4, 5 and 6 present the calculations, the mapping, the exposure estimates and the uncertainty results for PM_{10}, $PM_{2.5}$ and ozone respectively. Chapter 7 summarizes the conclusions on exposure estimates and their interpolation uncertainties involved with the interpolated mapping of the air pollutant indicators. Annex 1 presents separate urban background maps for urbanised areas only, aimed to better visualise the actual urban background concentration levels, without the influence of the dominating pattern of extended rural areas.

As of the 2012 maps onward, i.e. from this paper onward, we implement changes in legend class intervals and colour schemes. The adapted legends incorporate and resolve more thresholds as defined by the EU and WHO. Furthermore, the original intention was to match the colour scheme more with EEA's house style. However, from tests we conclude that adapting EEA's house style results in less intuitive map interpretations, disliked by the test-public. Best was to stick close to current colour scheme and implement just very limited adaptions in the colour settings. Annex 2 highlights the implemented changes in the intervals and its colour scheme and that be used from now onward, and it proposes legends for indicator maps that might be produced in the future.

2 Used methodology

2.1 Mapping method

Previous technical papers prepared by the ETC/ACM, resp. ETC/ACC (Technical Papers 2013/13, 2012/12, 2011/11, 2011/5, 2010/10, 2010/9, 2009/16, 2009/9, 2008/8, 2007/7, 2006/6, 2005/8, 2005/7) discuss methodological developments and details on spatial interpolations and their uncertainties. No changes took place in the methodology in comparison with the four preceding reports (Horálek et al., 2014a and references cited therein), respectively with the $PM_{2.5}$ mapping methodology paper (Denby et al., 2011c). In this chapter a summary on the currently applied methods is given.

2.1.1 Pseudo $PM_{2.5}$ station data estimation

To supplement measured $PM_{2.5}$ data, in the mapping procedure we also use data from so-called *pseudo $PM_{2.5}$ stations*. These data are the estimates of $PM_{2.5}$ concentrations at the locations of PM_{10} stations with no $PM_{2.5}$ measurement. These estimates are based on measured PM_{10} data and different supplementary data, using linear regression:

$$\hat{Z}_{PM2.5}(s) = c + b.Z_{PM10}(s) + a_1.X_1(s) + ... + a_n.X_n(s) + \varepsilon(s) \qquad (2.1)$$

where $\hat{Z}_{PM2.5}(\mathrm{s})$ is the estimated value of $PM_{2.5}$ at the station *s*,
$Z_{PM10}(\mathrm{s})$ is the measured value of PM_{10} at the station *s*,
$X_1(s), ..., X_n(s)$ are the values of other supplementary variables at the station *s*,
$c, b, a_1,, ..., a_n$ are the parameters of the linear regression model calculated based on the data at the points of measuring stations with both $PM_{2.5}$ and PM_{10} measurements,
n is the number of other supplementary variables used in the linear regression model (apart from PM_{10}).

When applying this estimation method, rural and urban/suburban background stations are handled together. For details, see Denby et al. (2011c).

2.1.2 Interpolation

The mapping method used is a linear regression model followed by kriging of the residuals produced from that model (residual kriging). Interpolation is therefore carried out according to the relation:

$$\hat{Z}(s_0) = c + a_1.X_1(s_0) + a_2.X_2(s_0) + ... + a_n.X_n(s_0) + \eta(s_0) \qquad (2.2)$$

where $\hat{Z}(\mathrm{s}_0)$ is the estimated value of the air pollution indicator at the point s_o,
$X_1(s_0), X_2(s_0), ..., X_n(s_0)$ are the *n* number of individual supplementary variables at the point s_o
$c, a_1, a_2,, ..., a_n$ are the *n+1* parameters of the linear regression model calculated based on the data at the points of measurement,
$\eta(s_0)$ is the spatial interpolation of the residuals of the linear regression model at the point s_o calculated based on the residuals at the points of measurement.

For different pollutants and area types (rural, urban), different supplementary data are used, depending on their improvement to the fit of the regression. Ordinary kriging is used to interpolate the residuals:

$$\hat{R}(s_0) = \sum_{i=1}^{N} \lambda_i R(s_i), \ \sum_{i=1}^{N} \lambda_i = 1, \qquad (2.3)$$

where $R(s_i)$ are the residuals in the points of the measuring stations s_i,
$\lambda_1, ..., \lambda_N$ are the weights estimated based on variogram,
N is the number of the stations used in the interpolation.

The variogram (as a measure of a spatial correlation) is estimated using a spherical function (with parameters *nugget, sill, range*). For details, see Horálek et al. (2007), Section 2.3.5 and Cressie (1993).

For $PM_{2.5}$, both measured data and the estimated data from the pseudo $PM_{2.5}$ stations are used.

For the PM_{10} and $PM_{2.5}$ indicators we apply, prior to linear regression and interpolation, a logarithmic transformation to measurement and EMEP model concentrations. In the case of $PM_{2.5}$ rural map creation, population density is also log-transformed. After interpolation, we apply a back-transformation. For details, see De Smet et al. (2011) and Denby et al. (2008). In the case of urban background $PM_{2.5}$ map, we do not use any supplementary data – we apply just lognormal kriging.

For the vegetation related indicators (AOT40 for crops and forests) we only construct rural maps based on rural background stations, based on the assumption that no vegetation is located in urban areas. For the health related indicators, we construct the rural and urban background maps separately and then we merge them.

2.1.3 Merging of rural and urban background maps

Health related indicator maps are constructed (using linear regression with kriging of its residuals) for the rural and urban background areas separately on a grid at 10x10 km resolution. The rural map is based on rural background stations and the urban background map on urban and suburban background stations. Subsequent to this, the rural and urban background maps are merged into one combined air quality indicator map using a European-wide population density grid at 1x1 km resolution. For the 1x1 km grid cells with a population density less than a defined value of α_1, we select the rural map value and for grid cells with a population density greater than a defined value α_2, we select the urban background map value. For areas with population density within the interval (α_1, α_2) a weighting function of α_1 and α_2 is applied (for details and the setting of the parameters α_1 and α_2, see Horálek et al., 2010, 2007 and 2005). This applies to the grid cells where the estimated rural value is lower (PM_{10} and $PM_{2.5}$) or higher (ozone), than the estimated urban background map value. In the exceptional cases when this criterion does not hold, we apply a joint urban/rural map (created using all background stations regardless their type), as far as its value lies in between the rural and urban background map value. For details, see De Smet et al. (2011).

Summarising, the separate rural, urban and joint urban/rural maps are constructed at a resolution of 10x10 km; their merging however takes place on basis of the 1x1 km resolution population density grid, resulting in a final combined pollutant indicator map on this 1x1 km resolution grid. This map is used for the population exposure estimates. We refer to the applied chain of optimised combinations of spatial resolutions, the process of *interpolation -> merging -> exposure estimate*, as the '10-1-1' (in km). For presentational purposes of European map illustrations, a spatial aggregation to 10x10 km resolution is sufficient and as such applied in this paper.

In all calculations and map presentations the EEA standard projection and datum defined as EEA ETRS89-LAEA5210 is used. The interpolation and mapping domain consists of the areas of all EEA member and cooperating countries, as far as they fall into the EEA map extent *Map_1c* (EEA, 2011).

For further details and discussion on subjects briefly addressed in this section, refer to De Smet et al. (2011), chapter 2.

2.2 Calculation of population and vegetation exposure

Population and vegetation exposure estimates are based on the interpolated concentration maps, population density data and land cover data.

2.2.1 Population exposure

Population exposure for individual countries and for Europe as a whole is calculated from the air quality maps and population density data, both at 1x1 km resolution. For each concentration class, the total population per country as well as the European-wide total is determined. In addition, we express per-country and European-wide exposure as the population-weighted concentration, i.e. the average concentration weighted according to the population in a grid cell:

$$\hat{c} = \frac{\sum_{i=1}^{N} c_i p_i}{\sum_{i=1}^{N} p_i} \tag{2.4}$$

where $\hat{c}$ is the population-weighted average concentration in the country or in the whole Europe,

p_i is the population in the i^{th} grid cell,

c_i is the concentration in the i^{th} grid cell,

N is the number of grid cells in the country or in Europe as a whole.

2.2.2 Vegetation exposure

Vegetation exposure for individual countries and for Europe as a whole is calculated based on the air quality maps and land cover data, both in 2x2 km grid resolution. For each concentration class, the total vegetation area per country as well as European-wide is determined.

2.3 Methods for uncertainty analysis

The uncertainty estimation of the European map is based on cross-validation. The cross-validation method computes the quality of the spatial interpolation for each measurement point from all available information except from the point in question, i.e. it withholds one data point and then makes a prediction at the spatial location of that point. This procedure is repeated for all measurement points in the available set. The predicted and measured values at these points are plotted in the form of a scatter plot. With help of statistical indicators the quality of the predictions is demonstrated objectively. The advantage of the nature of this cross-validation technique is that it enables evaluation of the quality of the predicted values at locations without measurements, as long as they are within the area covered by the measurements.

In addition, we make a simple comparison between the point measurements and interpolated values of the 10x10 km grid (or the 2x2 km grid in the case of AOT40). Where the 10x10 km grid is used, the grid value is the averaged result of the 1x1 km interpolations in each 10 x 10 km grid area. The interpolated value within a grid cell will only approximate the predicted value(s) at the station(s) lying within that cell.

Another method to estimate uncertainties is based on geostatistical theory: together with the prediction, the prediction standard error is computed at all the grid cells, which represents in fact the interpolation uncertainty map (see Cressie, 1993 for a detailed discussion). Based on the concentration and the uncertainty map, the exceedance probability map is created (Section 2.3.3).

2.3.1 Cross-validation

The results of cross-validation are described by the statistical indicators and scatter plots. The main indicator used is root mean squared error (RMSE) and additional is bias (mean prediction error, MPE):

$$RMSE = \sqrt{\frac{1}{N}\sum_{i=1}^{N}(\hat{Z}(s_i) - Z(s_i))^2} \tag{2.5}$$

$$bias(MPE) = \frac{1}{N}\sum_{i=1}^{N}(\hat{Z}(s_i) - Z(s_i)) \tag{2.6}$$

where $Z(s_i)$ is the air quality indicator value derived from the measured concentration at the i^{th} point, $i = 1, ..., N$,

$\hat{Z}(s_i)$ is the air quality estimated indicator value at the i^{th} point using other information, without the indicator value derived from the measured concentration at the i^{th} point,

N is the number of the measuring points.

Next to the RMSE expressed in the absolute units, one could express this uncertainty in relative terms by relating the RMSE to the mean of the air pollution indicator value for all stations:

$$RRMSE = \frac{RMSE}{\overline{Z}}.100 \tag{2.7}$$

where $RRMSE$ is the relative RMSE, expressed in percent,

$\overline{Z}$ is the arithmetic average of the indicator values $Z(s_1), \ldots, Z(s_N)$, as derived from measurement concentrations at the station points $i = 1, \ldots, N$.

Other indicators are R^2 and the regression equation parameters *slope* and *intercept*, following from the scatter plot between the predicted (using cross-validation) and the observed concentrations

RMSE should be as small as possible, bias (MPE) should be as close to zero as possible, R^2 should be as close to *1* as possible, slope *a* should be as close to *1* as possible, and intercept *c* should be as close to zero as possible (in the regression equation $y = a.x + c$).

In the cross-validation of $PM_{2.5}$, only stations with measured $PM_{2.5}$ data are used (not the pseudo $PM_{2.5}$ stations).

2.3.2 Comparison of the point measured and interpolated grid values

The comparison of measured and predicted grid values is described by the linear regression equation and its parameters and statistical values. The comparison is executed separately for rural and urban background maps. In the case of $PM_{2.5}$, only the stations with actual measured $PM_{2.5}$ data are used (not the pseudo $PM_{2.5}$ stations).

The point observation – point cross-validation prediction analysis (Section 2.3.1) describes interpolation performance at point locations when there is no observation (as it follows the leave-one-out approach). In this case, the smoothing effect of the interpolation is most prevalent.

The point observation – grid prediction approach indicates performance of the value for the 10x10 km (resp. 1x1 km or 2x2 km) grid cell with respect to the observations that are located within that cell. As such, some variability is due to smoothing but it also includes smoothing due to spatial averaging into the 10x10 km (resp. 1x1 km or 2x2 km) grid cells. Therefore, the point-grid approach tells us how well our interpolated and aggregated values approximate the measurements at the actual stations locations. Whereas, the point-point approach tells us how well our interpolated values estimate the indicator when there are no measurements at a location (under the constrained that it is within the area covered by measurements).

2.3.3 Exceedance probability mapping

The maps with the probability of exceedance (PoE) of a specific threshold value (e.g. limit or target value) are constructed using the concentration and uncertainty maps:

$$PoE(x) = 1 - \Phi\left(\frac{LV - C_c(x)}{\delta_c(x)}\right) \tag{2.6}$$

where $PoE(x)$ is the probability of limit/target value (LV/TV) exceedance in the grid cell x,
$\Phi(\,)$ is the cumulative distribution function of the normal distribution,
LV is the limit or target value of the relevant indicator,
$C_c(x)$ is the interpolated concentration in the grid cell x,
$\delta_c(x)$ is the standard error of the estimation in the grid cell x.

The standard error of the probability map of the combined (rural and urban background) map is calculated from the standard errors of the separate rural and urban background maps; see Horálek et al. (2008), Section 2.3 and De Smet et al. (2011), Chapter 2. The maps with the probability of threshold value exceedance (PoE) are constructed in 10 x 10 km grid resolution.

3 Input data

The types of input data in this paper are not different from that of Horálek et al. (2014a, 2013). The air quality, meteorological and where possible, the supplementary data has been updated. No further changes in selecting and processing of the input data have been implemented. For readability of this paper, we reproduce here the list of the input data. The key data is the air quality measurements at the monitoring stations extracted from AirBase, including geographical coordinates (*latitude*, *longitude*). The supplementary data cover the whole mapping domain and are converted into the EEA reference projection ETRS89-LAEA5210 on a 10 x 10 km grid resolution. The data for the AOT40 maps, however, we converted – like last year – into a 2 x 2 km resolution to allow accurate land cover exposure estimates to be prepared for use in Core Set Indicator 005 of the EEA.

3.1 Measured air quality data

Air quality station monitoring data for the relevant year are extracted from the European monitoring database AirBase (http://acm.eionet.europa.eu/databases/airbase/index_html). This data set is supplemented by several rural stations from the database EBAS (NILU, 2014) not reported to AirBase. Only data from stations classified by AirBase and/or EBAS of the type *background* for the areas *rural*, *suburban* and *urban* are used. *Industrial* and *traffic* station types are not considered; they represent local scale concentration levels not applicable at the mapping resolution employed. The following substances and their indicators are considered:

PM_{10} – annual average [$\mu g.m^{-3}$], year 2012
– 36th highest daily average value [$\mu g.m^{-3}$], year 2012

$PM_{2.5}$ – annual average [$\mu g.m^{-3}$], year 2012

Ozone – 26th highest daily maximum 8-hour average value [$\mu g.m^{-3}$], year 2012
– SOMO35 [$\mu g.m^{-3}.day$], year 2012
– AOT40 for crops [$\mu g.m^{-3}.hour$], year 2012
– AOT40 for forests [$\mu g.m^{-3}.hour$], year 2012

SOMO35 is the annual sum of the differences between maximum daily 8-hour concentrations above 70 $\mu g.m^{-3}$ (i.e. 35 ppb) and 70 $\mu g.m^{-3}$. AOT40 is the sum of the differences between hourly concentrations greater than 80 $\mu g.m^{-3}$ (i.e. 40 ppb) and 80 $\mu g.m^{-3}$, using only observations between 7:00 and 19:00 UTC, calculated over the three months from May to July (AOT40 for crops), respectively over the six months from April to September (AOT40 for forests). Note that the term *vegetation* as used in the ozone directive is not further defined. Comparing the definitions in the Mapping Manual (UNECE, 2004) and those in the ozone directive suggests that we have to interpret the term *vegetation* in the ozone directive as agricultural crops. The exposure of *agricultural crops* has been evaluated here on basis of the AOT40 for vegetation as defined in the ozone directive.

For the indicators relevant to human health (i.e. PM_{10}, $PM_{2.5}$ and for ozone the 26th highest daily maximum 8-hour average and SOMO35) data from *rural*, *urban* and *suburban background* stations are considered. For the indicators relevant to vegetation damage (both AOT40 parameters for ozone) only *rural background* stations are considered.

Only the stations with annual data coverage of at least 75 percent are used. We excluded the stations from French overseas areas (departments), Svalbard, Azores, Madeira and Canary Islands. These areas were excluded from the interpolation and mapping domain. The stations from eastern Turkey (which is outside the EEA map extent *Map_1c* (EEA, 2011)) were used in the interpolation, but they are not shown in the maps. To reach a more extended spatial coverage by measurement data we use, in addition to the AirBase data, four additional rural background stations for PM_{10} and one for $PM_{2.5}$ from the EBAS database (NILU, 2014). Table 3.1 shows the number of the measurement stations selected for the individual pollutants and their respective indicators. Compared to 2011, the number of rural background stations selected for 2012 increased by approximately 1-3% for PM_{10} and $PM_{2.5}$ stations, while decreased by approximately 1-3 % for ozone. The number of the urban/suburban background stations increased by approximately 7 % for PM_{10}, by approximately 4 % for $PM_{2.5}$, and by about 1 % for ozone. The increase in the number of the urban/suburban PM_{10} stations is influenced by the inclusion of the eastern Turkish stations into the interpolation (without such stations the increase is only about 4 %).

Table 3.1 Number of stations selected for individual indicators and areas – rural background stations used for rural areas, urban and suburban background stations used for urban background areas.

	PM_{10}		$PM_{2.5}$	ozone			
	annual average	36th daily maximum	annual average	26th highest daily max. 8h	SOMO35	AOT40 for crops	AOT40 for forests
rural	336	330	139	504	504	506	515
urban	1204	1198	469	1024	1024		

For $PM_{2.5}$ mapping an additional 207 rural background and 776 urban/suburban background PM_{10} stations (in the places with no $PM_{2.5}$ measurement) were also used for the purpose of calculating the pseudo $PM_{2.5}$ station data.

Due to a lack of rural stations in Turkey for PM_{10}, $PM_{2.5}$ and ozone no proper interpolation results could be presented for this country in a rural map for all the indicators. Therefore, we excluded Turkey also from the production process of the final maps of this paper.

3.2 EMEP MSC-W model output

The chemical dispersion model used was the EMEP MSC-W (formerly called Unified EMEP) model (version rv4.5), which is an Eulerian model with a resolution of circa 50x50 km. Information from this model was converted to 10x10 km grid resolution (for health related indicators), resp. into the 2x2 km grid resolution (for vegetation related indicators) for the interpolation process.

As per the previous year, we received the EMEP data in the form of daily means for PM_{10} and $PM_{2.5}$ and hourly means for ozone. We aggregated these primary data to the same set of parameters as we have for the air quality observations:

PM_{10} – annual average [$\mu g.m^{-3}$], year 2012 (aggregated from daily means)
– 36th highest daily average value [$\mu g.m^{-3}$], year 2012 (aggregated from daily means)

$PM_{2.5}$ – annual average [$\mu g.m^{-3}$], year 2012 (aggregated from daily means)

Ozone – 26th highest daily maximum 8-hour average value [$\mu g.m^{-3}$], year 2011 (aggregated from hourly means)
– SOMO35 [$\mu g.m^{-3}.day$], year 2011 (aggregated from hourly means)
– AOT40 for crops [$\mu g.m^{-3}.hour$], year 2011 (aggregated from hourly means)
– AOT40 for forests [$\mu g.m^{-3}.hour$], year 2011 (aggregated from hourly means)

Simpson et al. (2012, 2013) and https://wiki.met.no/emep/page1/emepmscw_opensource (web site of Norwegian Meteorological Institute) describe the model in more detail. Emissions for the relevant year (Mareckova et al., 2014) are used and the model is driven by ECMWF meteorology. EMEP (2014) provides details on the EMEP modelling for 2012.

In the original format, a point represents the centre of a grid cell (in 50x50 km resolution). The data are imported into *ArcGIS* as a point shapefile and converted into ETRS89-LAEA5210 projection, subsequently converted into a 100x100 m resolution raster grid and spatially aggregated into the reference EEA 10x10 km grid (for health related indicators), resp. into the 2x2 km grid (for vegetation related indicators).

3.3 Altitude

We use the altitude data field (in meters) of Global Multi-resolution Terrain Elevation Data 2010 (GMTED2010), with an original grid resolution of 15x15 arcseconds (some 463x463 m at 60N).

Source: U.S. Geological Survey Earth Resources Observation and Science, see Danielson et al. (2011). We converted the field into the ETRS 1989 LAEA projection. (The resolution after projection was in 449.2x449.2 m). In the following step, we resampled the raster dataset to 100x100 m resolution and shifted it to the extent of EEA reference grid. As a final step, the dataset was spatially aggregated into 2x2 km and 10x10 km resolutions.

3.4 Meteorological parameters

Actual meteorological surface layer parameters we extracted from the Meteorological Archival and Retrieval System (MARS) of the ECMWF (European Centre for Medium-range Weather Forecasts). Currently we use the following ECMWF variables (details specified in Horálek et al. 2007, Section 4.5) on a 0.25x0.25 degrees (about 28x28 km at 60N) resolution as supplementary data in the regressions:

Wind speed – annual average [$m.s^{-1}$], year 2012
Surface solar radiation – annual average of daily sum [$MWs.m^{-2}$], year 2012

The data are imported into *ArcGIS* as a point shapefile. Each point represents the centre of a grid cell. The shapefile is converted into ETRS89-LAEA5210 projection, converted into a 100x100 m resolution raster grid and spatially aggregated into the reference EEA 10x10 km grid, resp. and into the 2x2 km grid.

3.5 Population density and population totals

Population density (in $inhbs.km^{-2}$, census 2001) is based on JRC data for the majority of countries (JRC, 2009) – source: EEA, pop01clcv5.tif, official version 5, 24 Sep. 2009, resolution 100x100 m.

For countries (Andorra, Albania, Bosnia-Herzegovina, Iceland, Liechtenstein, FYR of Macedonia, Montenegro, Norway, Serbia, Switzerland and Turkey) and regions (Faroe Islands, Jersey, Guernsey, Man and northern part of Cyprus), which are not included in this map we used population density data from an alternative source: ORNL LandScan Global Population Dataset (ORNL, 2008). This dataset is in 30x30 arcsec resolution; its values are based on the annual mid-year national population estimates for 2008 from the Geographic Studies Branch, US Bureau of Census, http://www.census.gov.

The ORNL data is reprojected and converted from its original WGS1984 30x30 arcsec grids into EEA's reference projection ETRS89-LAEA5210 at 1x1 km resolution by EEA (eea_r_3035_1_km_landscan-eurmed_2008, EEA, 2008). The JRC 100x100 m population density data is spatially aggregated into the reference 1x1 km EEA grid; in the areas with the lack of data (see above) it is supplemented with the ORNL data. Thus, the supplemented JRC 1x1 km data covers the entire examined area.

In order to verify the correctness of the merger of JRC and ORNL, we compared ORNL and JRC data for countries covered by both data sources, using the national population totals of the individual countries. Next to this, we compared the national population totals for the JRC gridded data supplemented with the ORNL and the Eurostat national population data for 2012 (Eurostat, 2014). Figure 3.1 presents both these comparisons.

From the comparisons, one can see the high correlation of the compared population datasets and a similar level of the JRC and the ORNL population data. Slight underestimation of the supplemented JRC data in comparison with the Eurostat data can be seen, which is caused by the fact that the Eurostat data is more up-to-date than both JRC and ORNL data. Based on this, the population totals in the report are presented using these actual Eurostat data, see below.

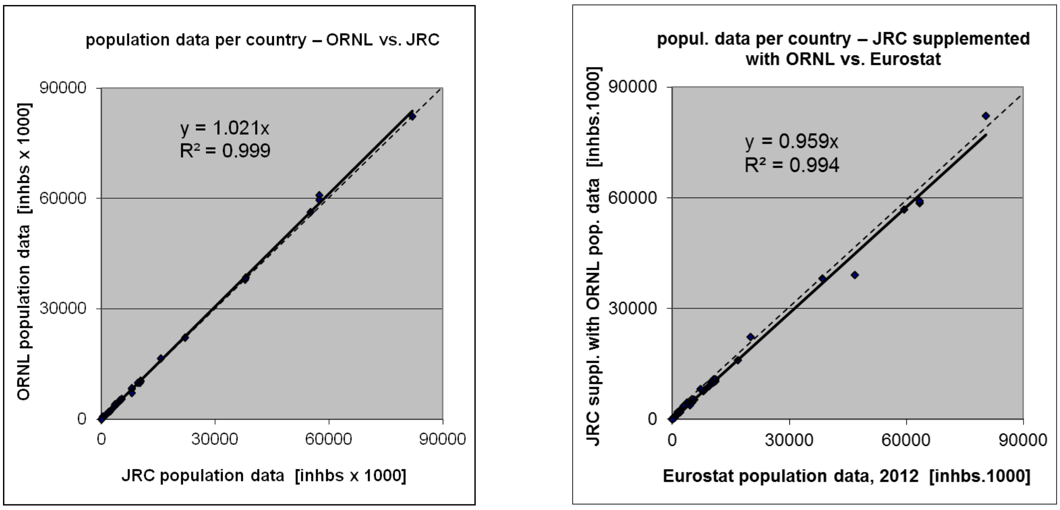

Figure 3.1 Correlation between ORNL (y-axis, left) and JRC (x-axis, left) and between JRC supplemented with ORNL (y-axis, right) and Eurostat 2012 revision (x-axis, right) for national population totals.

Population density data can be used to classify the spatial distribution of each type of area (rural, urban or mixed population density) in Europe. We use this information to select and weight the air quality value, grid cell by grid cell. Furthermore, we use it to estimate population health exposure and exceedance numbers per country and for Europe as a whole, including involved uncertainties. These activities take place on the 1x1 km resolution grid in accordance with the recommendations of Horálek et al. (2010). The supplemented JRC data (as described above) are used in all the calculations.

Population totals for individual countries presented in exposure tables in Sections 4.1.2, 4.2.2, 5.1.2, 6.1.2 and 6.2.2 are based on Eurostat national population data for 2011 (Eurostat, 2013). For Monaco, which is not included in the Eurostat database, the population total is based on UN (2010) for 2010.

3.6 Land cover

CORINE Land Cover 2006 – grid 100 x 100 m, Version 17 (12/2013) is used (CLC2006 – 100m, g100_06.zip; EEA, 2013a). The countries missing in this database are Andorra and Greece. Greece is missing in the CLC2006 but present in the CLC2000 version that we used in previous mapping years. Therefore, we inserted for Greece the CLC2000 data (grid 100 x 100 m, Version 17, 12/2013 EEA, 2013b). Due to lacking land cover data for Andorra, we excluded these countries from the process of exposure estimates related to the vegetation based AOT40 ozone indicators.

4 PM_{10} maps

This chapter presents the 2012 updates (for the interpolated maps and exposure tables) of the two PM_{10} health related indicators: annual average and 36th highest daily average. The separate rural and urban background concentration maps were calculated on the 10x10 km resolution grid and the subsequent combined concentration map was based on the 1x1 km gridded population density map. The population exposure tables were calculated at 1x1 km grid resolution. All maps here are presented using the 10x10 km grid resolution. The standard EEA ETRS89-LAEA5210 coordinate reference system was applied.

4.1 Annual average

4.1.1 Concentration map

Figure 4.1 presents the combined final map for the 2012 PM_{10} annual average as the result of interpolation and merging of the separate maps as described in detail in De Smet et al. (2011) and Horálek et al. (2007). Red and purple areas and stations exceed the limit value (LV) of 40 μg.m^{-3}. Supplementary data in the regression used for rural areas consisted of EMEP model output, altitude, wind speed and surface solar radiation and for urban background areas it was EMEP model output only. The relevant linear regression submodels have been identified earlier in Horálek et al. (2008) and De Smet et al. (2009, 2010, 2011).

As one can observe and like in 2011, in a few areas of the map (e.g. Bulgaria, Poland) the high urban background measurement values do not seem to influence the interpolation results despite their clustering. The main reason is that the map presented here is an aggregation of 1x1 km grid values to a 10x10 km resolution and this aggregation smooths out the elevated values one would more likely be able to distinguish in the higher resolution map, especially in the case of urban background stations representing the urban areas. (Therefore, the exposure estimates of Table 4.2 are derived just from the 1x1 km grid map). Another less prominent reason is the smoothing effect kriging has in general. However, kriging would in the case of clustering not mask these elevations in the separate 1x1 km rural and urban background maps.

Table 4.1 presents the estimated parameters of the linear regression models (c, a_1, a_2,…) and of the residual kriging (*nugget, sill, range*) and includes the statistical indicators of both the regression and the kriging. The adjusted R^2 and standard error are indicators for the fit of the regression relationship, where the adjusted R^2 should be as close to 1 as possible and the standard error should be as small as possible. The adjusted R^2 was 0.52 for the rural areas and 0.24 for urban areas. The R^2 values show both for rural and urban areas in 2012 the second best fit, compared to its all previous years, see Horálek et al. (2014a) and references cited therein. The continued better regression fit for urban areas as of 2010 is most likely attributable to improvements of the EMEP model since 2010. The reason probably is the improvement of the EMEP model. RMSE and bias are the cross-validation indicators, showing the quality of the resulting map; the bias indicates to what extent the estimation is un-biased. Sections 4.1.2 and 4.1.3 deal with a more detailed analysis and compares with results of the years 2005 – 2011.

As indicated in Table 4.1, surface solar radiation was, in contrast to 2010–2011 (and like in 2006-2009), found to be statistically significant and thus used in 2011 mapping. However, its significance is quite weak (P = 0.043, where it can be no more than 0.5) and its further use is still to be considered.

In the case of PM_{10}, the linear regression is applied for the logarithmically transformed data of both measured and modelled PM_{10} values. Thus, in Table 4.1 the standard error and variogram parameters refer to these transformed data, whereas RMSE and bias refer to the interpolation after the back-transformation.

Table 4.1 Parameters of the linear regression models (Eq. 2.2) and of the ordinary kriging (OK) variograms (nugget, sill, range) – and their statistics – of PM_{10} indicator annual average for 2012 in rural (left) and urban (right) areas as used for the combined final map.

linear regr. model + OK of its residuals	rural areas parameter values	urban areas parameter values
c (constant)	1.71	1.63
a1 (log. EMEP model 2012)	0.613	0.64
a2 (altitude GTOPO)	-0.00047	
a3 (wind speed 2012)	-0.101	
a4 (s. solar radiation 2012)	0.014	
adjusted R^2	**0.52**	**0.24**
standard error [μg.m^{-3}]	**0.27**	**0.35**
nugget	0.024	0.018
sill	0.068	0.075
range [km]	480	750
RMSE [μg.m^{-3}]	**3.77**	**6.05**
Relative RMSE [%]	**21.4**	**22.1**
bias (MPE) [μg.m^{-3}]	**0.09**	**-0.03**

The concentration map presented in Figure 4.1 is spatially aggregated from 1x1 km to a 10x10 km grid resolution, see Section 2.1.3. As a result, the urban areas are not properly resolved in this map, due to the smoothing effect of the aggregation. Section 4.1.3 discusses the level of the representation of the urban areas in this final combined aggregated 10x10 km map. For better visualising the actual urban concentration levels at the actual urbanised areas, i.e. without the influence of the dominating pattern of extended rural areas, a separate 1x1 km urban background map is presented in Annex 1, Figure A1.1. In this map, the non-urban areas are masked and the 'mixed' areas, i.e. areas with population density weighting of rural – urban characteristics, are semi-transparent.

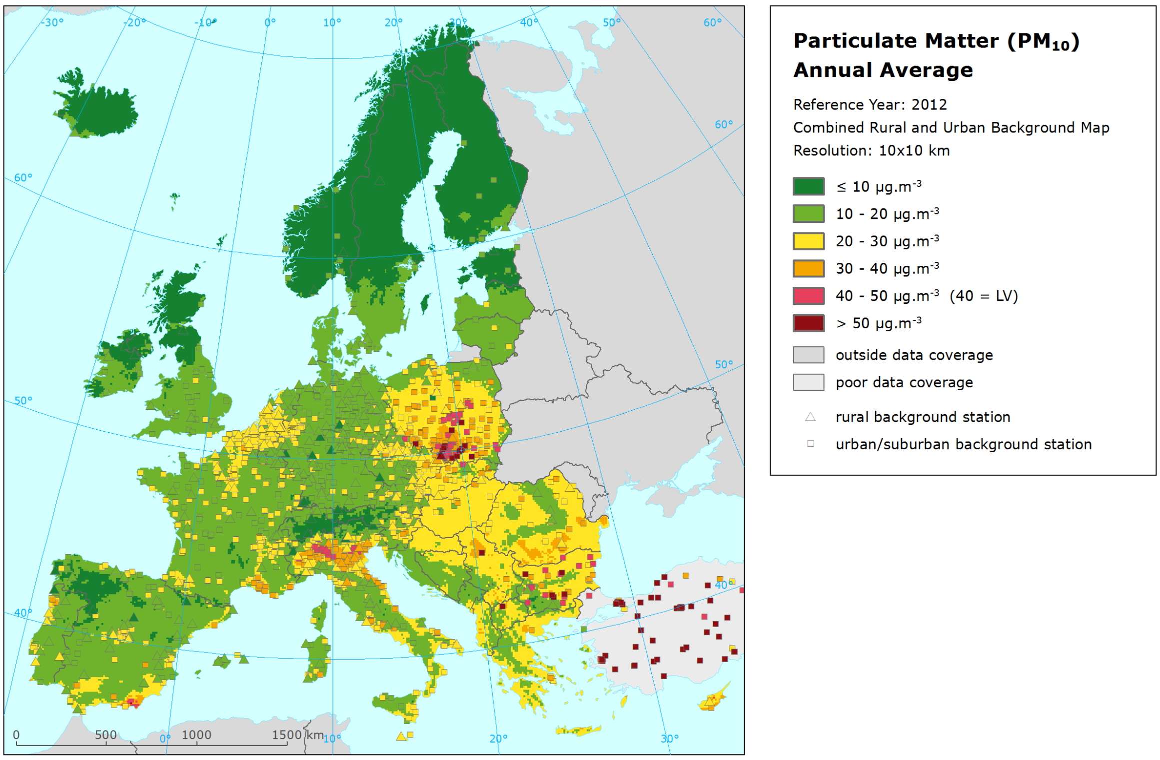

Figure 4.1 Combined rural and urban concentration map of PM_{10} – annual average, year 2012. Spatial interpolated concentration field (10x10 km grid resolution, excluding Turkey due to lack of rural air quality data) and the measured values in the measurement points. Units: μg.m^{-3}.

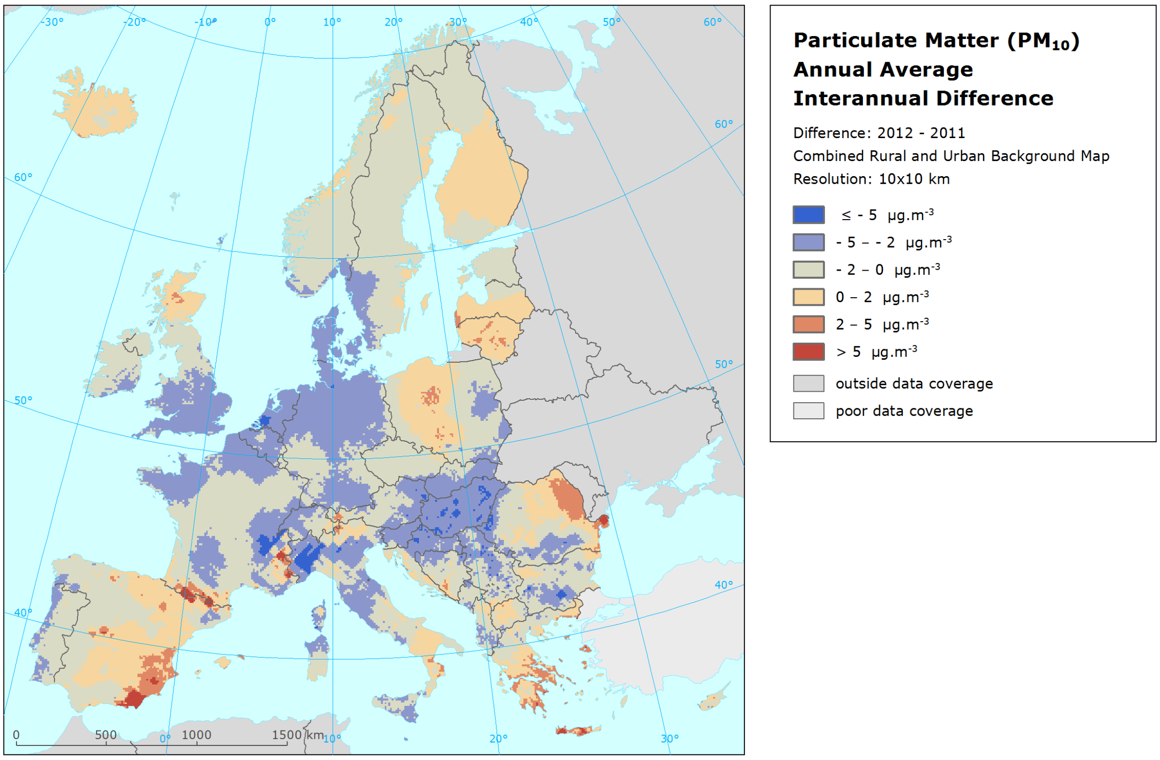

Figure 4.2 Inter-annual difference between mapped concentrations for 2012 and 2011 – PM_{10}, annual average. Units: µg.m^{-3}.

Figure 4.2 presents the inter-annual difference between 2011 and 2010 for annual average PM_{10}. Red areas show an increase of PM_{10} concentration, while blue areas show a decrease. The highest increases are observed in eastern part of the Iberian Peninsula, the Pyrenees, the western and eastern part of the Alps, and the north-eastern part of Romania. In past year's paper (Horálek et al (2014a) the comparison of the difference between 2011 and 2010 showed an increase at these areas as well, indicating a continued increase in concentrations from 2010 through 2012. Other areas with smaller increases (orange) in 2012, showed decreases in 2011 compared to 2010. For example, central part of Poland, Latvia, Lithuania, Finland, central part of Spain and Greece. Contrary to that, many areas in Europe demonstrate decreased concentrations in 2012 compared to 2011 (blue) versus an increase in 2011 compared to 2010, indicating a temporal elevation in 2011 of concentrations. For example, the Po Valley and northern and central Italy, the region covering southern UK, Normandy and Bretagne, Belgium, The Netherlands, Germany, Denmark and South-West Sweden, and parts of Central Europe with Hungary in its centre.

4.1.2 Population exposure

Table 4.2 gives the population frequency distribution for a limited number of exposure classes calculated at the 1x1 km grid resolution, as well as the population-weighted concentration for individual countries and for Europe as a whole according to Equation 2.3.

About 55 % of the European population (and also of the EU-28 population) has been exposed to annual average concentrations above 20 µg.m^{-3}, the WHO (World Health Organization) air quality guideline. EEA (2014) estimates that about 64-83 % of the urban population in the EU-28 is exposed to levels above the WHO guideline reference level. The latter estimate accounts for the urban population mainly in the larger cities of the EU-28 It therefore represents areas where, in general, considerably higher PM_{10} concentrations occur throughout the year. The estimates in Table 4.2 includes the total European (resp. EU-28) population, including inhabitants in the rural areas, the smaller cities and the villages that are in general exposed to lower levels of PM_{10} throughout the year. It is important to note that this difference in WHO reference level exposure estimates is explained by the use of different area representation in the calculations.

Slightly more than half (52 %) of the European population in 2012 lived in areas where the PM_{10} annual mean concentration was estimated to be between 20 and 40 $\mu g.m^{-3}$. About 3.4 % of the population lived in areas where the PM_{10} annual limit value was exceeded, with Bulgaria, Cyprus, FYR of Macedonia, Poland and Serbia showing a population-weighted concentration of more than 5 % above the LV. However, as the next Section 4.1.3 discusses, the current mapping methodology tends to underestimate high values. Therefore, the exceedance percentage would most likely be underestimated; additional exceedances might be expected in countries like Albania, Czech Republic Greece and Romania.

The evolution of population exposure in the last eight years is presented in Table 4.3. It is based on results presented in previous reports (Horálek et al., 2014a, and references cited therein) for the years 2008 – 2011, based on the recalculated results for 2005 and 2007 and based on the paper with the tests of a new methodology (Horálek et al., 2010) for 2006. The overall picture of the population-weighted concentration of the European totals in Table 4.3 demonstrates a slightly continuous downward trend for the years 2005 – 2012. For these years, the EEA CSI 004 (urban population weighted concentration of the EU-28 2003 – 2012) does observe a less prominent downward trend in urban population exposure. The difference has most likely its cause in the fact that the EEA CSI 004 is based on the stations, which are irregularly distributed across Europe, while in the countries with smaller density of the stations (e.g. Portugal, Romania, Sweden) the downward trend is more prominent than in the countries with higher station density (e.g. Germany, France)..

The frequency distribution shows large variability over Europe, with several countries showing in 2012 exposures above the limit value, like in 2011 but most of them with an increased percentage in exceedance (e.g. Albania, Bulgaria, Cyprus, FYR of Macedonia, Poland). Italy shows a decrease of almost 14 % in 2011 to just 0.1 % in 2012. In the period 2005 – 2012, the year 2012 appears to show a slight increase in the number of population being exposed to annual averaged concentrations above the limit value for 2012, but it is still lower than in the years 2005 – 2010. In many cases the reduction in 2011 is not continued in 2012, where the levels seem to be close to those of 2010. Compared to 2011, an overall increase of 1.0 % occurred in 2012.

In a number of countries in northern and north-western Europe, the LV of 40 $\mu g.m^{-3}$ seems to continue not to be exceeded. When comparing between years the total population exposed to the low levels, i.e. below 20 $\mu g.m^{-3}$, it is found that the percentage for 2012 of 45 % is higher than the four previous years 2008 – 2011 (with 29 – 40 %), which on its turn higher is than for the years 2007 with 24 % and 2006 with 20 %. The tendency of reduced exposure of population living in areas with concentrations above the limit value, established in previous years (from 10.3 % in 2006 to 5 – 6 % in 2007 – 2010)) seems to continue with values of between 2.5 – 5 % in the years 2011 – 2012. The tendency comes with a degree of uncertainty however and should not be qualified as a clear downward trend without more detailed analysis.

Considering the average for the whole of Europe in Table 4.3, the overall population-weighted annual mean PM_{10} concentration in 2012 was 22.7 $\mu g.m^{-3}$. This is almost the same as in previous year. One may observe a steady reduction of the population-weighted concentration over the period of time 2005 – 2011, with perhaps some consolidation effect in 2012.

Table 4.2 Population exposure and population-weighted concentration – PM_{10}, annual average, year 2012. Resolution: 1x1 km.

Country		Population	PM_{10} annual average, exposed population [%]						Population weighted conc.
			< LV				> LV		
			< 10	10 - 20	20 - 30	30 - 40	40 - 45	> 45	
		[inhbs . 1000]	$\mu g.m^{-3}$	$\mu g.m^{-3}$	$\mu g.m^{-3}$	$\mu g.m^{-3}$	$\mu g.m^{-3}$	$\mu g.m^{-3}$	[$\mu g.m^{-3}$]
Albania	AL	2 865	0.0	8.3	27.1	61.4	3.2		32.0
Andorra	AD	78		10.5	8.4	81.1			33.2
Austria	AT	8 408	1.6	39.3	59.1				20.0
Belgium	BE	11 095		8.9	91.1				23.2
Bosnia & Herzegovina	BA	3 839		16.1	40.9	43.1			27.2
Bulgaria	BG	7 327	0.0	4.3	23.7	26.3	38.7	6.9	36.6
Croatia	HR	4 276		9.5	85.9	4.5			24.7
Cyprus	CY	862		0.2	12.6	12.2	73.3	1.7	42.9
Czech Republic	CZ	10 505	0.0	13.5	73.8	8.4	4.3		25.4
Denmark	DK	5 581	0.1	99.3	0.6				16.3
Estonia	EE	1 325	27.0	73.0					12.1
Finland	FI	5 401	38.6	61.4					10.2
France	FR	63 379	0.1	42.0	56.5	1.5	0.0		21.4
Germany	DE	80 328	0.1	78.3	21.6				18.4
Greece	GR	11 123		3.5	71.3	20.3	1.4	3.6	30.3
Hungary	HU	9 932		0.2	93.4	6.4			26.1
Iceland	IS	320	68.6	31.4					9.6
Ireland	IE	4 583	14.9	85.1	0.0				12.4
Italy	IT	59 394	0.1	15.5	55.4	28.9	0.1		27.0
Latvia	LV	2 045	2.3	54.2	43.5				18.0
Liechtenstein	LI	36	1.4	98.6					14.3
Lithuania	LT	3 004		87.4	12.6				18.1
Luxembourg	LU	525		100.0					17.2
Macedonia, FYR of	MK	2 060		6.2	14.5	16.1	30.4	32.7	42.3
Malta	MT	418			100.0				25.4
Monaco	MC	37		0.1	99.9				28.0
Montenegro	ME	621	0.1	23.1	28.2	47.7	0.9		28.3
Netherlands	NL	16 730		24.3	75.7				21.1
Norway	NO	4 986	37.9	61.0	1.1				12.2
Poland	PL	38 538		5.3	37.4	37.6	19.7		32.4
Portugal	PT	10 542	0.4	42.7	56.8	0.1			19.9
Romania	RO	20 096		4.1	63.2	28.6	4.2		28.9
San Marino	SM	32		11.6	88.4				25.8
Serbia (incl. Kosovo)	RS	9 015	0.0	2.6	27.0	47.4	21.7	1.3	34.9
Slovakia	SK	5 404		1.6	68.7	29.7	0.0		27.9
Slovenia	SI	2 055	0.0	12.8	87.2				24.3
Spain	ES	46 818	1.7	37.7	59.2	0.7	0.7	0.0	20.9
Sweden	SE	9 483	19.1	80.9					12.4
Switzerland	CH	7 955	2.1	86.2	11.7				17.6
United Kingdom	UK	63 495	2.4	95.2	2.4				16.5
Total		**534 518**	**1.8**	**43.1**	**41.0**	**10.7**	**3.1**	**0.3**	**22.7**
			44.9				**3.4**		
EU-28		**502 673**	**1.5**	**43.7**	**42.4**	**9.5**	**2.7**	**0.2**	**22.4**
			45.2				**2.9**		

Note1: Turkey is not included in the calculation due to lacking air quality data in rural areas.
Note2: The percentage value "0.0" indicates an exposed population exists, but is small and estimated less than 0.05 %. Empty cells mean: no population in exposure.

Table 4.3 Evolution of percentage population living in above limit value (left) and population-weighted concentration (right) in the years 2005-2012 – PM_{10}, annual average. Resolution: 1x1 km.

Country		Population above LV 40 μg.m^{-3} [%]									Population-weighted conc. [μg.m^{-3}]								
		2005	2006	2007	2008	2009	2010	2011	2012	diff. '12 - '11	2005	2006	2007	2008	2009	2010	2011	2012	diff. '12 - '11
Albania	AL	59.4	3.1	0.1	6.5	52.1	62.6	0.9	3.2	2.3	36.3	31.8	31.6	33.3	35.3	45.5	26.5	32.0	5.6
Andorra	AD	0	0	0	0	0	0	0	0	0	19.5	22.5	20.5	18.7	17.7	17.9	18.0	33.2	15.2
Austria	AT	0	0	0	0	0	0	0	0	0	25.4	26.0	22.1	21.3	21.6	22.7	20.8	20.0	-0.8
Belgium	BE	0	0	0	0	0	0	0	0	0	29.2	31.3	24.8	23.9	26.5	25.7	24.8	23.2	-1.6
Bosnia-Herzegovina	BA	32.1	6.9	3.3	0.0	51.6	17.2	0.7	0	-0.7	34.3	33.1	32.4	29.3	37.2	30.8	22.3	27.2	4.9
Bulgaria	BG	46.4	49.9	42.1	62.1	53.8	49.0	7.4	45.6	38.2	42.6	41.6	40.2	44.2	39.8	38.0	27.3	36.6	9.3
Croatia	HR	15.2	0.1	0	0	3.0	0	0	0	0	33.6	31.5	30.0	28.1	29.0	27.3	25.0	24.7	-0.4
Cyprus	CY	71.1	0	0	87.0	73.0	82.7	12.8	75.0	62.2	38.9	35.4	33.9	76.1	41.0	50.2	31.1	42.9	11.9
Czech Republic	CZ	11.5	13.8	1.8	1.7	3.3	9.4	0.9	4.3	3.4	32.9	33.5	25.6	24.2	25.3	28.3	23.7	25.4	1.7
Denmark	DK	0	0	0	0	0	0	0	0	0	21.3	23.5	20.8	18.8	16.3	15.7	18.4	16.3	-2.2
Estonia	EE	0	0	0	0	0	0	0	0	0	17.7	19.7	15.7	12.9	13.4	14.1	9.8	12.1	2.3
Finland	FI	0	0	0	0	0	0	0	0	0	14.2	17.0	13.7	12.5	11.7	12.2	9.5	10.2	0.7
France	FR	0	0	0	0	0	0	0	0.0	0.0	19.3	20.4	24.6	22.6	24.0	23.0	21.8	21.4	-0.4
Germany	DE	0	0	0	0	0	0	0	0	0	23.0	24.2	20.7	19.6	20.7	21.2	19.6	18.4	-1.1
Greece	GR	65.4	3.6	1.5	37.0	23.4	20.9	5.7	5.0	-0.7	38.0	33.6	33.5	39.7	35.3	37.3	24.6	30.3	5.6
Hungary	HU	5.41	2.2	0	0	0	0	0	0	0	34.8	32.9	28.7	26.8	27.6	28.1	29.1	26.1	-3.0
Iceland	IS	0	0	0	0	0	0.1	0	0	0.0	13.8	17.4	12.2	15.2	9.0	10.7	9.3	9.6	0.3
Ireland	IE	0	0	0	0	0	0	0	0	0	12.7	14.9	14.7	15.4	12.8	13.7	12.8	12.4	-0.4
Italy	IT	28.9	24.2	19.8	2.7	8.8	0	13.7	0.1	-13.6	34.9	33.9	33.2	30.1	28.7	26.4	27.7	27.0	-0.7
Latvia	LV	0	0	0	0	0	0	0	0	0	19.8	21.9	17.8	19.1	18.8	21.5	14.6	18.0	3.4
Liechtenstein	LI	0	0	0	0	0	0	0	0	0	23.4	24.9	20.7	20.6	18.3	17.3	11.3	14.3	3.0
Lithuania	LT	0	0	0	0	0	0	0	0	0	20.7	22.5	18.5	17.3	19.0	22.0	14.8	18.1	3.3
Luxembourg	LU	0	0	0	0	0	0	0	0	0	18.7	20.8	19.5	18.2	21.0	19.4	16.4	17.2	0.8
Macedonia, FYR of	MK	69.3	61.3	52.1	67.8	74.5	70.0	2.3	63.2	60.8	46.2	39.3	38.5	41.6	45.4	43.9	23.0	42.3	19.3
Malta	MT	0	0	0	0	0	0	0	0	0	37.1	29.4	27.0	27.5	27.2	32.5	27.8	25.4	-2.4
Monaco	MC		0	0	0	0	0	0	0	0		36.7	34.5	29.5	26.8	24.0	22.8	28.0	5.2
Montenegro	ME	63.5	9.7	1.3	38.7	61.1	42.1	0	0.9	0.9	35.1	33.1	33.1	33.6	35.0	32.8	21.5	28.3	6.8
Netherlands	NL	0	0	0	0	0	0	0	0	0	29.2	29.1	25.8	24.0	24.3	24.3	25.1	21.1	-4.0
Norway	NO	0	0	0	0	0	0	0	0	0	18.1	19.6	15.6	15.7	14.1	14.7	9.3	12.2	2.9
Poland	PL	21.6	28.5	13.4	12.4	14.7	30.0	5.2	19.7	14.5	32.7	37.0	28.8	28.3	30.8	35.2	27.2	32.4	5.2
Portugal	PT	11.5	0	0	0	0	0	0	0	0	30.9	28.4	27.0	21.8	22.9	21.7	20.8	19.9	-0.9
Romania	RO	61.2	47.0	32.0	19.6	4.0	2.0	0.9	4.2	3.3	42.7	39.1	35.0	30.8	28.9	25.2	27.2	28.9	1.7
San Marino	SM	0	0	0	0	0	0	0	0	0	31.7	33.9	31.2	29.6	26.0	25.0	20.9	25.8	4.9
Serbia (incl. Kosovo)	RS	69.5	66.0	59.1	61.8	55.5	20.7	13.4	23.0	9.6	44.2	41.8	39.4	40.1	39.5	33.1	30.1	34.9	4.8
Slovakia	SK	16.3	16.3	2.4	1.7	1.2	3.0	0.1	0.0	-0.1	34.3	33.8	29.1	26.7	26.9	30.2	27.4	27.9	0.6
Slovenia	SI	2.4	0	0	0	0	0	0	0	0	30.8	29.0	27.2	25.0	25.2	26.0	25.4	24.3	-1.1
Spain	ES	3.5	7.5	2.6	1.3	0	0	0	0.8	0.8	29.6	31.4	29.6	25.2	23.7	21.4	18.8	20.9	2.1
Sweden	SE	0	0	0	0	0	0	0	0	0	16.9	19.0	15.7	16.3	13.8	12.8	12.3	12.4	0.1
Switzerland	CH	0.8	0.9	0	0	0	0	0	0	0	21.3	23.2	21.4	20.5	21.0	19.8	17.7	17.6	-0.1
United Kingdom	UK	0	0	0	0	0	0	0	0	0	21.4	23.2	21.6	19.5	18.4	18.2	17.5	16.5	-1.0
Total		**13.3**	**10.3**	**6.8**	**5.8**	**6.0**	**5.2**	**2.5**	**3.4**	**1.0**	**28.0**	**28.5**	**26.2**	**24.8**	**24.6**	**24.3**	**22.1**	**22.7**	**0.6**
EU-28		**11.4**	**9.3**	**5.9**	**4.4**	**4.1**	**4.1**	**2.4**	**2.9**	**0.6**	**27.6**	**28.3**	**26.0**	**24.4**	**24.2**	**24.0**	**22.1**	**22.4**	**0.3**

4.1.3 Uncertainties

Uncertainty estimated by cross-validation

Using RMSE as the most common indicator, the *absolute mean uncertainty* of the combined final map at areas 'in between' the station measurements can be expressed in μg.m^{-3}. Table 4.1 shows that the absolute mean uncertainty of the combined final map of PM_{10} annual average expressed by RMSE is 3.8 μg.m^{-3} for the rural areas and 6.1 μg.m^{-3} for the urban areas. The RMSE for urban areas is in line with the results of previous years; the RMSE for rural areas is the lowest one obtained so far. Alternatively, one could express this uncertainty in relative terms by relating the absolute RMSE uncertainty to the mean air pollution indicator value for all stations. This *relative mean uncertainty*

(RRMSE) of the combined final map of PM_{10} annual average is 21.4 % for rural areas and 22.1 % for urban areas. This is, for rural areas, slightly higher than in 2011 (21.1 %), but lower that in the period 2005 – 2010. The somewhat higher uncertainty levels for urban areas in the years 2008 – 2012, compared to the years 2005 – 2007, are caused specifically by addition of Turkish urban background stations reported only since 2008. (Turkish urban stations show high concentrations, uncertainty statistics are sensitive to such values.) These data have been used in the calculations since 2008 (although the interpolation result for Turkey is not present in the map due to lack of rural air quality data for Turkey). These relative uncertainty values fulfil the data quality objectives for models as set in Annex I of the air quality Directive 2008/50/EC (EC, 2008). Table 7.5 summarises both the absolute and relative uncertainties over these past eight years.

Figure 4.3 shows the cross-validation scatter plots, obtained according Section 2.3, for both rural and urban areas. The R^2 indicates that for the rural areas about 67 % and for the urban areas about 76 % of the variability is attributable to the interpolation. The 2012 interpolation performance at both the rural and urban locations is slightly above the average of the earlier seven years (see Table 7.5).

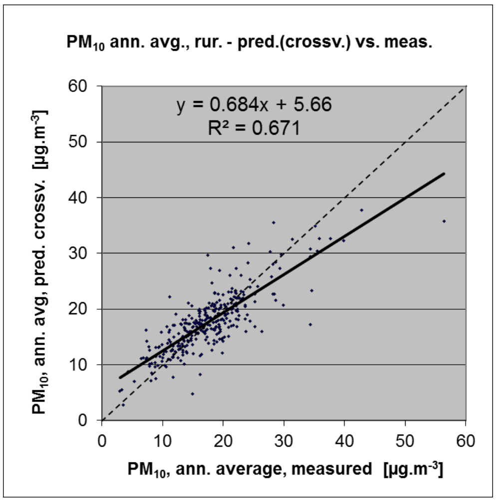

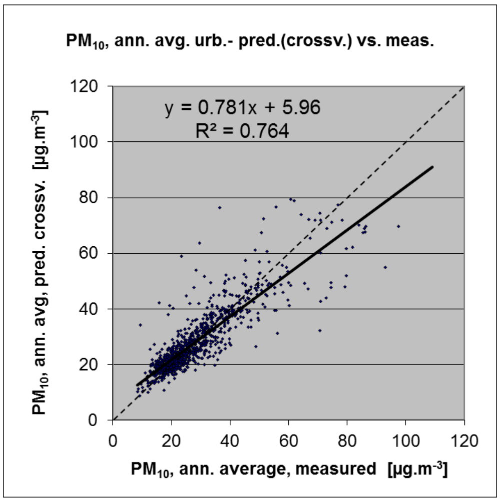

Figure 4.3 Correlation between cross-validation predicted values (y-axis) and measurements (x-axis) for the PM_{10} annual average for 2012 for rural (left) and urban (right) areas. R^2 and the slope a (from the linear regression equation $y = a \cdot x + c$) should be as close 1 as possible, the intercept c should be as close 0 as possible

The scatter plots indicate that in areas with high concentrations the interpolation methods tend to underestimate the levels. For example, in rural areas an observed value of 40 $\mu g.m^{-3}$ is estimated in the interpolations to be about 33 $\mu g.m^{-3}$, about 17 % too low. This underestimation at high values is natural to all spatial interpolations. It can be reduced by either using a higher number of stations with an improved spatial distribution, or by introducing a closer improved regression by using other supplementary data.

Comparison of point measurement values with the predicted grid value

In addition to the above point observation – point prediction cross-validation discussed in the previous subsection, a simple comparison has been made between the point observation values and interpolated prediction values spatially averaged at grid cells. This *point-grid* comparison indicates to what extent the predicted value of a grid cell represents the corresponding measured values at stations located in that cell. The comparison has been executed primarily for the separate rural and separate urban background map at 10x10 km resolution. (One can directly relate this comparison result to the cross-validation results of Figure 4.3.)

Next to this, the comparison has been done also for the final combined maps at 1x1 km resolution and for the spatial aggregated final maps at 10x10 km resolution. Figure 4.4 shows the scatterplots for these comparisons.

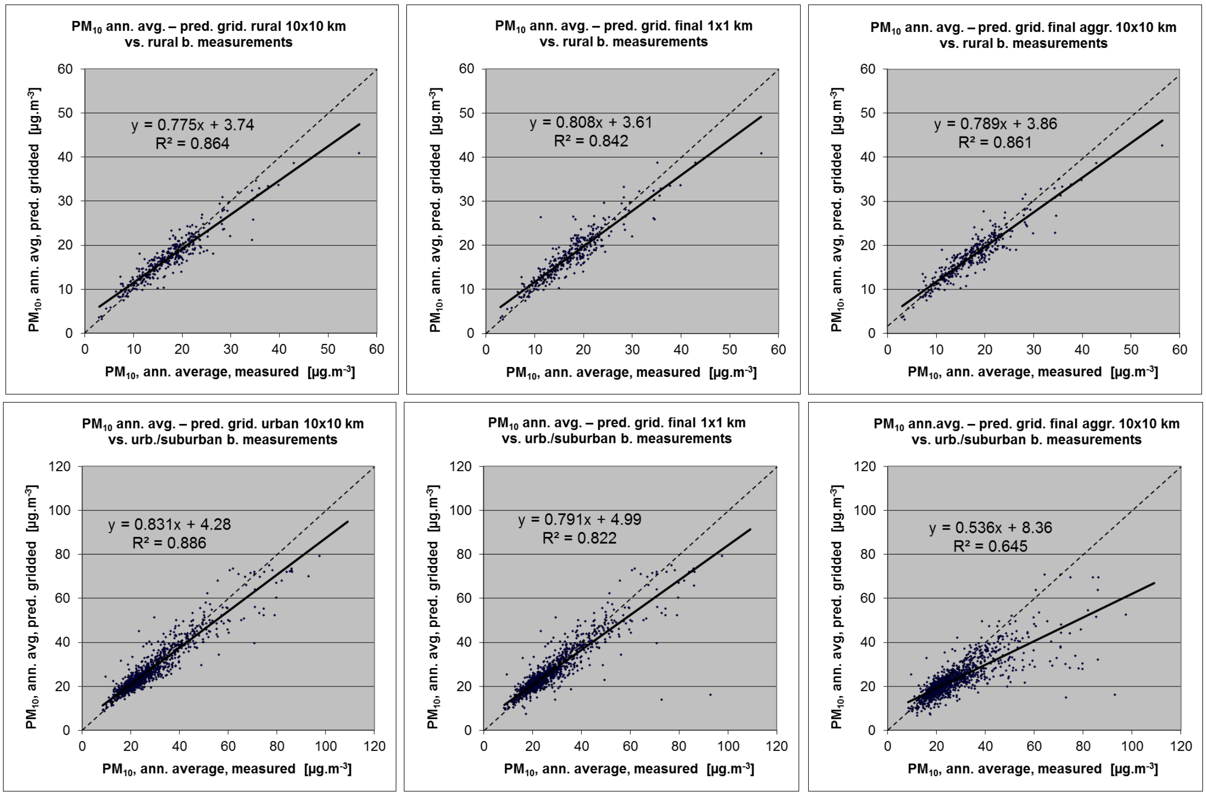

Figure 4.4 Correlation between predicted grid values from rural 10x10 km (upper left), urban 10x10 km (bottom left), final combined 1x1 km (upper and bottom middle) and final combined spatially aggregated 10x10 km (upper and bottom right) map (y-axis) versus measurements from rural (top), resp. urban/suburban (bottom) background stations (x-axis) for PM_{10} annual average 2012.

The results of the point observation – point prediction cross-validation of Figure 4.3 and those of the point-grid validation for separate rural and separate urban background maps, and for the final combined maps at both resolutions are summarised in Table 4.4.

By the comparing the scatterplots and the statistical indicators for the separate rural and separate urban background map with the final combined maps in both resolutions, one can evaluate the level of representation of the rural resp. urban background areas in the final combined maps. The rural air quality is fairly well represented in both the 1x1 km and the aggregated 10x10 km final combined map. The urban air quality is quite well represented in the final combined 1x1 km map, but not in the aggregated final combined 10x10 km map as one can deduce from its higher RMSE, its bias being further from zero and its lower R^2. Therefore, we present in Figure A1.1 of Annex 1 the 1x1 km urban background map in addition to the 10x10 km final combined map of Figure 4.1.

The Table 4.4 shows a better relation (i.e. lower RMSE, higher R^2, smaller intercept and slope closer to 1) between station measurements and the interpolated values of the corresponding grid cells at both rural and urban background map areas than it does at the point cross-validation predictions. That is because the simple comparison between point measurements and the gridded interpolated values shows the uncertainty at the actual station locations (points), while the point cross-validation prediction simulates the behaviour of the interpolation at point positions assuming no actual measurement would exist at that point. The uncertainty at measurement locations is caused partly by the smoothing effect of the interpolation and partly by the spatial averaging of the values in the 10x10 km grid cells. The level of the smoothing effect leading to underestimation at areas with high values is there smaller than it is in situations where no measurement is represented in such areas. For example, in urban areas the predicted interpolation gridded value in the separate urban background map will be about 58 $\mu g.m^{-3}$ at the corresponding station point with the measured value of 65 $\mu g.m^{-3}$. This means an underestimation of about 10 %. It is less than the prediction underestimation of 13 % at the same point location, when leaving out this one actual measurement point and one does the interpolation without this station (see the previous subsection).

Table 4.4 Statistical indicators RMSE, bias, coefficient of determination R^2 and linear regression equation from the scatter plots for the predicted point values based on cross-validation and the predicted grid values from separate (rural resp. urban) 10x10 km, final combined 1x1 km and final combined spatially aggregated 10x10 km map versus the measured point values for rural (left) and urban (right) background stations for PM_{10} annual average of 2012.

	rural backgr. stations				urb./suburban backgr. stations			
	RMSE	bias	R^2	equation	RMSE	bias	R^2	equation
cross-valid. prediction, separate (r or ub) map	3.8	0.1	0.671	y = 0.684x + 5.66	6.1	0.0	0.764	y = 0.781x + 5.96
grid prediction, 10x10 km separate (r or ub) map	2.5	-0.2	0.864	y = 0.775x + 3.74	4.3	-0.3	0.886	y = 0.831x + 4.26
grid prediction, 1x1 km final merged map	2.6	0.3	0.842	y = 0.808x + 3.61	5.3	-0.7	0.822	y = 0.791x + 4.99
grid prediction, aggr. 10x10 km final merged map	2.5	0.2	0.861	y = 0.789x + 3.86	8.7	-4.2	0.645	y = 0.536x + 8.36

Probability of Limit Value exceedance

Next to the point cross-validation analysis, we constructed the map of probability of limit value exceedance. For this purpose, we used the final combined concentration map in the 10x10 km grid resolution. Based on this map, we derived, with support of the 10x10 km uncertainty map and the limit value (40 µg.m^{-3}), the probability of exceedance (PoE) map at that same resolution (Figure 4.5). It is important to emphasize that the exceedance of the spatial average of a 10x10 km grid cell can show low probability even though some smaller (e.g. urban) areas inside such a grid cell show high probability of exceedance (using finer grid cell resolution). Next to this – keeping in mind that the interpolated maps refer to the rural or (sub)urban *background* situations only, it cannot be excluded that exceedances of limit values may occur at different *hotspot* and traffic locations.

The map demonstrates areas with a probability of limit value exceedance above 75 % marked in red (*high* probability) and areas below 25 % in green (*low* probability). Red indicates areas for which exceedance is *very likely* to occur due to either high concentrations close to or already above the LV accompanied with such uncertainty that exceedance is very likely, or areas with lower concentrations accompanied with high uncertainty levels reaching above the LV that excess is very likely. Vice versa, in the green areas it is *not likely* to have predicted concentrations and accompanying uncertainties at levels that do reach above the LV.

In the probability maps, the areas with 25-50 % and 50-75 % probability of LV exceedance are marked in yellow and orange respectively. The yellow colour indicates the areas with the estimated concentrations below limit value, but for which there exists a *modest* probability of exceeding the limit. On the contrary, the orange areas have estimated concentrations above the limit value, but with a chance of non-exceedance caused by its accompanying uncertainty. Table 4.5 summarises the classes and terminology for probability (i.e. likelihood) that are distinguished in this paper.

Table 4.5 Probability mapping classes and terminology use in this paper.

Map class colour	Percentage probability of threshold exceedance	Degree of probability (or likelihood) of exceedance	Likelihood of exceedance
Green	0 – 25	Low/ Little	Not likely
Yellow	25 – 50	Modest	Somewhat likely
Orange	50 – 75	Moderate	Rather Likely
Red	75 – 100	High / Large	Very likely

The patterns in the spatial distribution of the different PoE classes over Europe differ in 2012 somewhat from those of 2011. The patterns in the spatial distribution of the different PoE classes over Europe differ in 2012 somewhat from those of 2011. The region of southern Poland – north-eastern

Czech Republic with the industrial zones of Krakow, Katowice (PL) and Ostrava (CZ) shows in 2012, like 2011, a smaller area with the highest probability of exceedance (75-100 %) compared to 2010.The Po Valley in Italy shows a considerable reduced probability of exceedance compared to 2011. In south-eastern Europe, where relatively few measurement stations are located, especially at some larger cities with mostly high traffic density and heavy industry, only somewhat elevated PoE do show up at a few cities. In comparison with 2011, their number has reduced considerably. In other parts of Europe there exists just little likelihood of exceedance, with the exception of the area around Almería, Spain, where a high likelihood of exceedance appears to exist. In general, one can conclude that the likelihood of exceedance in 2012 has reduced compared to the levels of 2011.

It should be noted that the PoE is related to the aggregated 10x10 km grid. In case we would produce such map on a 1x1 km grid resolution the map pattern would demonstrate elevated PoE levels clearly distinguishing smaller cities and towns as well, which are not resolved at the 10x10 km grid resolution. Furthermore, one should bear in mind that the map is based on rural and (sub)urban *background* station data only. As such the map reflects rural and urban background situations only. Therefore, this type of map will not resolve the exceedances of limit values that may occur at the many *hotspot* and traffic locations throughout Europe.

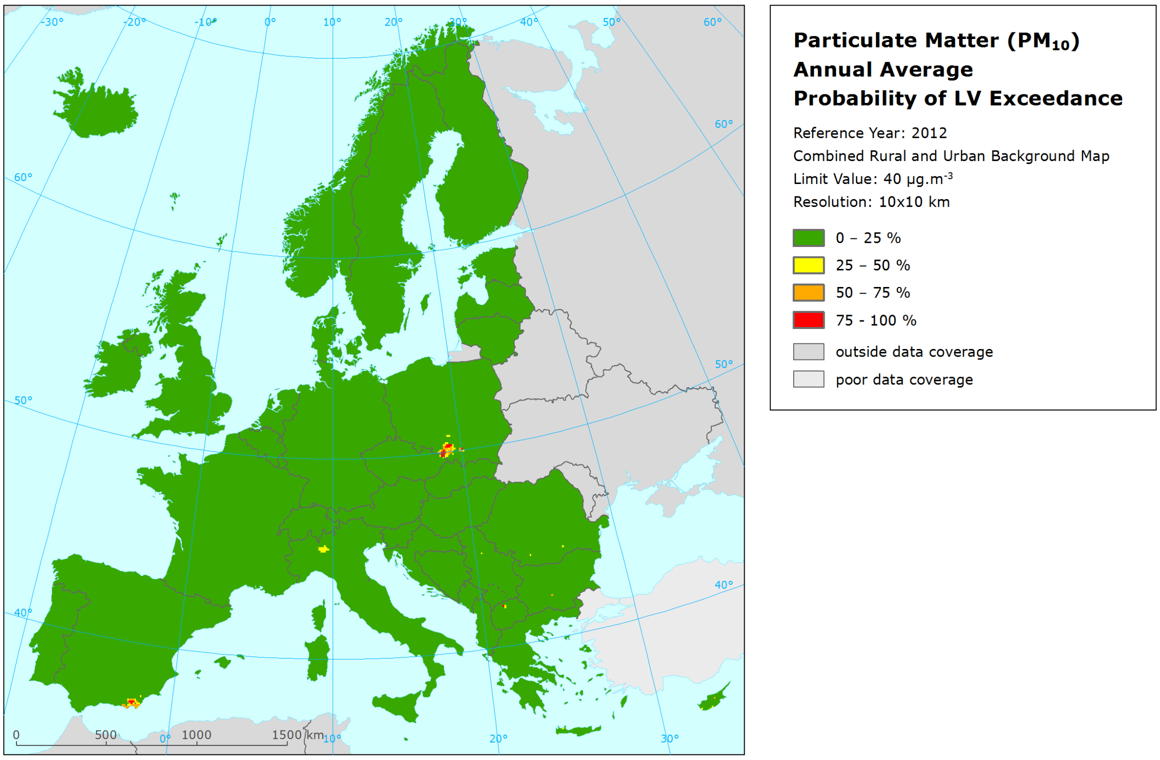

Figure 4.5 Map with the probability of the limit value exceedance for PM_{10} annual average (µg.m^{-3}) for 2012 on European scale calculated on the 10 x 10 km grid resolution. Interpolation uncertainty is considered only, no other sources of uncertainty.

4.2 36^{th} highest daily average

4.2.1 Concentration map

Similar to the PM_{10} annual average map, the combined final map of 36^{th} highest daily value has been derived from the separate rural, urban and joint rural/urban maps, using the same set of supplementary data parameters (Section 4.1.1) in the regression models and interpolation of residuals. Table 4.6 presents the estimated parameters of the linear regression models and of the residual kriging, including their statistical indicators.

Surface solar radiation was, like in 2010–2011 (and in contrast to 2006-2009), found to be statistically non-significant and thus it was not used in 2012 mapping.

Like in the case of annual average, the linear regression is applied for the logarithmically transformed data of both measured and modelled PM_{10} values. Thus, in Table 4.6 the standard error and variogram parameters refer to these transformed data, whereas RMSE and bias refer to the interpolation after the back-transformation.

The regressions on the 2012 data have an adjusted R^2 of 0.52 for rural areas and 0.22 for urban areas. Such a fit for rural areas is the same as in 2011 (0.55) and better than all other previous years. In urban areas, the fit was less than for 2010 (0.34) but much better than for other previous years, see Horálek et al. (2014a) and references cited therein. RMSE and bias are the cross-validation indicators for the quality of the resulting map. Section 4.2.3 discusses in more detail the RMSE analysis and the comparison with 2005 – 2011.

Table 4.6 Parameters of the linear regression models (Eq.2.1) and of their residual ordinary kriging (OK) variograms (nugget, sill, range) - and their statistics - of PM_{10} indicator 36^{th} highest daily mean for 2012 in the rural (left) and urban (right) areas as used for final mapping.

linear regr. model + OK on its residuals	rural areas parameter values	urban areas parameter values
c (constant)	2.06	1.80
a1 (lnEMEP model 2012)	0.637	0.638
a2 (altitude GTOPO)	-0.00050	
a3 (wind speed 2012)	-0.123	
a4 (s. solar radiation 2012)	n. sign.	
adjusted R^2	**0.52**	**0.22**
standard error [μg.m^{-3}]	**0.27**	**0.37**
nugget	0.029	0.016
sill	0.065	0.095
range [km]	480	660
RMSE [μg.m^{-3}]	**7.73**	**11.86**
relative RMSE [%]	**24.5**	**24.5**
bias (MPE) [μg.m^{-3}]	**0.13**	**-0.06**

Figure 4.6 presents the combined final map, where areas and stations exceeding the limit value (LV) of 50 μg.m^{-3} on more than 35 days are coloured red and purple.

As one can observe in a few areas of the map, the high urban background measurement values do not seem to influence the interpolation results despite their clustering (e.g. in Bulgaria). The main reason is that the map presented here is an aggregation of 1x1 km grid values to a 10x10 km resolution and this aggregation smooths out the elevated values one would more likely be able to distinguish in the higher resolution map, especially in the case of urban background stations representing the urban areas. Another less prominent reason is the smoothing effect kriging has in general. However, kriging would in the case of clustering, not mask these elevations in the separate 1x1 km urban and rural maps.

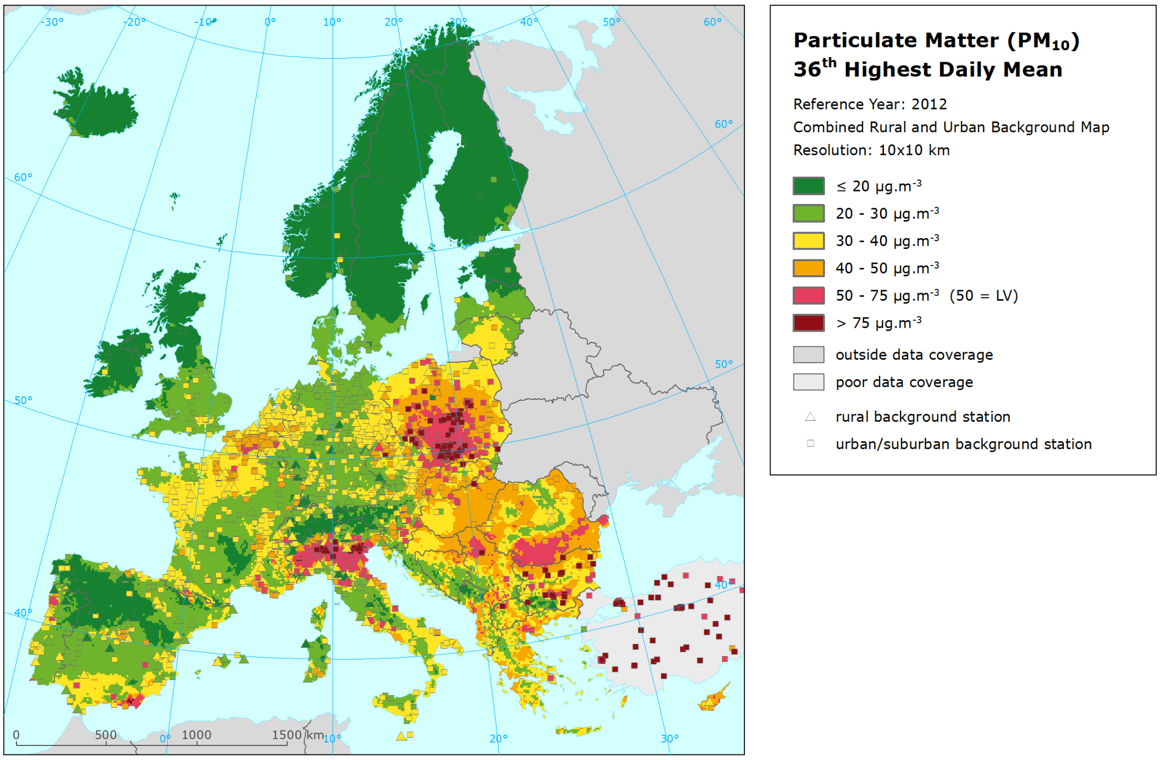

Figure 4.6 Combined rural and urban concentration map of PM_{10} – 36th highest daily average value, year 2012. Spatial interpolated concentration field (10x10 km grid resolution, excluding Turkey due to lack of rural air quality data) and the measured values in the measuring points. Units: µg.m^{-3}.

The concentration map presented in Figure 4.6 is spatially aggregated from a 1x1 km to a 10x10 km grid resolution. The urban areas are not properly resolved in this map, due to the smoothing effect of the aggregation. Section 4.2.3 discusses the level of the representation of the urban areas in this final combined aggregated 10x10 km map. For better visualising the actual urban concentration levels, without the influence of the dominating pattern of extended rural areas, a separate urban background map is presented in Annex 1, Figure A1.2.

Figure 4.7 presents the inter-annual difference between 2012 and 2011 for 36th highest daily mean. Red areas show an increase of PM_{10} concentration, while blue areas show a decrease. The highest increase s are observed in the eastern part of the Iberian Peninsula, the Pyrenees, the western part of the Alps and the eastern part of Romania, similar to that of the increases observed in the '2011-2010' difference map (Horálek et al, 2014a). The steepest decrease is observed in central Europe with Hungary in its centre. The Netherlands, East UK, Denmark, northern Germany and South-West Sweden. At these areas, the indicator value appears to show some elevation in 2011, compared to the ones of 2012 and 2010 and in some cases also of 2009. Contrary to that, Greece, central Italy, central Poland, Lithuania, Latvia and Finland show decreased indicator values in 2011, compared to the those of 2012 and 2010.

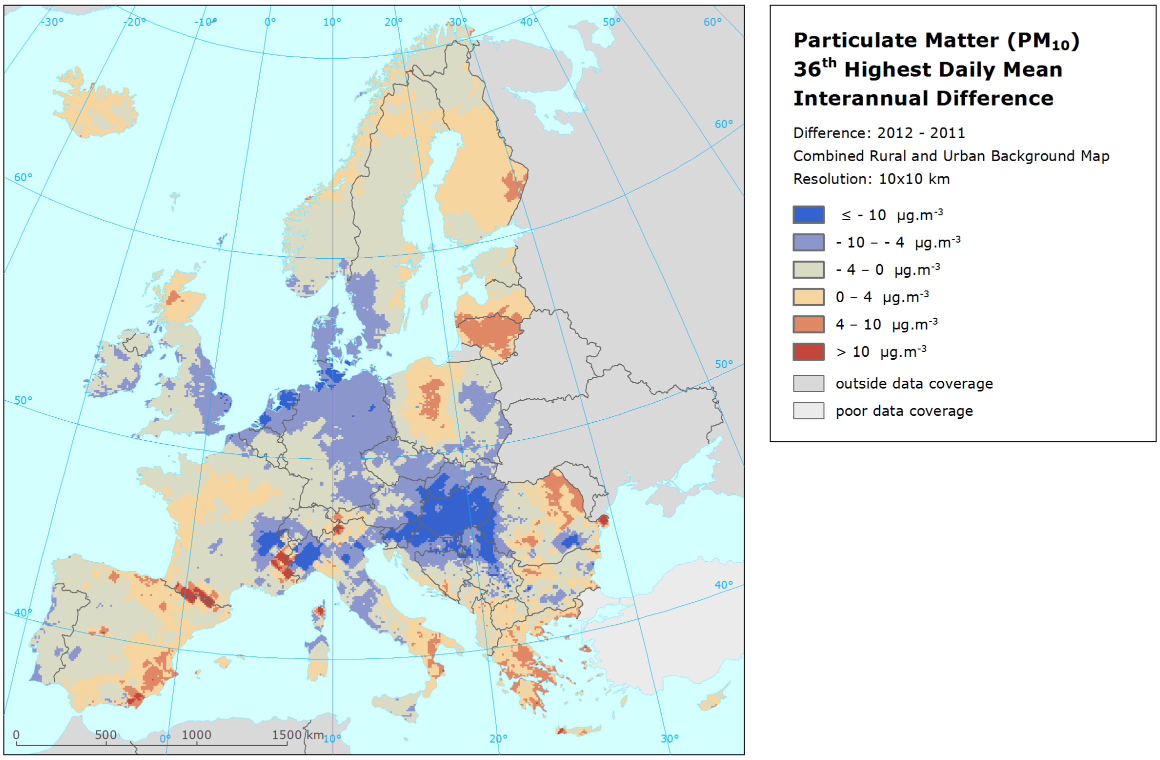

Figure 4.7 Inter-annual difference between mapped concentrations for 2012 and 2011 – PM_{10}, 36^{th} highest daily average value. Units: µg.m^{-3}. Resolution: 10x10 km.

4.2.2 Population exposure

Table 4.7 gives the population frequency distribution for a limited number of exposure classes calculated at 1x1 km grid resolution, as well as the population-weighted concentration for individual countries and for Europe as a whole. Table 4.8 shows the evolution of the population exposure in the last seven years.

It has been estimated that in 2012 about 16 % of the European population lived in areas where the 36^{th} highest daily mean of PM_{10} exceeded the limit value of 50 µg.m^{-3}. This is 0.7 % more than in 2011, the same as in 2009, and less than in the years 2010 and 2005 – 2008. In Albania, Andorra, Bosnia & Herzegovina, Bulgaria, Cyprus, FYR of Macedonia, Montenegro, Poland and Serbia both the population-weighted indicator concentration and the median were above the LV, implying that in these countries the average concentration exceeded the LV and more than half of the population was exposed to concentrations exceeding the LV. Slovakia has a population-weighted concentration just above the LV, but its median dropped below the LV to 42 % of the population. In comparison with 2011, an increase of both population living above the LV and an increased population-weighted concentration occurs in many countries of south-eastern Europe (in Albania, Bosnia-Herzegovina, Bulgaria, Cyprus, Greece, Montenegro, FYR of Macedonia). A decrease of both exposure indicators is detected in Austria, Belgium, Croatia, Germany, Hungary, Italy, Slovakia and Slovenia.

In the EU-28, almost 15 % of the population lived in areas above the limit value. According to EEA (2014), in 2012 about 21 % of the urban population in the EU-28 was exposed to PM_{10} above the limit value. The difference between the two estimates is caused by the fact that the EEA estimated only for the urban population of the larger cities, while in Table 4.8 the total population of the EU-28, including inhabitants in rural areas, smaller cities and villages has been considered.

The European-wide population-weighted concentration of the 36^{th} highest daily mean is estimated for the year 2012 at 39.7 µg.m^{-3}, being the just slightly higher than in 2011 and lower than in the period of 2006 – 2010.

Table 4.7 Population exposure and population-weighted concentration – PM_{10}, 36th highest daily average value, year 2012. Resolution: 1x1 km.

Country		Population	PM_{10}, 36th highest d. a., exposed population [%]						Pop. weighted conc.
			< LV				> LV		
		[inhbs . 1000]	< 20 $\mu g.m^{-3}$	20 - 30 $\mu g.m^{-3}$	30 - 40 $\mu g.m^{-3}$	40 - 50 $\mu g.m^{-3}$	50 - 75 $\mu g.m^{-3}$	> 75 $\mu g.m^{-3}$	[$\mu g.m^{-3}$]
Albania	AL	2 865	0.0	4.5	10.4	18.5	64.6	2.0	56.1
Andorra	AD	78		3.2	3.7	4.7	8.9	79.5	75.2
Austria	AT	8 408	2.4	18.2	45.6	33.7	0.0		35.8
Belgium	BE	11 095		2.0	9.5	88.5			43.5
Bosnia & Herzegovina	BA	3 839	0.3	9.6	15.0	15.8	59.2	0.1	50.8
Bulgaria	BG	7 327	0.2	1.9	10.0	13.8	45.8	28.4	65.8
Croatia	HR	4 276	0.1	4.1	19.6	58.4	17.8		44.8
Cyprus	CY	862		0.1	2.1	16.5	81.3		60.2
Czech Republic	CZ	10 505	0.0	3.9	20.0	53.6	15.7	6.7	46.7
Denmark	DK	5 581	0.9	97.4	1.4	0.3			25.9
Estonia	EE	1 325	30.1	69.9					21.4
Finland	FI	5 401	90.3	9.7					18.1
France	FR	63 379	0.4	12.1	49.0	37.1	1.3	0.0	37.6
Germany	DE	80 328	0.1	23.8	74.6	1.5			32.6
Greece	GR	11 123	0.0	1.9	13.9	59.3	21.3	3.4	47.1
Hungary	HU	9 932		0.0	14.4	67.4	18.2		46.0
Iceland	IS	320	97.0	2.9	0.1				17.1
Ireland	IE	4 583	36.0	63.9	0.1				21.2
Italy	IT	59 394	0.3	8.4	30.3	26.5	29.6	5.0	47.2
Latvia	LV	2 045	4.0	29.1	65.0	1.9			33.0
Liechtenstein	LI	36	1.8	98.2					27.6
Lithuania	LT	3 004		14.8	81.9	3.3			33.1
Luxembourg	LU	525		27.9	72.1				30.0
Macedonia, FYR of	MK	2 060	0.1	3.1	9.1	7.1	17.8	62.8	78.3
Malta	MT	418			100.0				37.2
Monaco	MC	37			0.1	100			45.5
Montenegro	ME	621	3.1	15.9	7.1	6.7	66.3	0.9	53.5
Netherlands	NL	16 730		6.6	90.3	3			35.1
Norway	NO	4 986	43.1	37.7	19.2				21.6
Poland	PL	38 538		0.2	11.4	23.1	43.9	21.4	60.6
Portugal	PT	10 542	2.5	23.9	49.9	22.1	1.6		35.1
Romania	RO	20 096		1.2	18.2	44.9	33.6	2.2	48.8
San Marino	SM	32		4.6	8.1	87			43.8
Serbia (incl. Kosovo)	RS	9 015	0.0	1.6	6.2	17.9	60.1	14.2	62.1
Slovakia	SK	5 404		0.3	6.5	52.1	39.8	1.3	50.4
Slovenia	SI	2 055	0.1	6.1	22.7	51.6	19.6		43.5
Spain	ES	46 818	4.3	22.4	62.9	9.2	1.1	0.0	33.5
Sweden	SE	9 483	36.3	63.6	0.0				20.5
Switzerland	CH	7 955	2.3	19.2	76.0	1.7	0.9		32.6
United Kingdom	UK	63 495	3.4	49.1	47.6				28.8
Total		**534 518**	**3.3**	**18.6**	**41.3**	**20.4**	**13.0**	**3.4**	**39.7**
			83.5				**16.5**		
EU-28		**502 673**	**3.0**	**19.0**	**42.4**	**21.0**	**11.6**	**3.1**	**39.2**
			85.3				**14.7**		

Note1: Turkey is not included in the calculation due to lacking air quality data in rural areas.
Note2: The percentage value "0.0" indicates an exposed population exists, but is small and estimated less than 0.05 %. Empty cells mean: no population in exposure.

Like at previous years, for 2012 the comparison between the examined PM_{10} exceedances, i.e. the annual average of section 4.1.2 with the 36th highest daily average in this section, leads to the conclusion that the daily average limit value is more stringent of the two.

Table 4.8 Evolution of percentage population living in above limit value (left) and population-weighted concentration (right) in the years 2005-2012 – PM_{10}, 36^{th} highest daily average value. Resolution: 1x1 km.

Country		Population above LV 50 μg.m^{-3} [%]									Population-weighted conc. [μg.m^{-3}]								
		2005	2006	2007	2008	2009	2010	2011	2012	diff. '12 - '11	2005	2006	2007	2008	2009	2010	2011	2012	diff. '12 - '11
Albania	AL	68.7	70.6	74.5	76.6	62.4	78.4	21.2	66.6	45.4	59.8	54.0	53.3	55.7	51.3	69.5	42.8	56.1	13.3
Andorra	AD	0	0	0	0	0	0	0	88.4	88.4	31.1	35.7	32.1	29.3	29.4	28.5	29.2	75.2	46.0
Austria	AT	39.2	43.9	3.4	0	0	23.8	22.8	0	-22.7	45.7	47.1	39.9	36.9	36.7	42.8	38.7	35.8	-2.8
Belgium	BE	28.4	73.1	4.2	0	3.3	0	7.0	0	-7.0	46.9	51.3	43.5	38.4	45.8	42.7	45.1	43.5	-1.6
Bosnia-Herzegovina	BA	66.6	80.0	68.8	68.0	65.7	64.9	19.1	59.3	40.2	57.3	57.4	52.7	50.6	57.8	53.7	40.8	50.8	10.0
Bulgaria	BG	63.3	81.8	76.6	75.4	73.4	80.2	20.8	74.2	53.4	73.3	74.2	67.5	78.2	70.3	69.2	46.6	65.8	19.2
Croatia	HR	68.4	80.2	46.2	35.0	27.7	58.6	37.6	17.8	-19.8	57.6	53.7	49.6	48.6	46.9	50.5	46.6	44.8	-1.8
Cyprus	CY	80.9	81.5	91.8	98.3	80.6	99.0	12.9	81.3	68.4	63.7	58.2	54.4	130.7	68.6	74.5	46.2	60.2	14.0
Czech Republic	CZ	79.6	76.6	20.9	13.1	14.7	47.2	31.0	22.4	-8.6	60.2	57.5	46.2	42.5	43.6	53.7	46.2	46.7	0.6
Denmark	DK	0	0	0	0	0	0	0	0	0	34.5	37.0	32.5	29.0	26.0	25.5	31.6	25.9	-5.7
Estonia	EE	0	0	0	0	0	0	0	0	0	31.7	34.1	28.0	22.4	22.4	25.8	17.6	21.4	3.8
Finland	FI	0	0	0	0	0	0	0	0	0	24.2	29.5	23.9	21.9	19.4	22.7	16.9	18.1	1.2
France	FR	0.0	1.7	5.0	0.6	3.0	0	3.2	1.4	-1.9	29.8	32.9	41.0	36.3	39.2	37.1	36.6	37.6	1.0
Germany	DE	2.5	2.0	0	0	0	0.5	0.5	0	-0.5	38.6	41.3	35.7	31.7	34.4	37.2	35.7	32.6	-3.2
Greece	GR	71.0	78.6	79.5	84.9	38.2	95.7	7.5	24.8	17.3	59.9	54.3	53.0	64.9	54.7	64.8	37.6	47.1	9.5
Hungary	HU	94.6	96.9	44	35.4	24.4	69.4	92.1	18.2	-73.9	61.6	58.5	48.5	47.5	46.4	52.3	55.4	46.0	-9.4
Iceland	IS	0	0.1	0	0	0	0.0	0	0	0	19.0	27.2	21.4	25.4	15.8	16.8	15.8	17.1	1.2
Ireland	IE	0	0	0	0	0	0	0	0	0	17.8	24.1	24.8	25.8	21.7	23.2	23.2	21.2	-2.0
Italy	IT	70.5	58.4	63.3	46.2	31.9	31.2	39.5	34.6	-4.9	60.2	58.6	57.4	51.7	48.6	45.2	48.6	47.2	-1.4
Latvia	LV	0	0	0	0	0	0	0	0	0	35.9	40.0	31.9	32.7	33.4	37.8	26.7	33.0	6.4
Liechtenstein	LI	0	0	0	0	0	0	0	0	0	40.2	47.5	39.3	38.5	31.5	33.6	21.3	27.6	6.3
Lithuania	LT	0	0	0	0	0	0	0	0	0	37.7	39.7	33.2	29.5	32.7	39.5	26.6	33.1	6.4
Luxembourg	LU	0	0	0	0	0	0	0	0	0	31.2	35.9	32.5	29.1	34.3	31.9	29.4	30.0	0.6
Macedonia, FYR of	MK	74.2	74.5	78.3	73.8	80.3	87.7	3.5	80.7	77.1	77.5	69.9	57.8	71.5	75.6	80.1	37.9	78.3	40.4
Malta	MT	95.8	0	0	0	0	3.3	0	0	0	62.7	44.8	42.6	40.3	38.7	49.4	39.7	37.2	-2.5
Monaco	MC		100	0	0	0	0	0	0	0		59.7	46.2	46.0	41.5	36.1	37.0	45.5	8.5
Montenegro	ME	67.6	69.5	71.6	70.8	65.7	66.9	12.3	67.2	54.9	58.7	57.9	53.6	56.7	51.8	54.0	36.2	53.5	17.2
Netherlands	NL	26.2	3.9	0	0	0	0	0	0	0	47.5	46.1	41.9	37.7	39.0	40.2	44.0	35.1	-8.9
Norway	NO	0	0	0	0	0	0	0	0	0	29.3	31.9	26.3	26.1	24.0	25.7	16.3	21.6	5.3
Poland	PL	60.3	75.2	47.1	38.3	60.5	71.3	41.3	65.3	24.0	58.6	64.0	50.8	48.6	55.4	65.7	51.4	60.6	9.2
Portugal	PT	55.9	57.2	23.6	0	0	0.2	4.9	1.6	-3.3	52.0	48.3	45.0	35.5	38.5	35.6	35.4	35.1	-0.2
Romania	RO	85.5	91.2	73.0	53.5	39.8	28.2	43.3	35.7	-7.6	73.4	65.4	57.7	53.1	49.0	45.2	48.1	48.8	0.7
San Marino	SM	80.8	84.8	100	25.9	0	0	0	0	0	51.7	57.4	54.1	48.9	40.6	44.0	35.9	43.8	7.8
Serbia (incl. Kosovo)	RS	82.1	87.5	81.5	77.5	77.8	80.5	52.9	74.3	21.4	73.1	73.1	61.8	68.6	67.6	60.1	54.6	62.1	7.5
Slovakia	SK	86.9	83.8	43.7	38.2	33.5	82.3	62.4	41.1	-21.3	60.9	58.5	50.5	47.5	46.2	56.0	51.5	50.4	-1.1
Slovenia	SI	63.9	63.3	40	5.5	0	38.6	39.1	19.6	-19.5	53.7	49.2	46.1	42.7	41.9	47.2	48.1	43.5	-4.6
Spain	ES	48.6	55.6	40.5	12.5	1.0	0.1	1.1	1.1	0.0	46.7	49.3	46.9	40.1	38.0	33.4	30.5	33.5	3.0
Sweden	SE	0	0	0	0	0	0	0	0	0	28	32.0	25.8	26.4	23.3	22.1	21.1	20.5	-0.6
Switzerland	CH	3.3	8.3	2.5	1.9	0.9	0	1.3	0.9	-0.5	36.0	43.9	39.9	36.5	37.1	36.3	33.0	32.6	-0.4
United Kingdom	UK	0	0	0	0	0	0	0	0	0	33	35.5	34.7	32.1	30.1	28.8	30.3	28.8	-1.5
Total		**34.3**	**35.7**	**26.2**	**19.4**	**16.5**	**20.6**	**15.8**	**16.5**	**0.7**	**46.8**	**47.8**	**44.1**	**41.3**	**41.2**	**41.9**	**39.0**	**39.7**	**0.7**
EU-28		**33.1**	**34.5**	**24.7**	**17.3**	**14.6**	**18.8**	**15.4**	**14.7**	**-0.8**	**46.1**	**47.2**	**43.8**	**40.5**	**40.5**	**41.3**	**39.0**	**39.2**	**0.2**

4.2.3 Uncertainties

Uncertainty estimated by cross-validation

Cross-validation analysis determines the uncertainty. For the combined map of PM_{10} indicator 36^{th} highest daily mean in 2012, Table 4.6 shows an absolute mean uncertainty (expressed as the RMSE) of 7.7 μg.m^{-3} for rural areas and 11.9 μg.m^{-3} for urban areas. This indicates the best fit for rural areas compared to all its previous years and a better fit for urban areas compared to 2008 – 2011. The relative mean uncertainty (absolute RMSE relative to the mean indicator value) of the 2012 map of PM_{10} indicator 36^{th} highest daily mean is 24.5 % for both rural and urban areas. In urban areas, the higher uncertainty for 2008 – 2012, compared to its preceding years is caused specifically by Turkish urban background stations reported and used in the calculations as of 2008. (An interpolation result for Turkey is not presented in the map due to lack of population density data). Table 7.5 summarises both the absolute and relative uncertainties over the past eight years.

Figure 4.8 shows the cross-validation scatter plots for both rural and urban areas. The R^2 indicates that for rural areas about 64 % and for urban areas about 75 % of the variability is attributable to the interpolation. Corresponding values with those of the years 2011 – 2006 (see Table 7.5) do show that the fit of 2012 is for both rural and urban areas comparable to some of the other years.

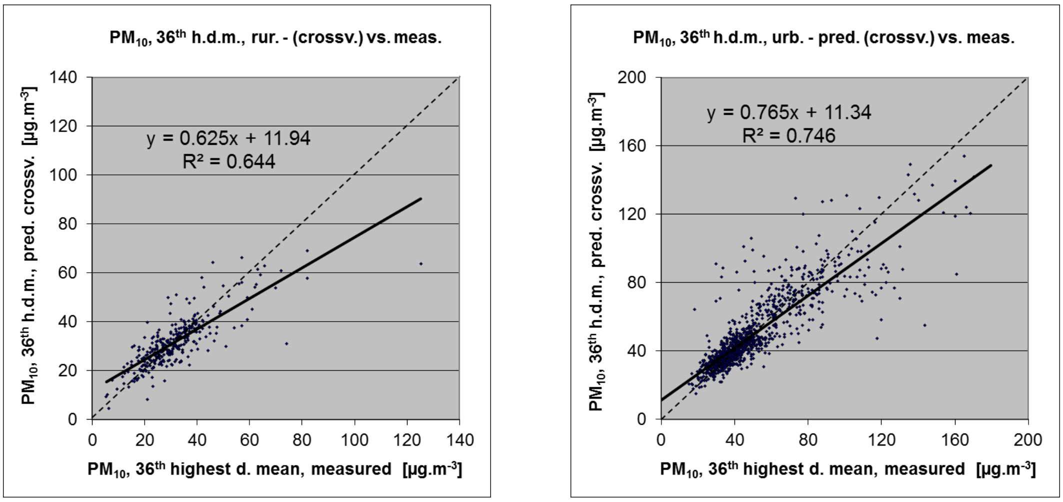

Figure 4.8 Correlation between cross-validation predicted values (y-axis) and measurements (x-axis) for the PM_{10} indicator 36^{th} highest daily mean for 2012 for rural (left) and urban (right) areas.

The scatter plots indicate that in areas with high concentrations the interpolation methods tend to underestimate the levels. For example, in urban areas (Figure 4.8, right panel) an observed value of 130 $\mu g.m^{-3}$ would be estimated in the interpolation as about 110 $\mu g.m^{-3}$, i.e. about 15 % too low. For rural areas, the underestimation is slightly stronger.

Comparison of point measurement values with the predicted grid value

In addition to the point observation – point prediction cross-validation, a simple comparison was made between the point observation values and interpolation predicted grid values. The comparison has been executed primarily for the separate rural and separate urban background maps at 10x10 km resolution. (This comparison result one can directly relate to the cross-validation results of Figure 4.8.)

Next to this, the comparison has been done also for the final combined maps at 1x1 km resolution and for the spatial aggregated final maps at 10x10 km resolution. Figure 4.9 shows the scatterplots for these comparisons.

The results of the point observation – point prediction cross-validation of Figure 4.8 and those of the point-grid validation for separate rural and separate urban background maps, and for the final combined maps at both resolutions are summarised in Table 4.9.

By the comparing the scatterplots and the statistical indicators for the separate rural and separate urban background map with the final combined maps in both resolutions, one can evaluate the level of representation of the rural resp. urban background areas in the final combined maps. The rural air quality is fairly well represented in both the 1x1 km and the aggregated 10x10 km final combined map. The urban air quality is quite well represented in the final combined 1x1 km map, but not in the aggregated final combined 10x10 km map as one can deduce from its higher RMSE, its bias being further from zero and its lower R^2. Therefore, we present in Figure A1.2 of Annex 1 the 1x1 km urban background map in addition to the 10x10 km final combined map of Figure 4.6.

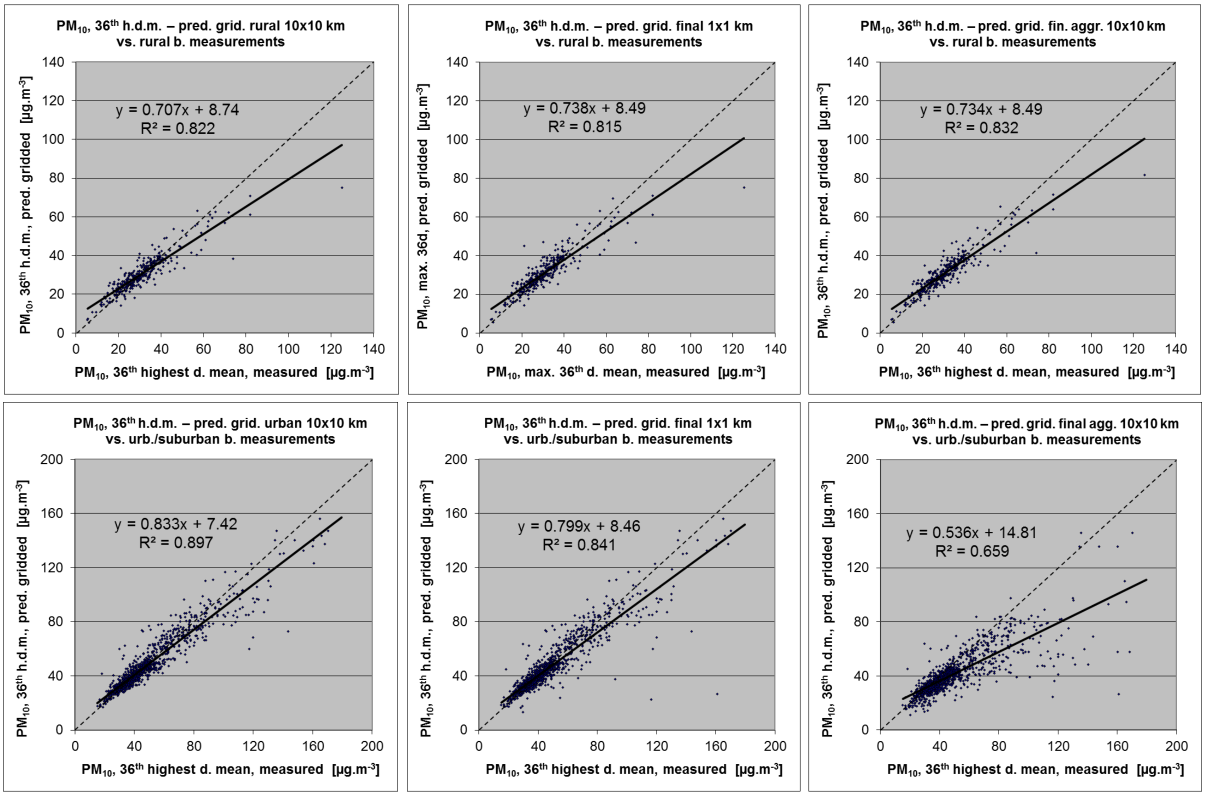

Figure 4.9 Correlation between predicted grid values from rural 10x10 km (upper left), urban 10x10 km (bottom left), final combined 1x1 km (upper and bottom middle) and final combined spatially aggregated 10x10 km (upper and bottom right) map (y-axis) versus measurements from rural (top), resp. urban/suburban (bottom) background stations (x-axis) for PM_{10} indicator 36^{th} highest daily mean 2012.

The comparison of the cross-validation with the gridded validation shows higher correlation of the gridded validation for both the rural and the urban background maps. That is because the simple grid validation shows the uncertainty at the actual measurement locations, while the point cross-validation prediction simulates the behaviour of the interpolation at points assuming no actual measurements would exist at these points. The uncertainty at measurement locations is caused partly by the smoothing effect of the interpolation and partly by the spatial averaging of the values in the 10x10 km grid cells. The level of smoothing, which leads to underestimation in areas with high values, is weaker in areas where measurements exist than in areas where a measurement point is not available. For example, in urban areas the predicted interpolation gridded value in the separate urban background map would be about 115 $\mu g.m^{-3}$ at a corresponding station point with a measurement value of 130 $\mu g.m^{-3}$. This is an underestimation of 11 %. It is less than the prediction underestimation of 15 % at the point locations without measuring stations (see the previous subsection).

Table 4.9 Statistical indicators RMSE, bias, coefficient of determination R^2 and linear regression equation from the scatter plots for the predicted point values based on cross-validation and the predicted grid values from separate (rural resp. urban) 10x10 km, final combined 1x1 km and final combined spatially aggregated 10x10 km map versus the measured point values for rural (left) and urban (right) background stations for PM_{10} indicator 36^{th} highest daily mean for 2012.

	rural backgr. stations				urb./suburban backgr. stations			
	RMSE	bias	R^2	equation	RMSE	bias	R^2	equation
cross-valid. prediction, separate (r or ub) map	7.7	0.1	0.644	y = 0.625x + 11.9	11.9	-0.1	0.746	y = 0.765x + 11.3
grid prediction, 10x10 km separate (r or ub) map	5.6	-0.4	0.822	y = 0.707x + 8.7	7.7	-0.6	0.897	y = 0.833x + 7.4
grid prediction, 1x1 km final merged map	5.6	0.3	0.815	y = 0.738x + 8.5	9.4	-1.2	0.841	y = 0.799x + 8.5
grid prediction, aggr. 10x10 km final merged map	5.4	0.2	0.832	y = 0.734x + 8.5	16.0	-7.5	0.659	y = 0.536x + 14.8

Probability of Limit Value exceedance

Again, we constructed the map with the probability of the limit value exceedance (PoE), using an aggregated 10x10 km gridded concentration map, the 10x10 km gridded uncertainty map and the limit value (LV, 50 $\mu g.m^{-3}$). Figure 4.10 presents the probability of exceedance 10x10 km gridded map classifying the areas with probability of LV exceedance below 25 % (little PoE) in green, between 25-50 % (modest PoE) in yellow, between 50-75 % (moderate PoE) in orange and above 75 % in red (large PoE). Section 4.1.3 explains in more detail the significance of the colour classes in the map.

Comparing the probabilities of exceedance (PoE) of 2011 (Horálek et al., 2014a) and 2010 (see Horálek et al, 2013) with those of 2012, one can conclude that a decrease in the spatial extents and PoE levels in south-eastern Europe continues to occur in 2012.

The Po Valley in northern Italy has quite a similar PoE pattern to 2010 and has slightly reduced PoE pattern compared to 2011. Throughout the years 2009 – 2012, areas with continued increased PoE levels do occur in southern Poland and north-eastern Czech Republic. However, their extent towards northern and southern direction (central Poland, Slovakia, and Hungary) reduced considerably compared to 2010 and 2011. Northern Serbia, eastern and southern Romania, and the centre of Bulgaria show throughout the years 2010 – 2012 areas with continued high PoE levels.

The areas of western Belgium and north-western France are back to green in 2012, like in 2010, with a temporal increased levels of PoE in 2011.The increased levels of PoE area around Almería, southern Spain, has extended in 2012 compared to the years 2009 – 2011.

It should be noted that the PoE is related to the aggregated 10x10 km grid. In case we would produce such map on a 1x1 km grid resolution the map pattern would demonstrate elevated PoE levels clearly distinguishing smaller cities and towns as well, which are not resolved at the 10x10 km grid resolution. Next to this – bearing in mind that the interpolated maps refer to the rural or (sub)urban background situations only, it cannot be excluded that exceedances of limit values may occur at the many *hotspot* and traffic locations throughout Europe, which are not resolved by this type of map.

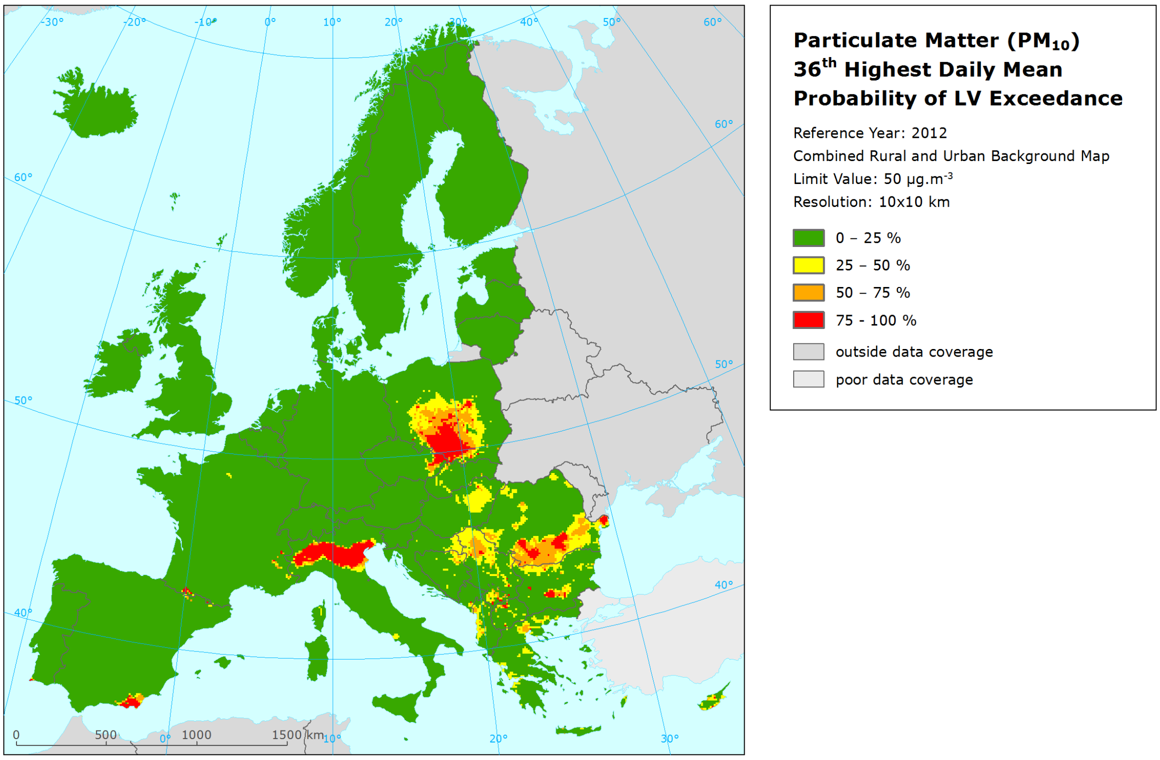

Figure 4.10 Map with the probability of the limit value exceedance for PM_{10} indicators 36^{th} highest daily mean ($\mu g.m^{-3}$) for 2012 on the European scale calculated on the 10 x 10 km grid resolution. Interpolation uncertainty is considered only, no other sources of uncertainty.

5 $PM_{2.5}$ maps

This chapter presents the health indicator $PM_{2.5}$ annual average, based on the mapping methodology developed in Denby et al. (2011b, 2011c). To increase the spatial coverage of measurements, pseudo $PM_{2.5}$ stations data were used in addition to quite limited number of stations with measured $PM_{2.5}$ data. The separate urban and rural concentration maps were calculated on a grid of 10x10 km resolution and the subsequent combined concentration map was based on the 1x1 km gridded population density map. Population exposure tables are calculated on a grid of 1x1 km resolution. All maps are presented in at 10x10 km resolution. The standard EEA ETRS89-LAEA5210 coordinate reference system was applied.

5.1 Annual average

5.1.1 Concentration map

Figure 5.1 presents the combined final map for the 2012 $PM_{2.5}$ annual average as the result of the interpolation and merging of the separate maps as described in detail in De Smet et al. (2011), using both measured $PM_{2.5}$ and pseudo $PM_{2.5}$ station data, as described in Denby (2011c). The red and purple areas and stations exceed the limit value (LV) of 25 $\mu g.m^{-3}$. Pseudo $PM_{2.5}$ stations data are estimated using PM_{10} measured data, surface solar radiation, latitude and longitude. (Instead of latitude and longitude, the coordinates of ETRS89-LAEA5210 projection could be used alternatively.)

Supplementary data in the regression used for rural areas consist of EMEP model output, altitude, wind speed, surface solar radiation and population density. Based on advice of Horálek et al. (2014a), we tested at the urban areas again the level of improvement in the interpolations in case we would include EMEP model output as supplementary data source. The relevant supplementary data for the estimation of both pseudo $PM_{2.5}$ station data and the linear regression submodel and its residual kriging in the rural areas were identified earlier in Denby et al. (2011b, 2011c). The supplementary data selection for the urban areas is discussed in further detail below at Table 5.2 of this section.

As one can observe in a few areas of the map, the high urban background measurement values do not seem to influence the interpolation results despite their clustering. The main reason is that the map presented here is an aggregation of 1x1 km grid values to a 10x10 km resolution and this aggregation smoothes out the elevated values one would more likely be able to distinguish in a higher resolution map, especially in the case of urban stations representing the urban background areas. Another less prominent reason is the smoothing effect kriging has in general. However in the case of clustering, kriging would not mask these elevations in the separate 1x1 km urban and rural maps.

Table 5.1 presents the regression coefficients determined for pseudo $PM_{2.5}$ stations data estimation, based on the stations with both $PM_{2.5}$ and PM_{10} measurements (see Section 2.1.1). The number of such type of stations is 507. The same supplementary data as in Denby (2011c) are used. Nevertheless, population was detected as statistically non-significant (like in 2010 and 2011).

Table 5.1 Parameters of the linear regression model (Eq. 2.1) and its statistics for generation of pseudo $PM_{2.5}$ stations data, without regard to the rural or urban/suburban type of the stations, for $PM_{2.5}$ 2012 annual average.

linear regr. model	**both rural and urban areas**
	parameter values
c (constant)	21.82
b (PM_{10} measured data, 2012 annual avg.)	0.704
a1 (population)	n. sign.
a2 (surface solar radiation 2012)	-0.944
a3 (latitude)	-0.267
a4 (longitude)	0.095
adjusted R^2	**0.89**
standard error [$\mu g.m^{-3}$]	**2.48**

The R^2 values show a weaker fit of the regression than observed in 2010 (0.95), but stronger than observed in the year 2008 (0.84) and similar as observed in the years 2011 and 2007 (0.89). No $PM_{2.5}$ map was produced for 2009, as we only started producing such map on a regular basis for the year 2010 and onward.

Table 5.2 presents the estimated parameters of the linear regression models (*c, a_1, a_2,...*) and of the residual kriging (*nugget, sill, range*) and includes the statistical indicators of both the regression and the kriging. The adjusted R^2 and standard error are indicators for the quality of the fit of the regression relation, where the adjusted R^2 should at the best be as close to 1 as possible and the standard error should be as small as possible. The adjusted R^2 is 0.57 for the rural areas. Such a fit is worse than for 2011 (0.60), while better than for other previous years, see Horálek et al. (2014a) and references cited therein. For urban areas, no supplementary data were used in the last years, see Denby et al. (2011c).

RMSE and bias are the cross-validation indicators, showing the quality of the resulting map; the bias indicates to what extent the estimation is un-biased. Only stations with measured (i.e. non-pseudo) $PM_{2.5}$ data are used for calculating RMSE and bias. Section 5.1.3 deals with a more detailed cross-validation analysis.

Like in the case of PM_{10}, the linear regression is applied on the logarithmically transformed data of both measured and modelled $PM_{2.5}$ values. Thus, in Table 5.2 the standard error and variogram parameters refer to these transformed data, whereas RMSE and bias refer to the interpolation after the back-transformation.

As mentioned above, at the urban areas we tested again the use of EMEP model output as supplementary data in order to explore its contribution to the interpolation performance. We tested with all the data of 2012 in logarithmically transformed format. The use of the linear regression model including EMEP modelling data followed by kriging of its residuals resulted in a RMSE of 3.26 (Table 5.2). This is again a better result than when excluding the EMEP modelling data from the linear regression model and kriging of its residuals (Table 5.2, last column) and confirms the findings in Horálek et al. (2014a). Therefore, we decided to use the regression model including the EMEP model output to derive the maps and exposure tables. When it proves in the next year that the inclusion of EMEP modelling output in the linear regression model leads systematically to better interpolation results, then we will implement the EMEP modelling data as a default supplementary data source in the routine mapping of the urban areas from then onward.

Table 5.2 Parameters of the linear regression models (Eq. 2.2) and of their residual ordinary kriging (OK) variograms (nugget, sill, range) – and their statistics – of $PM_{2.5}$ indicator annual average for 2012 in the rural (left) and urban (right) areas as used for the combined final map.

linear regr. model + OK on its residuals	**used in presented maps and exposure tables**		**testing purposes**
	rural areas	**urban areas incl. use of**	**urban areas excl. use**
	parameter values	**parameter values**	**parameter values**
c (constant)	1.31	1.28	1.3085
a1 (log. EMEP model 2012)	0.600	0.72	0.7206
a2 (altitude GTOPO)	-0.00036		
a3 (wind speed 2012)	-0.082		
a4 (s. solar radiation 2012)	n. sign.		
a4 (log. population density)	0.032		
adjusted R^2	**0.57**	**0.35**	0.32
standard error [μg.m^{-3}]	**0.30**	**0.34**	0.33
nugget	0.032	0.019	0.027
sill	0.084	0.091	0.123
range [km]	620	900	900
RMSE [μg.m^{-3}]	**2.99**	**3.26**	**3.45**
relative RMSE [%]	**24.9**	**18.7**	**19.8**
bias (MPE) [μg.m^{-3}]	**-0.37**	**0.09**	**0.07**

The merging of the separate rural and urban background maps takes place on the 1x1 km resolution map of population density.

According to Figure 5.1, the most polluted areas seem to be the Katowice (PL) and Ostrava (CZ) industrial region, together with the Po Valley in Northern Italy. Furthermore, the southern part of Romania with Bucharest as in it suffers from elevated $PM_{2.5}$ annual average concentrations and to a somewhat less extent the area around cities Belgrade and Novi Sad in Serbia.

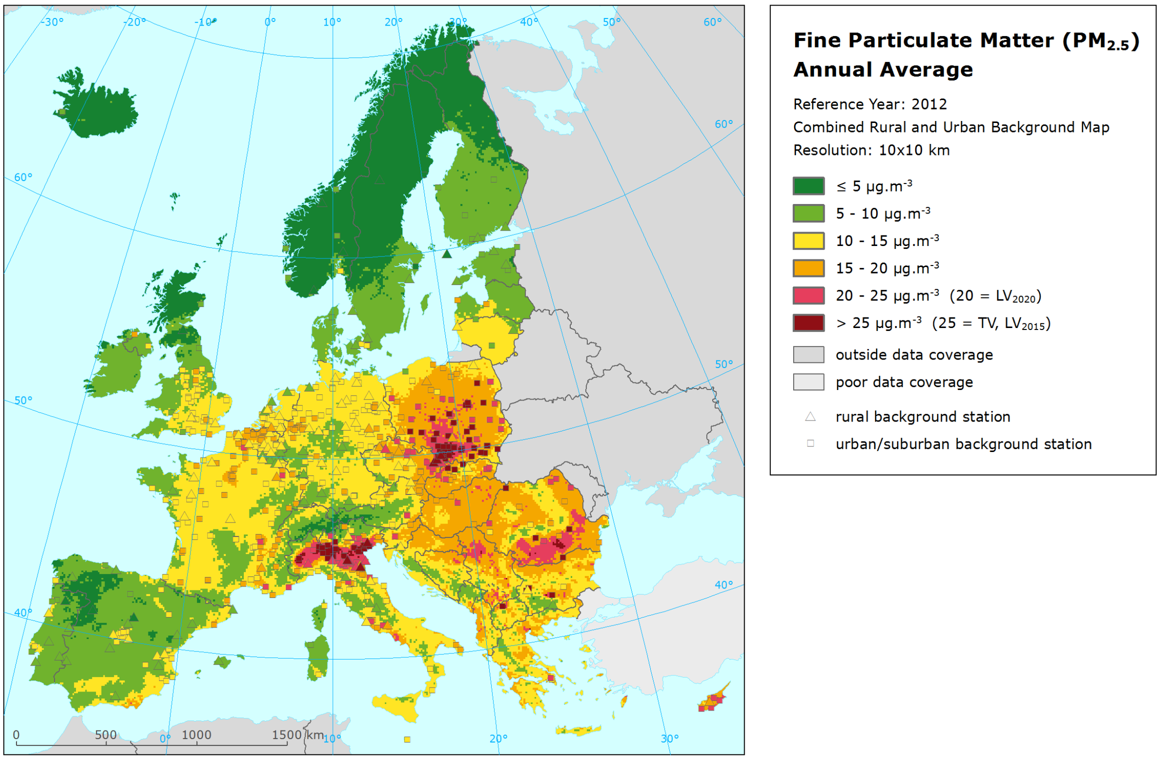

Figure 5.1 Combined rural and urban concentration map of $PM_{2.5}$ – annual average, year 2011. Spatial interpolated concentration field and the measured values in the measuring points. Units: µg.m^{-3}.

The concentration map presented in Figure 5.1 is spatially aggregated from 1x1 km to a 10x10 km grid resolution. As a result, the urban areas are not properly resolved in this map, due to the smoothing effect of this aggregation. Section 5.1.3 discusses the level of the representation of the urban areas in this final combined aggregated 10x10 km map. For better visualising the actual urban concentration levels at the actual urbanised areas, i.e. without the influence of the dominating pattern of extended rural areas, a separate 1x1 km urban background map is presented in Annex 1, Figure A1.3.

Figure 5.2 presents the inter-annual difference between 2012 and 2011 for annual average $PM_{2.5}$. Red areas show an increase of PM_{10} concentration, while blue areas show a decrease. The highest increases we see, like at PM_{10} annual average but somewhat less prominent, in the south-eastern part of Spain, the Pyrenees, the French Alps, the centre of Poland and the north-eastern part of Romania. Many areas in Europe demonstrate decreased concentrations in 2012 compared to 2011 (blue) versus an increase in 2011 compared to 2010, indicating a temporal elevation in 2011 of indicator concentrations. For example, the Po Valley and northern and central Italy, the region covering southern UK, Normandy and Bretagne, Belgium, The Netherlands, Germany, Denmark, South-West Sweden, and parts of Central Europe with Hungary in its centre.

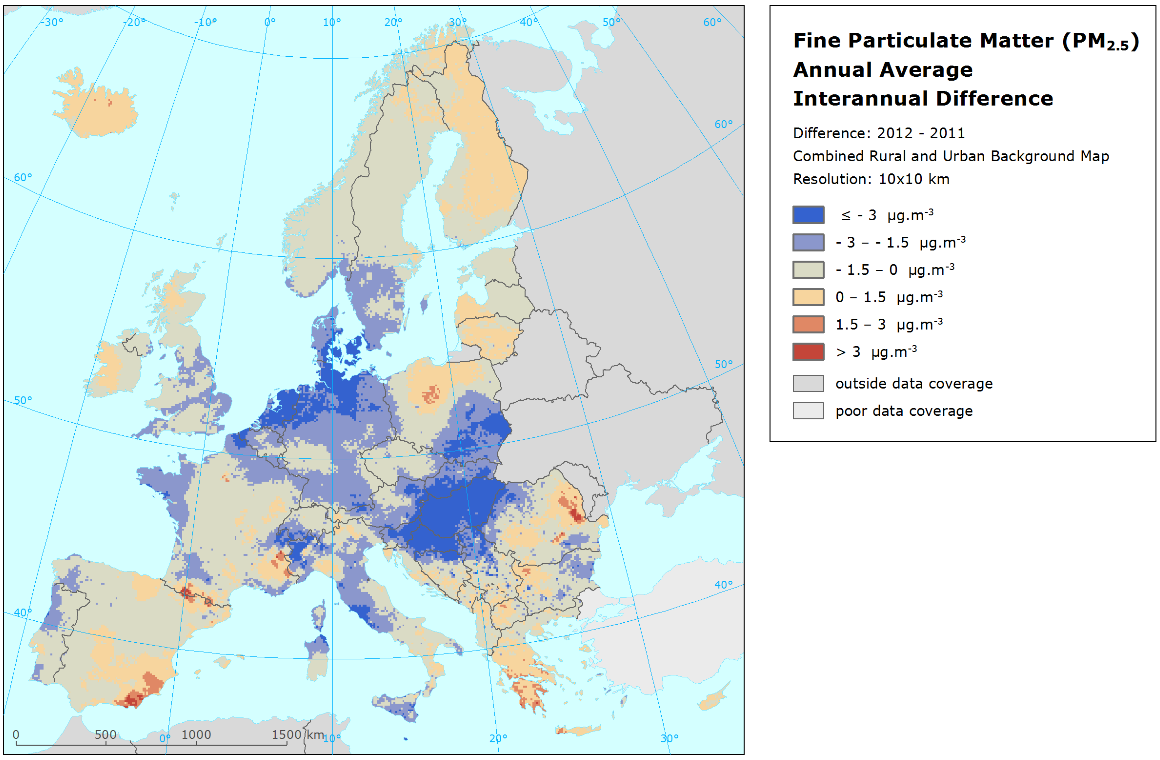

Figure 5.2 Inter-annual difference between mapped concentrations for 2012 and 2011 – $PM_{2.5}$, annual average. Units: µg.m^{-3}. Resolution: 10x10 km.

5.1.2 Population exposure

Table 5.3 gives the population frequency distribution for a limited number of exposure classes calculated on a grid of 1x1 km resolution, as well as the population-weighted concentration for individual countries and for Europe as a whole according to Equation 2.3.

In 2012, like in 2011, only 11 % of the European population has been exposed to $PM_{2.5}$ annual mean concentrations below 10 µg.m^{-3}, the WHO (World Health Organization) air quality guideline (WHO, 2005). Almost half of the population (47 %) lived in areas where the $PM_{2.5}$ annual mean concentration is estimated to be between 10 and 15 µg.m^{-3}, while almost a quarter of the population (24 %) lived in areas with $PM_{2.5}$ values between 15 and 25 µg.m^{-3}. About 18 % of the population lived in areas where the $PM_{2.5}$ annual mean exceeds the target value (TV). In Albania, Bulgaria, Cyprus, FYR of Macedonia, Poland and Serbia more than half of the population was exposure to levels above the target value. Of these countries the populated weighted concentration above the target value occurred at Cyprus and FYR of Macedonia, with Bulgaria, Poland and Serbia just below the target value. However, as the next section discusses, the current mapping methodology tends to underestimate high values. Therefore, the exceedance percentages and the number of countries with population exposed to concentrations above the target value will most likely be higher.

According to EEA (2014), about 11 % of the urban population in the EU-28 was exposed to $PM_{2.5}$ above the target value threshold in 2012. The difference with the estimated 8 % in Table 5.3 is caused by the different set of population taken into consideration. In the EEA estimate only the urban population in the larger cities is taken into account, while in Tables 5.3 and 5.4 it concerns the total population, including that of smaller cities, towns, villages and the rural areas.

Table 5.3 Population exposure and population-weighted concentration – $PM_{2.5}$, annual average, year 2012. Resolution: 1x1 km.

Country		Population	PM2.5 annual average, exposed population [%]						Population weighted conc.
			< LV2020				> LV2020		
			< TV					> TV	
			< 5	5 - 10	10 - 15	15 - 20	20 - 25	> 25	
		[inhbs . 1000]	µg.m-3	µg.m-3	µg.m-3	µg.m-3	µg.m-3	µg.m-3	[µg.m-3]
Albania	AL	2 865		0.9	14.3	22.8	33.5	28.5	21.1
Andorra	AD	78		10.3	8.6	81.1			15.9
Austria	AT	8 408	0.2	7.2	40.1	52.4	0.0		14.8
Belgium	BE	11 095		1.4	30.3	68.2			15.8
Bosnia & Herzegovina	BA	3 839		2.8	16.9	46.0	30.2	4.2	18.5
Bulgaria	BG	7 327	0.0	1.3	11.8	15.1	20.8	51.0	24.9
Croatia	HR	4 276		0.7	17.9	75.1	6.3		16.8
Cyprus	CY	862			0.7	13.6	12.9	72.8	25.0
Czech Republic	CZ	10 505		0.3	13.9	59.2	17.2	9.4	18.8
Denmark	DK	5 581	0.4	30.9	68.7				10.0
Estonia	EE	1 325	0.0	100.0					7.9
Finland	FI	5 401	1.4	98.6					7.1
France	FR	63 379	0.0	5.0	55.3	35.0	4.8		14.7
Germany	DE	80 328	0.0	3.3	80.3	16.4			13.3
Greece	GR	11 123		0.5	15.6	45.8	25.8	12.3	19.2
Hungary	HU	9 932			2.9	63.4	33.7	0.0	18.9
Iceland	IS	320	99.9	0.1					4.7
Ireland	IE	4 583	1.0	93.2	5.8				8.1
Italy	IT	59 394	0.0	2.8	29.2	29.2	19.3	19.5	18.9
Latvia	LV	2 045		24.1	49.7	26.2			12.4
Liechtenstein	LI	36	0.2	21.6	78.2				10.2
Lithuania	LT	3 004		1.7	97.5	0.9			12.9
Luxembourg	LU	525		7.9	92.1				12.6
Macedonia, FYR of	MK	2 060		1.4	11.0	8.3	9.8	69.5	29.2
Malta	MT	418			100.0				12.4
Monaco	MC	37			0.1	100			18.2
Montenegro	ME	621		10.9	15.4	23.9	48.2	1.5	18.7
Netherlands	NL	16 730		0.1	92.1	7.8			13.7
Norway	NO	4 986	33.6	45.6	20.7				7.2
Poland	PL	38 538		0.0	6.5	27.8	23.1	42.6	23.9
Portugal	PT	10 542	1.8	43.7	54.5				9.9
Romania	RO	20 096		0.1	6.3	46.0	28.7	18.9	20.8
San Marino	SM	32			12.7	87			16.7
Serbia (incl. Kosovo)	RS	9 015		0.4	4.4	21.9	24.9	48.3	24.3
Slovakia	SK	5 404		0.0	2.5	51.2	34.7	11.6	20.5
Slovenia	SI	2 055		0.2	13.3	68.8	17.6		17.7
Spain	ES	46 818	1.4	25.9	57.0	15.3	0.4		11.9
Sweden	SE	9 483	11.1	85.7	3.1				7.2
Switzerland	CH	7 955	0.4	11.1	86.0	1.6	0.9		12.6
United Kingdom	UK	63 495	0.9	12.2	86.9				11.9
Total		**534 518**	**0.8**	**10.3**	**47.2**	**23.7**	**9.1**	**9.0**	**15.6**
			11.1		**70.8**		**18.1**		
EU-28		**502 673**	**0.5**	**10.3**	**48.4**	**24.2**	**8.6**	**8.1**	**15.5**
			10.8		**72.5**		**16.7**		

Note1: Turkey is not included in the calculation due to lacking air quality data.
Note2: The percentage value "0.0" indicates an exposed population exists, but is small and estimated less than 0.05 %. Empty cells mean: no population in exposure.

The comparison of the $PM_{2.5}$ exposures of Table 5.3 with that of the PM_{10} exposure of Table 4.2 shows the $PM_{2.5}/PM_{10}$ ratio of population-weighted concentrations to be between 0.6 and 0.8, for most countries. The exceptions are Portugal, Spain, Andorra, Malta, Cyprus, Iceland, Norway and Sweden (between 0.45 and 0.6); a plausible cause for southern countries might be the influence of Saharan dust containing there a relative large fraction of coarse particles.

Considering the average for the whole of Europe, the overall population-weighted annual mean $PM_{2.5}$ concentration in 2012 was 15.6 µg.m^{-3}. This differs slightly from previous years as given in Table 5.4. This table shows the evolution of the population exposure for the years 2007 – 2012, except 2009 as for that year no $PM_{2.5}$ map has been produced. For all the years, the same mapping method has been used. The numbers for 2007 and 2008 were calculated while preparing the paper Denby et al. (2011c) and only for 2010 and onwards we started producing maps on a regular basis.

Table 5.4 Evolution of percentage population living in above target value (left) and population-weighted concentration (right) in the years 2007-2012 – $PM_{2.5}$, annual average. Resolution: 1x1 km.

Country		Population above TV 25 µg.m^{-3} [%]							Population-weighted conc. [µg.m^{-3}]						
		2007	2008	2009	2010	2011	2012	diff. '12 - '11	2007	2008	2009	2010	2011	2012	diff. '12 - '11
Albania	AL	1.6	1.6		53.4	1.6	28.5	26.9	20.8	19.6		25.1	17.2	21.1	3.9
Andorra	AD	0	0		0	0		0	11.5	11.3		12.4	13.7	15.9	2.1
Austria	AT	0	0		0	0		0	16.3	16.4		17.7	16.3	14.8	-1.5
Belgium	BE	0	0		0	0		0	16.6	17.1		18.8	17.3	15.8	-1.5
Bosnia-Herzegovina	BA	12.8	10.9		47.2	8.2	4.2	-4.0	21.7	20.3		22.2	17.2	18.5	1.3
Bulgaria	BG	68.8	68.4		60.9	8.4	51.0	42.5	28.8	28.4		24.5	18.3	24.9	6.6
Croatia	HR	0.2	0		1.0	2.2		-2.2	19.5	18.5		20.0	19.6	16.8	-2.8
Cyprus	CY	77.6	79.6		0	0.8	72.8	72.0	25.0	25.3		21.8	21.0	25.0	4.0
Czech Republic	CZ	8.0	8.3		15.7	10.2	9.4	-0.8	17.5	17.7		21.5	18.8	18.8	0.0
Denmark	DK	0	0		0	0		0	11.5	11.1		11.4	12.5	10.0	-2.6
Estonia	EE	0	0		0	0		0	8.8	8.9		8.9	8.0	7.9	-0.1
Finland	FI	0	0		0	0		0	7.7	7.4		7.8	7.4	7.1	-0.4
France	FR	0	0		0	0		0	14.9	14.7		16.2	15.3	14.7	-0.6
Germany	DE	0	0		0	0		0	14.0	14.1		16.3	14.8	13.3	-1.4
Greece	GR	18.5	18.4		6.3	7.0	12.3	5.3	22.0	21.7		20.0	16.8	19.2	2.4
Hungary	HU	0	0		6.7	22.2	0.0	-22.2	19.3	19.4		20.3	23.1	18.9	-4.2
Iceland	IS	0	0		0	0		0	7.1	7.1		6.9	4.6	4.7	0.1
Ireland	IE	0	0		0	0		0	8.5	9.6		10.3	7.9	8.1	0.2
Italy	IT	12.4	12.3		6.0	21.8	19.5	-2.3	19.0	19.1		17.5	19.8	18.9	-0.9
Latvia	LV	0	0	not	0	0		0	15.3	16.4	not	14.7	11.1	12.4	1.2
Liechtenstein	LI	0	0	mapped	0	0		0	15.5	15.5	mapped	15.3	8.5	10.2	1.7
Lithuania	LT	0	0		0	0		0	13.8	15.5		15.6	12.7	12.9	0.2
Luxembourg	LU	0	0		0	0		0	13.9	14.5		15.8	13.3	12.6	-0.7
Macedonia, FYR of	MK	61.5	61.0		73.8	2.8	69.5	66.7	24.4	23.6		27.5	15.8	29.2	13.4
Malta	MT	0	0		0	0		0	14.9	14.9		13.8	15.6	12.4	-3.2
Monaco	MC	0	0		0	0		0	16.5	16.5		14.9	16.4	18.2	1.8
Montenegro	ME	12.6	12.6		64.6	4.9	1.5	-3.3	21.4	19.9		24.6	15.1	18.7	3.6
Netherlands	NL	0	0		0	0		0	16.9	17.0		17.6	17.1	13.7	-3.4
Norway	NO	0	0		0	0		0	8.6	8.2		8.8	6.3	7.2	0.9
Poland	PL	20.6	21.0		53.1	24.4	42.6	18.1	20.8	21.1		26.4	21.8	23.9	2.1
Portugal	PT	0	0		0	0		0	11.5	10.9		10.5	10.5	9.9	-0.6
Romania	RO	28.5	27.7		7.8	14.0	18.9	4.8	22.4	21.8		17.0	20.5	20.8	0.3
San Marino	SM	0	0		0	0		0	18.2	18.2		16.3	14.7	16.7	2.0
Serbia (incl. Kosovo)	RS	69.4	64.7		30.6	18.3	48.3	30.0	26.6	25.4		22.7	21.2	24.3	3.1
Slovakia	SK	12.4	11.5		14.3	5.4	11.6	6.2	20.2	20.6		21.3	21.8	20.5	-1.3
Slovenia	SI	0	0		0	0		0	18.5	18.0		19.0	19.4	17.7	-1.7
Spain	ES	0	0		0	0		0	14.1	13.6		11.8	11.1	11.9	0.8
Sweden	SE	0	0		0	0		0	9.2	8.8		8.1	8.1	7.2	-0.9
Switzerland	CH	0	0		0	0		0	14.9	14.8		15.5	12.6	12.6	0.0
United Kingdom	UK	0	0		0	0		0	12.2	12.5		13.0	12.4	11.9	-0.4
Total		**7.8**	**7.6**		**8.3**	**6.2**	**9.0**	**2.7**	**16.3**	**16.3**		**16.8**	**15.9**	**15.6**	**-0.2**
EU-28		**6.4**	**6.3**		**7.1**	**6.2**	**6.2**	**0.0**	**16.1**	**16.1**		**16.7**	**15.9**	**15.5**	**-0.4**

In comparison with the year 2011, an increase of both the population exposed to levels above the TV and the population-weighted concentration in 2012 can be observed at Poland and the south-eastern part of Europe consisting of the countries Albania, Bulgaria, Cyprus, Greece, FYR of Macedonia, Romania and Serbia, while decreases for both are observed at Croatia, Hungary and Italy.

The increase in south-eastern Europe one can also observe in Figure 5.2. However, the results for this area, specifically the West-Balkan countries, are strongly influenced by the limited number of measurement stations.

5.1.3 Uncertainties

Uncertainty estimated by cross-validation

Using RMSE as the most common indicator, the *absolute mean uncertainty* of the combined final map at areas 'in between' the station measurements can be expressed in $\mu g.m^{-3}$. Table 5.2 shows that the absolute mean uncertainty of the combined final map of $PM_{2.5}$ annual average expressed as RMSE is 3.0 $\mu g.m^{-3}$ for the rural areas and 3.3 $\mu g.m^{-3}$ for the urban areas. Alternatively, one can express this uncertainty in relative terms by relating the absolute RMSE uncertainty to the mean air pollution indicator value for all stations. This *relative mean uncertainty* of the combined final map of PM_{10} annual average is 24.9 % for rural areas and 18.7 % for urban areas. These relative uncertainty values fulfil the data quality objectives for models as set in Annex I of the air quality Directive 2008/50/EC (EC, 2008). Table 7.6 summarises both the absolute and relative uncertainties of different years.

Figure 5.3 shows the cross-validation scatter plots, obtained according to Section 2.3, for both the rural and urban areas. The R^2 indicates that for the rural areas about 78 % and for the urban areas about 78 % of the variability is attributable to the interpolation.

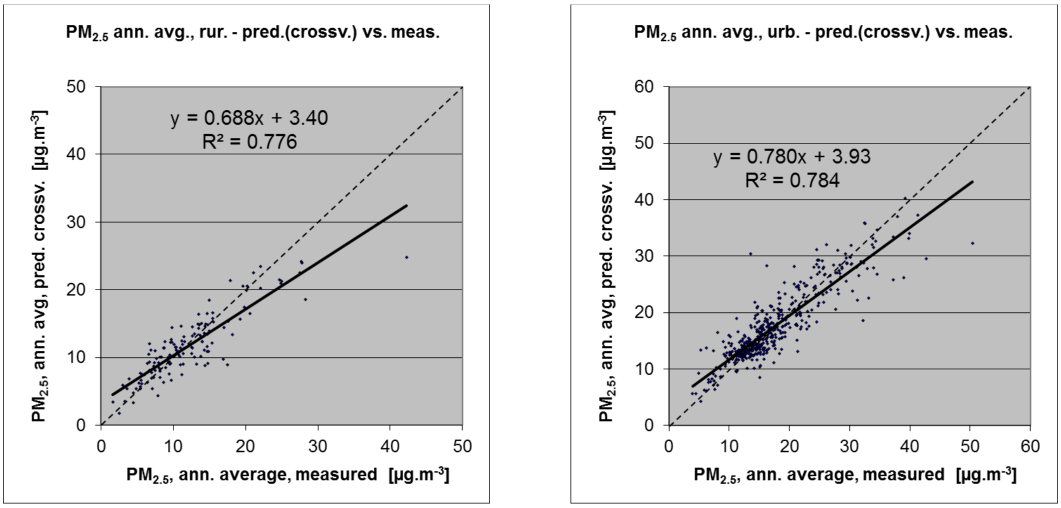

Figure 5.3 Correlation between cross-validation predicted values (y-axis) and measurements (x-axis) for the $PM_{2.5}$ annual average for 2012 for rural (left) and urban (right) areas. R^2 and the slope a (from the linear regression equation $y = a \cdot x + c$) should be as close 1 as possible, the intercept c should be as close 0 as possible

The scatter plots indicate that in areas with high concentrations the interpolation methods tend to underestimate the levels. For example, in urban areas an observed value of 30 $\mu g.m^{-3}$ is estimated in the interpolations to be about 27 $\mu g.m^{-3}$, about 9 % too low. This underestimation at high values is an inherent feature of all spatial interpolations. It can be reduced by either using a higher number of the stations at improved spatial distribution, or introducing a closer regression by using other supplementary data.

Comparison of point measurement values with the predicted grid value

In addition to the above point observation – point prediction cross-validation, a simple comparison has been made between the point observation values and interpolated prediction values spatially averaged in grid cells. This point-grid comparison indicates to what extent the predicted value of a grid cell represents the corresponding measured values at stations located in that cell.

The comparison has been executed primarily for the separate rural and separate urban background map at 10x10 km resolution. (One can directly relate this comparison result to the cross-validation results of Figure 5.3.)
Next to this, the comparison has been done also for the final combined maps at 1x1 km resolution and for the spatial aggregated final maps at 10x10 km resolution. Figure 5.4 shows the scatterplots for these comparisons.

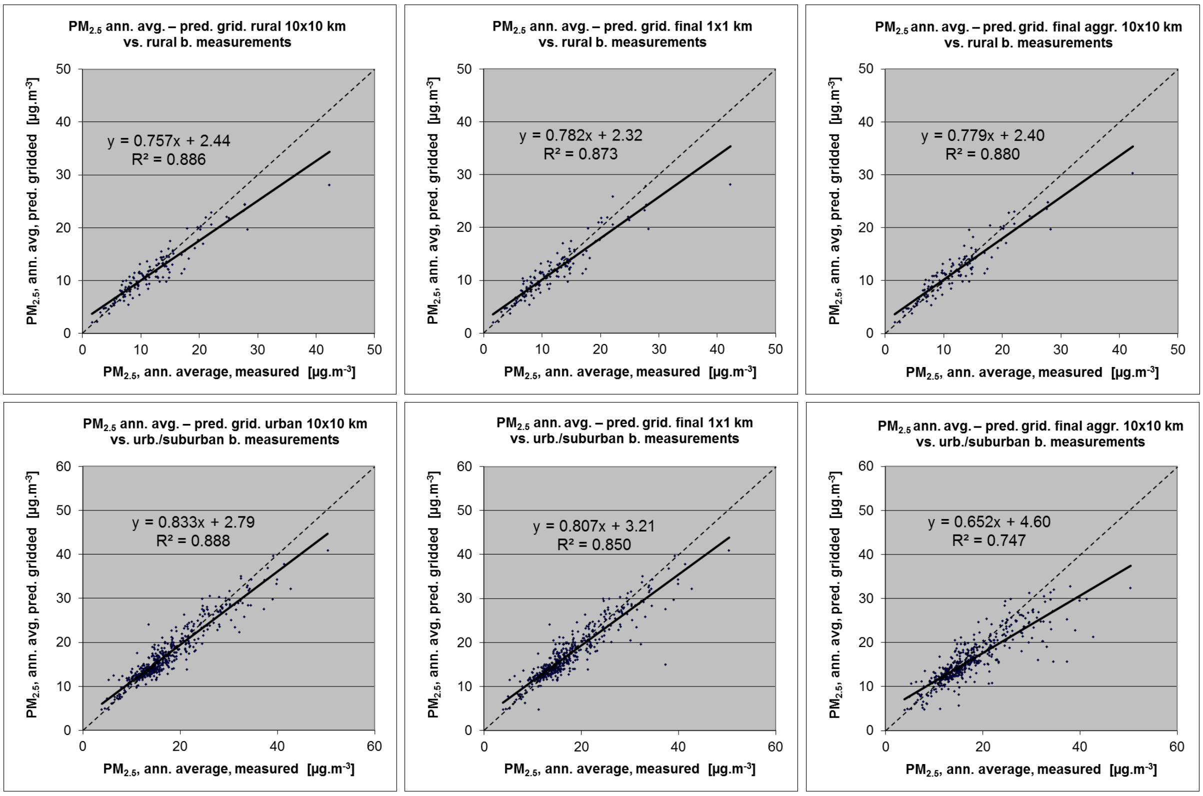

Figure 5.4 Correlation between predicted grid values from rural 10x10 km (upper left), urban 10x10 km (bottom left), final combined 1x1 km (upper and bottom middle) and final combined spatially aggregated 10x10 km (upper and bottom right) map (y-axis) versus measurements from rural (top), resp. urban/suburban (bottom) background stations (x-axis) for $PM_{2.5}$ annual average 2012.

The results of the point observation – point prediction cross-validation of Figure 5.3 and those of the point-grid validation for separate rural and separate urban background maps, and for the final combined maps at both resolutions are summarised in Table 5.4.

By the comparing the scatterplots and the statistical indicators for the separate rural and separate urban background map with the final combined maps in both resolutions, one can evaluate the level of representation of the rural resp. urban background areas in the final combined maps. The rural air quality is fairly well represented in both the 1x1 km and the aggregated 10x10 km final combined map. The urban air quality is quite well represented in the final combined 1x1 km map, but not in the aggregated final combined 10x10 km map as can be deduced from the higher RMSE, the bias being further from zero and the lower R^2. Therefore, we present in Figure A1.3 of Annex 1 the 1x1 km urban background map in addition to the 10x10 km final combined map of Figure 5.1.

Table 5.4 shows a better correlated relation between station measurements and the interpolated values of the corresponding grid cells (i.e. lower RMSE, higher R^2, smaller intercept and slope closer to 1) at both rural and urban background map areas than it does at the point cross-validation predictions. That is because the simple comparison between point measurements and the gridded interpolated values shows the uncertainty at the actual station locations (points), while the point cross-validation prediction simulates the behaviour of the interpolation at point positions assuming no actual measurements would exist at these points within the area covered by measurements. The uncertainty at measurement locations is caused partly by the smoothing effect of the interpolation and partly by the spatial averaging of the values in the 10x10 km grid cells. The level of smoothing, which leads to underestimation in areas with high values, is weaker in areas where measurements exist than in areas where a measurement point is not available. For example, in urban areas the predicted interpolation gridded value in the separate urban background map will be about 22 $\mu g.m^{-3}$ at the corresponding station point with the measured value of 28 $\mu g.m^{-3}$. %. It is less than the prediction underestimation of 9 % at the same point location, when leaving out this one actual measurement point and one does the interpolation without the station. (see the previous subsection).

Table 5.4 Statistical indicators RMSE, bias, coefficient of determination R^2 and linear regression equation from the scatter plots for the predicted point values based on cross-validation and the predicted grid values from separate (rural resp. urban) 10x10 km, final combined 1x1 km and final combined spatially aggregated 10x10 km map versus the measured point values for rural (left) and urban (right) background stations for $PM_{2.5}$ annual average of 2012.

	rural backgr. stations				urb./suburban backgr. stations			
	RMSE	bias	R^2	equation	RMSE	bias	R^2	equation
cross-valid. prediction, separate (r or ub) map	3.0	-0.4	0.776	y = 0.688x + 3.40	3.3	0.1	0.784	y = 0.780x + 3.93
grid prediction, 10x10 km separate (r or ub) map	2.3	-0.5	0.886	y = 0.757x + 2.44	2.4	-0.1	0.888	y = 0.833x + 2.79
grid prediction, 1x1 km final merged map	2.3	-0.3	0.873	y = 0.782x + 2.32	2.7	-0.1	0.850	y = 0.807x + 3.21
grid prediction, aggr. 10x10 km final merged map	2.2	-0.3	0.880	y = 0.779x + 2.40	3.9	-1.4	0.747	y = 0.652x + 4.60

Probability of Target Value exceedance

The probability of target value exceedance map was created for the $PM_{2.5}$ indicator in similar fashion as the PoE maps for PM_{10} indicators. This map at 10x10 km resolution is presented in Figure 5.4, with the Target Value (TV) of 25 $\mu g.m^{-3}$.

The areas with the highest probability of TV exceedance include the Po Valley in northern Italy with Turin and Milan, the region of southern Poland – north-eastern Czech Republic with the industrial zones of Krakow, Katowice and Ostrava, and the cities in the central part of Poland. Next to this, increased PoE do occur in south-eastern Europe at the larger cities of FYR of Macedonia, Serbia and in Romania, where only a rather limited set of measurement stations is located. They occur mostly in some urban areas or larger agglomerations such as Bucharest and Craiova with their rather high traffic density and heavy industry. In the other parts of Europe, there exists little to no likelihood of exceedance.

In comparison with 2011, a reduced area in the Po Valley with increased levels of PoE does occur. Furthermore, a reduction in areas with more elevated PoE is visible in larger areas and some agglomerations of Hungary, Serbia and Bulgaria (i.e. shifts from orange/yellow to green). In Bulgaria only limited reduction do occur.

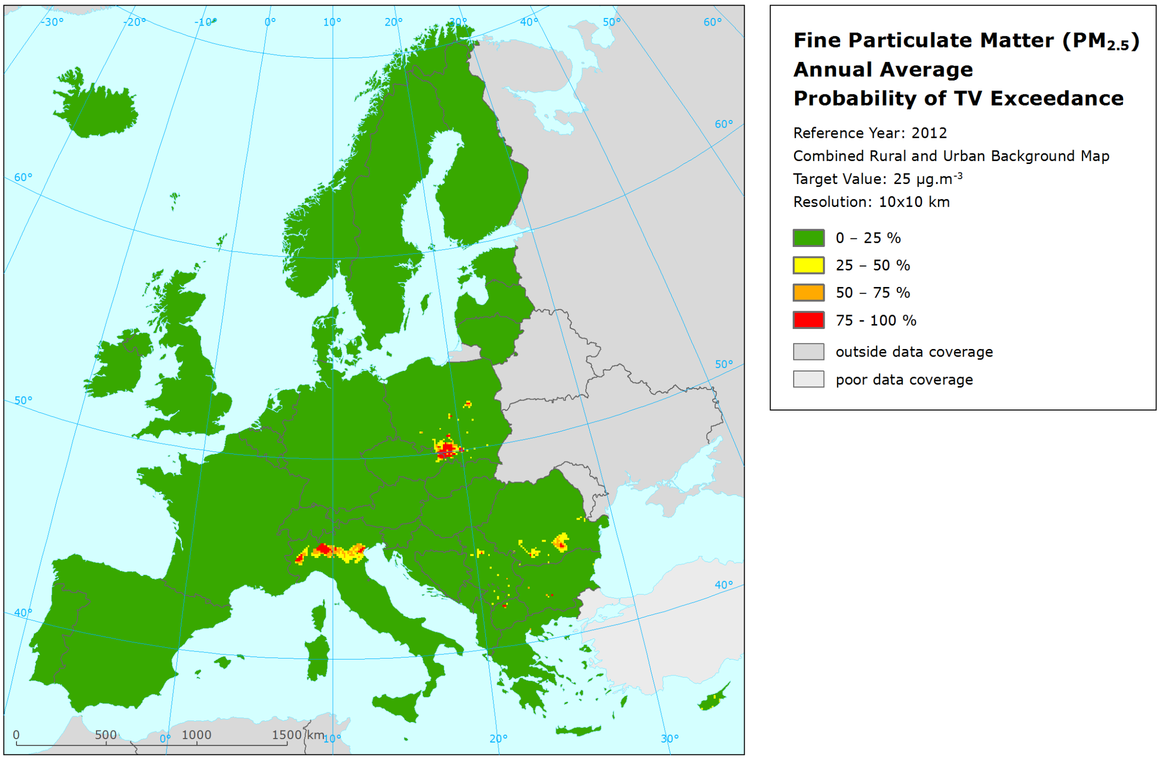

Figure 5.5 Map with the probability of the limit value exceedance for $PM_{2.5}$ annual average ($\mu g.m^{-3}$) for 2012 on European scale calculated on the 10 x 10 km grid resolution. Interpolation uncertainty is considered only.

It should be noted that the PoE is related to the aggregated 10x10 km grid. In case we would produce such map on a 1x1 km grid resolution the map pattern would demonstrate elevated PoE levels clearly distinguishing smaller cities and towns as well, which are not resolved at the 10x10 km grid resolution. Furthermore, one should bear in mind that the map is based on rural and (sub)urban *background* station data only. As such the map reflects rural and urban background situations only. Therefore, this type of map will not resolve the exceedances of limit values that may occur at the many *hotspot* and traffic locations throughout Europe.

6 Ozone maps

For ozone, the two health-related indicators (26th highest daily maximum 8-hour running mean and SOMO35) and the two vegetation-related indicators (AOT40 for crops and AOT40 for forests) are considered.

The separate urban and rural health-related indicator fields are calculated at a resolution of 10x10 km. The final health-related indicator maps are then created by combining rural and urban areas based on the 1x1 km resolution gridded population density map, as described in Chapter 2. We present the maps on a 10x10 km grid resolution.

The vegetation-related indicator maps are calculated and presented for rural areas only (assuming urban areas do not cover vegetation) and on a grid of 2x2 km resolution, covering the same mapping domain as at the human health indicators. This resolution serves the needs of the EEA Core Set Indicator 005 on ecosystem exposure to ozone. Map projection is the standard EEA ETRS89-LAEA5210.

6.1 26th highest daily maximum 8-hour average

6.1.1 Concentration map

Figure 6.1 presents the combined final map for 26th highest daily maximum 8-hour average as a result of combining the separate rural and urban interpolated map following the procedures as described in more detail in De Smet et al. (2011) and Horálek et al. (2007). Both separate maps were created by combining the measured ozone concentrations with supplementary data in a linear regression model, followed by kriging of its residuals. The supplementary data used in the regression model are EMEP model output, altitude and surface solar radiation for rural areas and EMEP model output, wind speed and surface solar radiation for urban areas, respectively.

Table 6.1 presents the estimated parameters of the linear regression models and of the residual kriging, including the statistical indicators of both the regression and the kriging.

Table 6.1 Parameters of the linear regression models (Eq. 2.2) and of the ordinary kriging (OK) variograms (nugget, sill, range) – and their statistics – of ozone indicator 26th highest daily maximum 8-hour mean for 2012 in the rural (left) and urban (right) areas as used for the combined final map.

linear regr. model + OK on its residuals	**rural areas parameter values**	**urban areas parameter values**
c (constant)	-9.7	12.8
a1 (EMEP model 2012)	1.00	0.89
a2 (altitude GTOPO)	0.0050	
a3 (wind speed 2012)		-2.62
a4 (s. solar radiation 2012)	0.93	0.39
adjusted R^2	**0.65**	**0.59**
standard error [μg.m^{-3}]	**9.25**	**10.55**
nugget	30	53
sill	74	82
range [km]	100	360
RMSE [μg.m^{-3}]	**8.49**	**9.06**
realtive RMSE [%]	**7.4**	**8.3**
bias (MPE) [μg.m^{-3}]	**0.18**	**-0.07**

The fit of the 2012 regression relationship, expressed as the adjusted R^2, is 0.65 for rural areas and 0.51 for urban areas. These values are better than in all the previous years, see Horálek et el. (2014a) and references cited therein. The numbers show that over the years the fit of the regressions are reasonably of the same order of magnitude at both the rural and the urban areas. RMSE and bias are the cross-validation indicators, showing the quality of the resulting map. Section 5.1.3 discusses in more detail the RMSE analysis and comparison with results of 2005 – 2011.

In the combined final map of Figure 6.1 the red and purple areas and stations do exceed the target value (TV) of 120 $\mu g.m^{-3}$. Note that in Directive 2008/50/EC the target value is defined as 120 $\mu g/m^3$ not to be exceeded on more than 25 days per calendar year *averaged over three years*.

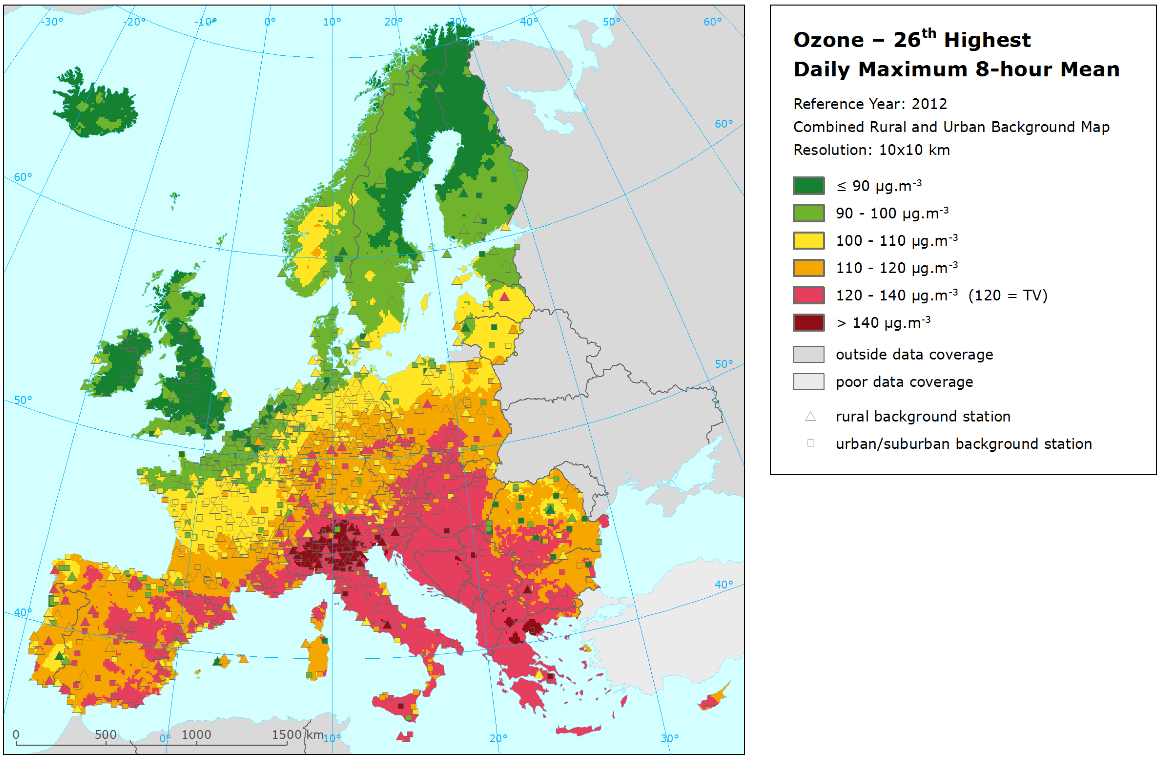

Figure 6.1 Combined rural and urban concentration map of ozone health indicator 26th highest daily maximum 8-hour value in $\mu g.m^{-3}$ for the year 2012. Its target value is 120 $\mu g.m^{-3}$. Resolution: 10x10 km.

As one can observe in a few areas of the map, the high measurement values do not seem to influence the interpolation results despite their clustering. The main reasons are (i) that the map presented here is an aggregation of 1x1 km values into a 10x10 km resolution and this aggregation smooths out the elevated values, and (ii) the smoothing effect kriging has in general.

The concentration map presented in Figure 6.1 is spatially aggregated from 1x1 km to a 10x10 km grid resolution. As a result the urban areas are not properly resolved in this map, due to the smoothing effect of this aggregation. Section 6.1.3 discusses the level of the representation of the urban areas in this final combined aggregated 10x10 km map. For better visualising the actual urban concentration levels at the actual urbanised areas, i.e. without the influence of the dominating pattern of extended rural areas, a separate 1x1 km urban background map is presented in Annex 1, Figure A1.4.

Figure 6.2 presents the inter-annual difference between 2012 and 2011 for 26th highest daily maximum 8-hour value. Red areas show an increase of ozone concentration, while blue areas show a decrease. The highest increases can be seen in northern and central Italy, and in south-eastern Europe, especially in Romania, Bulgaria, the Balkan countries and northern Greece. For most of these areas it is the second consecutive year with increases in concentrations. Somewhat less extended increases do occur at southern Italy, Hungary, Slovakia, eastern part of Poland, Lithuania, Latvia, the Iberian Peninsula, and Ireland. Considerable decreases are visible in most of France, and less prominent in South-East UK, the Benelux, Germany, north-western part of Poland, central and eastern Sweden and parts of Finland, of which for most of these areas the '2011 - 2010' difference map showed the opposite effect.

In general, we can observe a decrease of concentrations in the North-West of Europe and a increase the South-East. The reason lies probably in the meteorological conditions as we discovered a similar behaviour of inter-annual difference for the temperature.

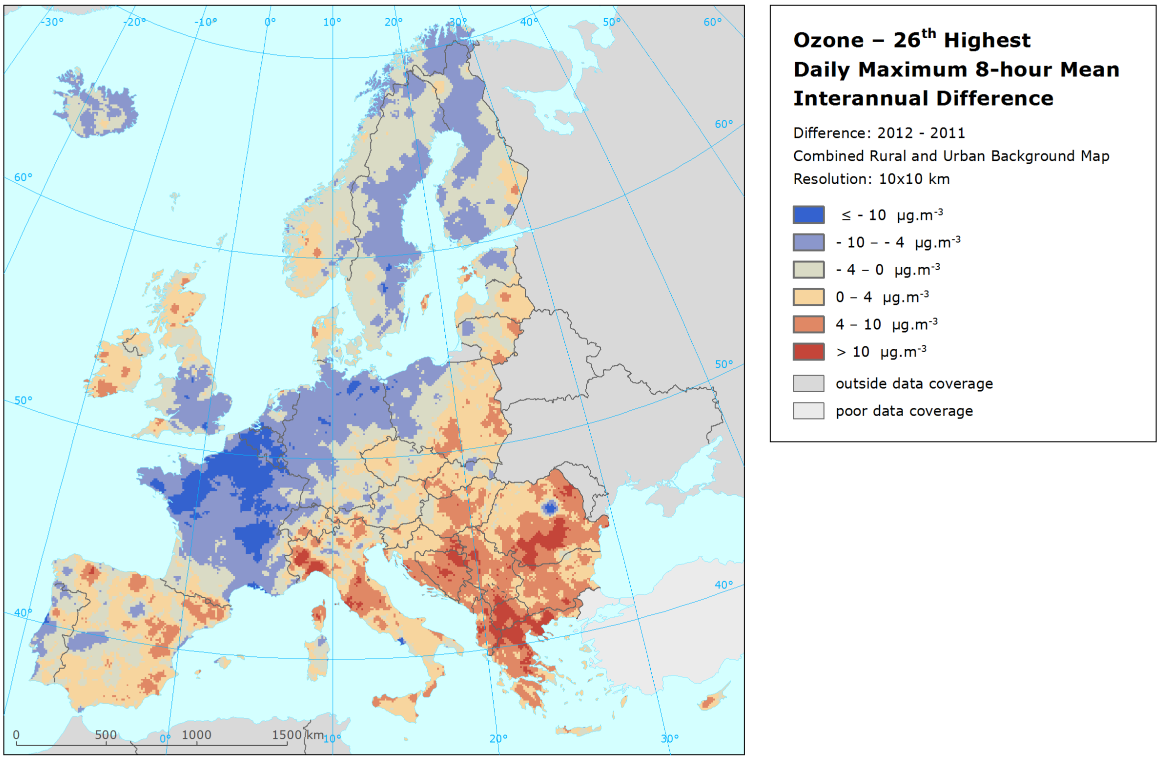

Figure 6.2 Inter-annual difference between mapped concentrations for 2012 and 2011 – ozone, 26th highest daily maximum 8-hour value. Units: µg.m^{-3}.

6.1.2 Population exposure

Table 6.2 gives, for 26th highest daily maximum 8-hour running mean, the population frequency distribution for a limited number of exposure classes, as well as the population-weighted concentration for individual countries and for Europe as a whole. In Table 6.3 the evolution of population exposure of the last eight years is presented.

It has been estimated that in 2012 some 20.7 % of the European population lived in areas where the ozone concentration exceeded the target value (TV of 120 µg.m^{-3}) of the 26th highest daily maximum 8-hour mean. This is about 4 – 5 percent point higher than in its four previous years (Table 6.3). Similar to previous years there are no exceedances in 2012 in Belgium, the Netherlands, Scandinavia and the Baltic countries, the UK, Ireland and Iceland.

Table 6.2 Population exposure and population weighted concentration – ozone, 26th highest daily maximum 8-hour mean for the year 2012.

Country		Population	Ozone, 26th highest dmax. 8-h, exposed population [%]						Population-weighted conc.
			< TV				> TV		
		[inhbs . 1000]	< 90 μg.m^{-3}	90 - 100 μg.m^{-3}	100 - 110 μg.m^{-3}	110 - 120 μg.m^{-3}	120 - 140 μg.m^{-3}	> 140 μg.m^{-3}	[μg.m^{-3}]
Albania	AL	2 865					100		133.4
Andorra	AD	78					100		122.2
Austria	AT	8 408			7.7	47.3	45.1	0.0	118.5
Belgium	BE	11 095	11.3	85.1	3.6				94.1
Bosnia & Herzegovina	BA	3 839				23.2	76.0	0.9	125.1
Bulgaria	BG	7 327		2.6	11.7	59.8	25.9		115.6
Croatia	HR	4 276				16.8	82.6	0.6	125.0
Cyprus	CY	862			9.4	74.3	16.3		115.5
Czech Republic	CZ	10 505			7.9	70.5	21.5		116.5
Denmark	DK	5 581	3.0	91.4	5.6	0.0			95.1
Estonia	EE	1 325	11.1	84.8	4.0				92.9
Finland	FI	5 401	70.9	28.6	0.4				88.4
France	FR	63 379	0.5	39.9	33.7	20.0	5.9	0.0	104.4
Germany	DE	80 328	0.1	24.7	37.0	37.7	0.4		106.7
Greece	GR	11 123				4.8	83.6	11.7	131.1
Hungary	HU	9 932		0.3	9.2	21.3	69.2		121.4
Iceland	IS	320	99.96	0.0					80.7
Ireland	IE	4 583	89.4	10.6					86.6
Italy	IT	59 394		0.5	1.5	21.0	50.6	26.4	129.9
Latvia	LV	2 045		74.1	25.6	0.3			97.9
Liechtenstein	LI	36				85.3	14.7		117.9
Lithuania	LT	3 004		58.9	39.5	1.6			100.4
Luxembourg	LU	525		70.3	25.9	3.8			98.2
Macedonia, FYR of	MK	2 060				1.3	93.6	5.1	134.6
Malta	MT	418				93.5	6.5		115.2
Monaco	MC	37				99.3	0.7		118.6
Montenegro	ME	621				12.3	87.7		126.1
Netherlands	NL	16 730	20.3	78.0	1.7				93.3
Norway	NO	4 986	52.2	45.3	2.5	0.0			90.6
Poland	PL	38 538		7.5	31.5	52.0	9.0		111.4
Portugal	PT	10 542		21.1	53.8	24.3	0.9		105.4
Romania	RO	20 096	13.5	39.8	17.3	21.3	8.1		102.4
San Marino	SM	32				84.7	15.3		120.9
Serbia (incl. Kosovo)	RS	9 015			2.0	30.8	66.8	0.4	122.5
Slovakia	SK	5 404			0.8	37.2	61.9		120.7
Slovenia	SI	2 055				3.7	95.5	0.8	125.4
Spain	ES	46 818	0.0	5.3	23.6	63.8	7.3		112.2
Sweden	SE	9 483	20.4	74.1	5.4	0.0			93.6
Switzerland	CH	7 955			3.4	83.9	10.0	2.8	117.0
United Kingdom	UK	63 495	94.9	5.0	0.1				83.6
Total		**534 518**	**14.7**	**20.3**	**17.3**	**27.0**	**17.5**	**3.2**	**107.9**
			35.0		**44.3**		**20.7**		
EU-28		**502 673**	**15.1**	**21.3**	**18.3**	**26.7**	**15.3**	**3.4**	**107.2**
			36.4		**45.0**		**18.6**		

Note1: Turkey is not included in the calculation due to lack of air quality data.
Note2: The percentage value "0.0" indicates an exposed population exists, but is small and estimated less than 0.05 %. Empty cells mean: no population in exposure.

Austria (45 %), Spain (7.5 %) and Malta (around 5 %) show similar percentage of inhabitants exposed to concentrations above the target value as in 2011. In Albania, Andorra, Bosnia & Herzegovina, Croatia, Hungary, Italy, FYR of Macedonia, Montenegro, Serbia and Slovakia both the population-weighted indicator concentration and the median were above the target value (TV), implying that in these countries the average concentration exceeded the TV and more than half of the population was exposed to concentrations exceeding the TV.

Table 6.3 Evolution of percentage population living in above target value (left) and population weighted concentration (right) in the years 2005-2012 – O_3, 26th highest daily maximum 8-hour mean. Resolution: 1x1 km.

Country		Population above TV 120 µg.m^{-3} [%]									Population-weighted conc. [µg.m^{-3}]								
		2005	2006	2007	2008	2009	2010	2011	2012	diff. '12 - '11	2005	2006	2007	2008	2009	2010	2011	2012	diff. '12 - '11
Albania	AL	39.8	24.9	67.6	6.6	13.2	0.0	52.6	100	47.4	122.7	117.9	126.9	115.3	114.7	109.5	121.1	133.4	12.3
Andorra	AD	100	26.8	18.9	78.2	13.5	100	100	100	0	127.2	119.1	118.6	122.0	115.6	122.4	120.6	122.2	1.7
Austria	AT	63.3	84.8	67.3	13.7	14.5	26.8	45.2	45.1	-0.1	120.6	124.9	122.8	114.8	116.4	118.4	118.6	118.5	-0.1
Belgium	BE	0.1	94.1	0	0	0	0	0	0	0	104.0	126.0	98.9	103.6	101.5	97.7	104.4	94.1	-10.3
Bosnia-Herzegovina	BA	38.3	34.9	63.8	7.5	25.7	16.5	24.1	76.8	52.7	119.9	118.1	122.5	113.7	114.5	107.4	109.9	125.1	15.2
Bulgaria	BG	21.9	0.8	34.2	6.6	16.3	0.3	2.2	25.9	23.7	109.9	105.0	115.7	114.4	112.0	103.8	105.1	115.6	10.6
Croatia	HR	76.9	79.6	85.8	8.8	19.2	20.3	40.4	83.2	42.8	122.8	124.8	124.7	115.5	115.6	114.3	118.3	125.0	6.7
Cyprus	CY	22.5	1.2	23.8	0.2	50.9	0.0	4.3	16.3	12.0	114.5	102.1	116.9	115.2	120.8	109.8	112.0	115.5	3.4
Czech Republic	CZ	75.1	95.6	59.1	6.8	6.6	0.9	11.1	21.5	10.4	121.6	126.5	121.0	114.6	113.5	114.1	114.8	116.5	1.7
Denmark	DK	0	0	0	0	0	0	0	0	0	95.0	104.9	95.2	102.6	95.5	91.4	96.9	95.1	-1.8
Estonia	EE	0	0	0	0	0	0	0	0	0	94.2	105.1	94.1	96.3	90.8	97.2	94.8	92.9	-1.9
Finland	FI	0	0	0	0	0	0	0	0	0	92.9	100.7	89.0	94.3	90.6	92.2	93.0	88.4	-4.6
France	FR	24.8	61.4	14.2	5.6	9.6	22.0	14.0	5.9	-8.1	113.8	122.0	109.0	107.3	107.3	111.6	112.8	104.4	-8.4
Germany	DE	23.8	88.0	13.1	10.6	2.0	13.0	3.8	0.4	-3.4	113.8	125.8	113.3	113.5	108.8	112.8	111.5	106.7	-4.8
Greece	GR	65.3	34.6	76.7	84.5	59.4	43.2	84.2	95.2	11.0	125.4	115.8	126.5	131.1	122.8	119.4	126.5	131.1	4.6
Hungary	HU	58.9	69.3	85.9	28.6	85.6	3.5	24.3	69.2	44.9	119.7	121.7	125.0	117.5	124.2	110.9	117.1	121.4	4.3
Iceland	IS	0	0	0	0	0	0	0	0	0	85.2	93.3	81.1	90.8	81.4	78.3	83.6	80.7	-2.9
Ireland	IE	0	0	0	0	0	0	0	0	0	86.5	90.2	84.2	92.1	84.9	85.6	84.4	86.6	2.2
Italy	IT	87.3	88.8	71.6	55.2	57.3	48.8	69.0	77.0	8.0	131.1	135.1	129.5	123.2	125.8	124.3	127.7	129.9	2.2
Latvia	LV	0	0	0	0	0	0	0	0	0	91.3	104.5	95.8	94.9	91.9	93.2	96.3	97.9	1.6
Liechtenstein	LI	1.5	100	21.8	9.4	17.8	100	9.5	14.7	5.2	106.9	127.3	119.9	119.4	118.9	123.3	116.4	117.9	1.4
Lithuania	LT	0	0	0	0	0	0	0	0	0	103.0	110.1	98.1	102.0	95.8	96.9	101.4	100.4	-1.1
Luxembourg	LU	39	100	0	0	0	2.9	1.8	0	-1.8	119.9	130.0	111.7	112.1	108.6	111.4	110.4	98.2	-12.2
Macedonia, FYR of	MK	31.5	15.0	29.7	78.4	16.6	0.0	17.7	98.7	81.0	117.5	110.3	121.1	121.0	111.3	109.0	117.4	134.6	17.2
Malta	MT	4.1	4.9	2.7	1.6	0	0.7	4.0	6.5	2.5	105.9	115.6	109.1	108.4	107.7	109.4	112.6	115.2	2.6
Monaco	MC		100	100	100	100	100	100	0.7	-99.3		142.4	127.3	123.1	127.2	124.0	126.6	118.6	-8.0
Montenegro	ME	35.2	23.7	35.4	12.3	14.5	5.3	31.0	87.7	56.6	120.8	114.3	122.3	118.1	111.7	108.6	115.1	126.1	11.0
Netherlands	NL	0	38.8	0	0	0	0	0	0	0	93.7	116.1	94.1	98.4	94.7	90.7	98.6	93.3	-5.2
Norway	NO	0.0	0	0	0	0	0	0	0	0	98.1	101.7	91.3	99.0	94.0	88.8	93.7	90.6	-3.1
Poland	PL	8.3	53.0	12.3	1.9	0.4	0.0	2.4	9.0	6.5	113.6	120.4	112.9	109.7	107.8	106.6	109.5	111.4	1.9
Portugal	PT	41.5	46.5	5.0	0.0	18.5	23.3	5.7	0.9	-4.9	119.0	119.4	111.0	102.7	112.4	112.0	108.4	105.4	-3.0
Romania	RO	13.4	0.6	36.7	3.1	8.0	0.0	0.7	8.1	7.4	112.1	105.7	116.9	110.1	108.8	94.0	91.1	102.4	11.3
San Marino	SM	100	22.9	100	14.1	13.8	11.6	13.8	15.3	1.5	130.8	120.8	130.4	119.0	118.1	116.1	117.9	120.9	3.0
Serbia (incl. Kosovo)	RS	28.3	6.3	62.2	20.2	38.2	4.1	16.5	67.2	50.7	115.6	108.5	122.5	117.3	115.8	102.5	112.0	122.5	10.6
Slovakia	SK	68.8	66.5	69.2	24.0	88.3	1.1	28.7	61.9	33.3	121.3	122.2	122.2	116.4	122.7	112.8	118.5	120.7	2.2
Slovenia	SI	79.7	100	99.9	22.7	38.2	56.5	99.5	96.3	-3.2	122.6	132.6	126.6	116.9	119.7	122.1	125.5	125.4	-0.2
Spain	ES	50.7	42.5	24.6	16.8	18.1	30.7	7.5	7.3	-0.2	117.7	116.2	115.4	110.7	113.1	115.4	112.1	112.2	0.1
Sweden	SE	0.0	0.1	0	0	0	0	0	0	0	97.6	104.5	93.5	97.6	94.2	91.2	96.1	93.6	-2.5
Switzerland	CH	74.7	100.0	53.6	11.1	15.4	99.5	40.6	12.8	-27.8	122.6	132.6	120.1	116.8	117.3	124.7	120.8	117.0	-3.9
United Kingdom	UK	0	0.0	0	0	0	0	0	0	0	87.2	98.0	83.3	93.1	86.8	81.6	87.8	83.6	-4.2
Total		**31.6**	**51.4**	**27.1**	**15.0**	**16.0**	**16.3**	**16.5**	**20.7**	**4.2**	**112.1**	**118.2**	**110.7**	**109.8**	**108.1**	**106.8**	**108.9**	**107.9**	**-1.0**
EU-28		**31.0**	**52.4**	**25.6**	**14.3**	**15.7**	**15.5**	**16.8**	**18.6**	**1.8**	**111.8**	**118.3**	**110.2**	**109.5**	**107.8**	**106.8**	**108.7**	**107.2**	**-1.5**

Compared with 2011, an increase of both the number of population living above the TV and the population-weighted concentration occurred in many countries in Central Europe, with Czech Republic, Slovakia, Hungary, Poland, Lichtenstein and Italy, and especially in south-eastern Europe, such as most of the Balkan countries, Romania, Bulgaria, Malta, Cyprus and Greece. A decrease of both exposure indicators is detected clearly in France, Germany, Luxembourg, Portugal, Slovenia and Switzerland.

Part of the population in Croatia, Serbia, Slovenia, Bosnia-Herzegovina (all lower than 1 %), Switzerland (2.8 %), FYR of Macedonia (5.1 %), Greece (11.7 %), and more substantially in Italy (about 26 %) was estimated to be exposed to ozone levels of more than 140 µg.m^{-3} (Table 6.2). As the current mapping methodology tends to underestimate high values due to interpolation smoothing, these actual numbers will most likely be even higher. Most of the western and northern European countries showed in 2012 a decrease in their population-weighted concentrations compared to 2011. The most prominent increases are observed for the Balkan countries, including Bulgaria and Romania.

The overall European population-weighted ozone concentration in terms of the 26th highest daily maximum 8-hour mean was estimated for 2012 as being 107.9 µg.m^{-3}, which is 1 µg.m^{-3} lower than in 2011.

6.1.3 Uncertainties

Uncertainty estimated by cross-validation

The basic uncertainty analysis is provided by cross-validation. Table 6.1 shows RMSE values of 8.5 µg.m^{-3} for the rural areas and 9.1 µg.m^{-3} for the urban areas of the combined final map. That is in the same order of magnitude as of the years 2011 – 2007, and lower than 2006 – 2005, (Horálek et al. 2014a and references cited therein). The relative mean uncertainty of the 2012 ozone map is 7.4 % for rural areas and 8.3 % for urban areas. Table 7.7 summarises both the absolute and relative uncertainties over the past eight years.

Figure 6.3 shows the cross-validation scatter plots for both the rural and urban areas of the 2012 map. The R^2, an indicator for the interpolation correlation with the observations, shows that for the rural areas about 71 % and for the urban areas about 70 % of the variability is attributable to the interpolation. Corresponding values for the years 2011 – 2005 do show a same or better fit of the 2012 interpolations than at previous years, see Table 7.7.

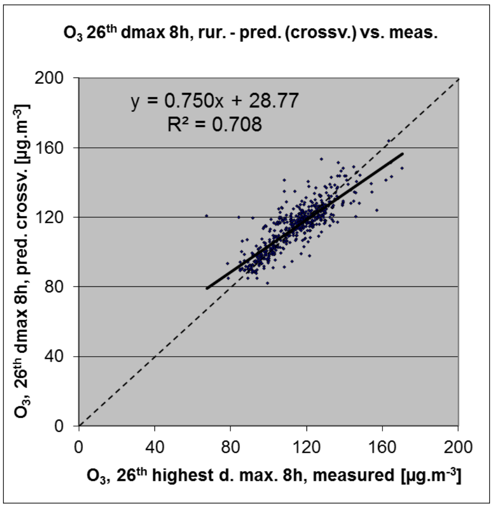

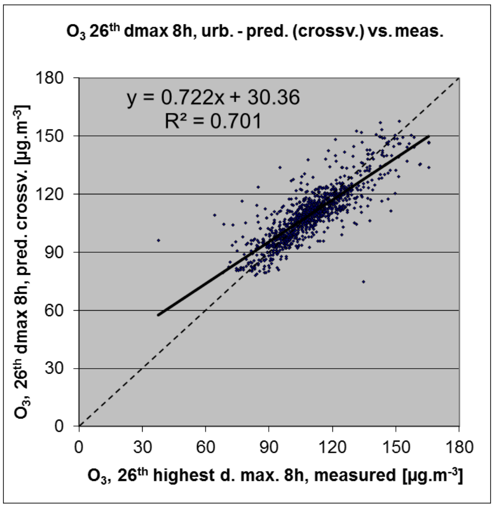

Figure 6.3 Correlation between cross-validation predicted values (y-axis) and measurements (x-axis) for the ozone indicator 26th highest daily maximum 8-hour mean for rural (left) and urban (right) areas in 2012.

The scatter plots indicate that the higher values are underestimated and the lower values somewhat overestimated by the interpolation method; a typical smoothing effect inherent to the interpolation method with the linear regression and its residuals kriging. For example, in rural areas (Figure 6.3, left panel) an observed value of 150 µg.m^{-3} is estimated in the interpolation as 141 µg.m^{-3}, which is 6 % too low.

Comparison of point measurement values with the predicted grid value

In addition to the above point observation – point prediction cross-validation, a simple comparison was made between the point observation values and interpolated predicted grid values.

The comparison has been executed primarily for the separate rural and separate urban background maps at 10x10 km resolution. (One can directly relate this comparison result to the cross-validation of Figure 6.3.) Next to this, the comparison has been done also for the final combined maps at 1x1 km resolution and for the spatial aggregated final maps at 10x10 km resolution. Figure 6.4 shows the scatterplots for these comparisons.

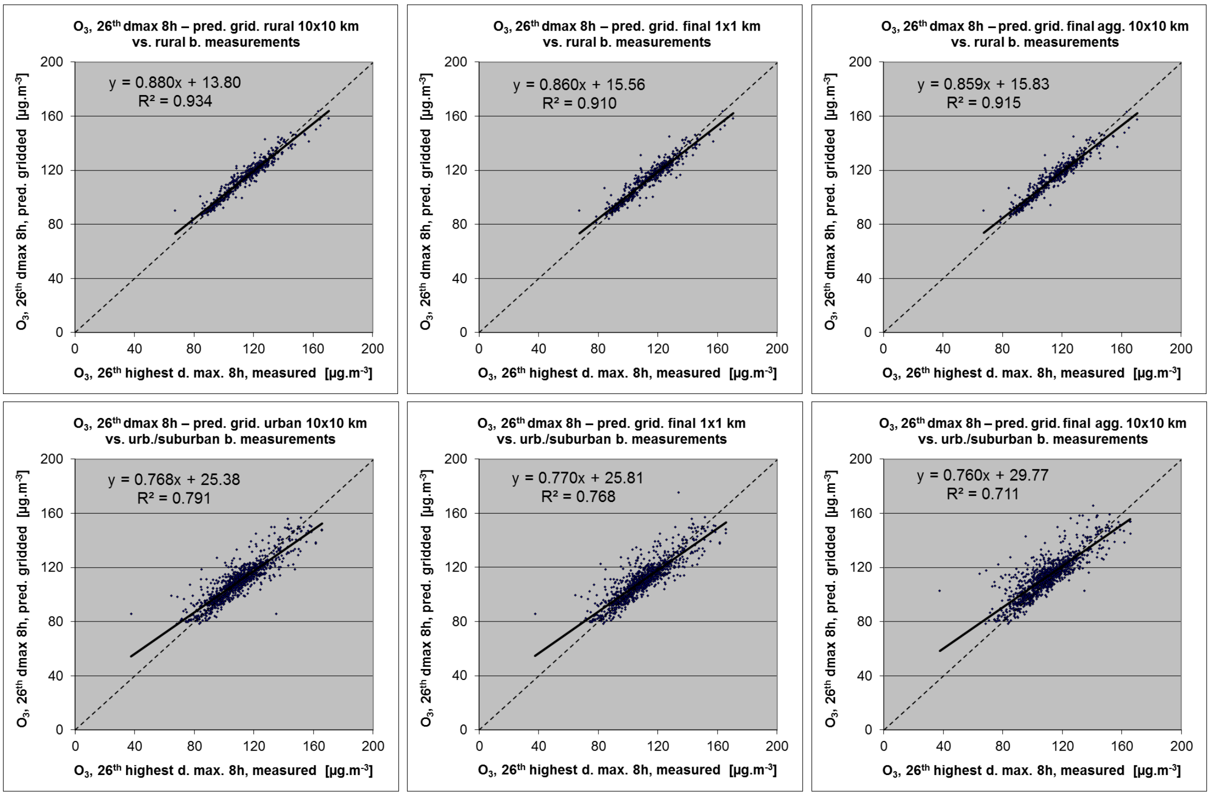

Figure 6.4 Correlation between predicted grid values from rural 10x10 km (upper left), urban 10x10 km (bottom left), final combined 1x1 km (upper and bottom middle) and final combined spatially aggregated 10x10 km (upper and bottom right) map (y-axis) versus measurements from rural (top), resp. urban/suburban (bottom) background stations (x-axis) for the ozone indicator 26th highest daily maximum 8-hour mean for 2012.

The results of the point observation – point prediction cross-validation of Figure 6.3 and those of the point-grid validation for the separate rural and the separate urban background map, and for the final combined maps at both resolutions (Figure 6.4), are summarised in Table 6.4.

By the comparing the scatterplots and the statistical indicators for the separate rural and separate urban background map with the final combined maps in both resolutions, one can evaluate the level of representation of the rural resp. urban background areas in the final combined maps. The rural air quality is fairly well represented in both the 1x1 km and the aggregated 10x10 km final combined map. The urban air quality is quite well represented in the final combined 1x1 km map, but not in the aggregated final combined 10x10 km map, as one can deduce from the higher RMSE, the bias being further from zero and the lower R^2. Therefore, we present in Figure A1.4 of Annex 1 the 1x1 km urban background map in addition to the 10x10 km final combined map of Figure 6.1.

The uncertainty of the rural and urban background maps at measurement locations is caused partly by the smoothing effect of interpolation and partly by the spatial averaging of the values in the 10x10 km grid cells. The level of smoothing, which leads to underestimation in areas with high values, is weaker in areas where measurements exist than in areas where a measurement point is not available. For example, in rural areas the predicted interpolation grid value in the separate rural map will be about 146 µg.m^{-3} at the corresponding station point with the observed value of 150 µg.m^{-3}. This is an underestimation of about 3 %. It is less than the prediction underestimation of 6 % at the same point location, when leaving out this one actual measurement point and one does the interpolation without this station (see the previous subsection).

Table 6.4 Statistical indicators RMSE, bias, coefficient of determination R^2 and linear regression equation from the scatter plots for the predicted point values based on cross-validation and the predicted grid values from separate (rural resp. urban) 10x10 km, final combined 1x1 km and final combined spatially aggregated 10x10 km map versus the measured point values for rural (left) and urban (right) background stations for the ozone indicator 26th highest daily maximum 8-hour mean of 2012.

	rural backgr. stations				urb./suburban backgr. stations			
	RMSE	bias	R^2	equation	RMSE	bias	R^2	equation
cross-valid. prediction, separate (r or ub) map	8.5	0.2	0.708	y = 0.750x + 28.8	9.1	-0.1	0.701	y = 0.722x + 30.4
grid prediction, 10x10 km separate (r or ub) map	4.1	0.1	0.934	y = 0.880x + 13.8	7.6	0.0	0.791	y = 0.768x + 25.4
grid prediction, 1x1 km final merged map	4.8	-0.4	0.910	y = 0.860x + 15.6	8.0	0.7	0.768	y = 0.770x + 25.8
grid prediction, aggr. 10x10 km final merged map	4.7	-0.3	0.915	y = 0.859x + 15.8	9.6	3.5	0.711	y = 0.760x + 29.8

Probability of Target Value exceedance

Figure 6.5 presents a gridded map of 10x10 km resolution showing the probability of target value exceedance. It was constructed on the basis of the 10x10 km gridded concentration map (Figure 6.1, derived from the 1x1 km resolution results), the 10x10 km gridded uncertainty map and the target value (TV) of 120 µg.m^{-3}. Section 4.1.3 explains the significance of the colour classes in the map.

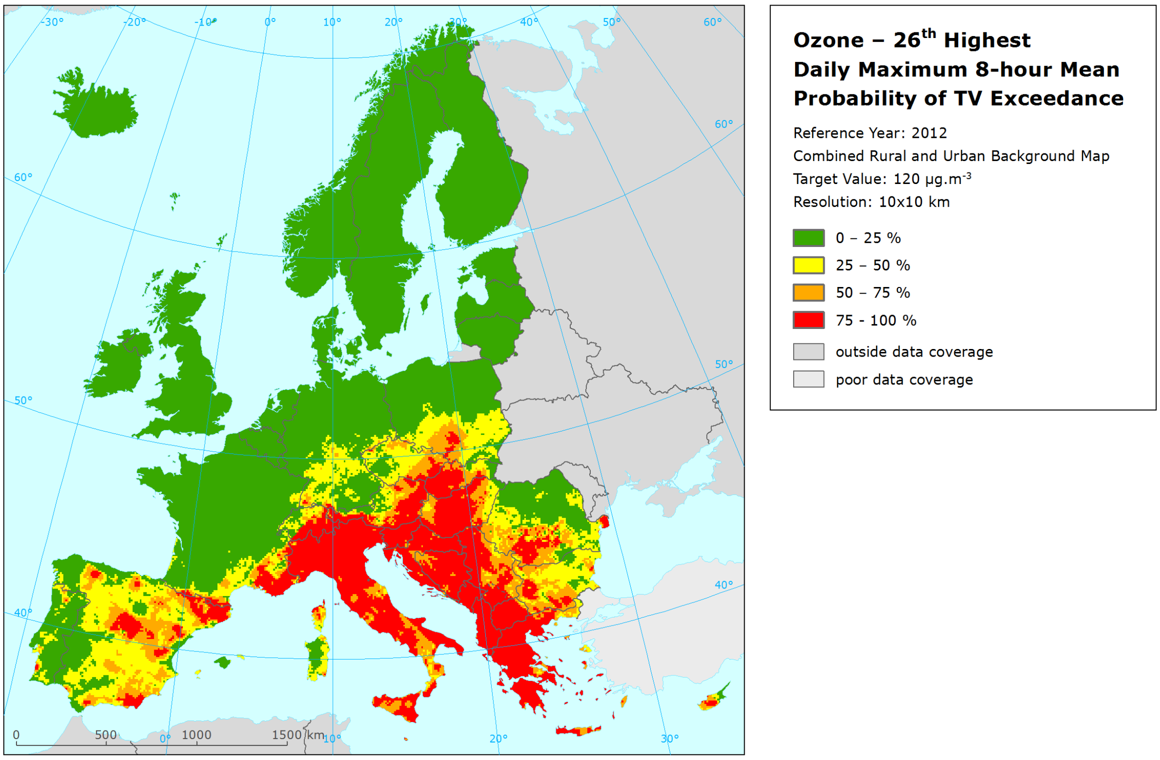

Figure 6.5 Map with the probability of the target value exceedance for ozone indicator 26th highest daily maximum 8-hour average (µg.m^{-3}) for 2012 on European scale calculated on the 10 x 10 km grid resolution. Interpolation uncertainty is considered only, no other sources of uncertainty.

The PoE map for 2012 compared to 2011, demonstrates that most of the red areas (high PoE) in the Alpine region, Italy, southern France, central Spain, Austria and Slovenia did not change compared to 2011. Especially in the Balkan countries, Hungary, Slovakia, Romania and Bulgaria the PoE increased considerably in its level (from 50 – 75 % in 2011 to more than 75 % in 2012, i.e. large PoE) and in general in its extent. North of the Alps the levels of PoE reduced somewhat reaching hardly anywhere levels more than 50 % (moderate; orange) and often changing from orange to yellow (modest) and from yellow to green (little).

In south-eastern Europe and in southern Italy there with its clear increases of the areas with elevated PoE one has to be aware that the small number of rural background stations in this area result in a high sensitivity of the map to the few (mainly urban background) measurement stations represented in this region.

On the Iberian Peninsula we observe in the more eastern part of the Spain some increases of areas with large PoE (red and orange) and further decreases in the more western part of the peninsula.

The meteorologically induced variations from year to year, combined with methodological uncertainties, the limited number of years considered here and the limited number of measurement stations at some regions do not allow for conclusions on whether, or not, there is any significant tendency on a European-wide range in this ozone indicator. For that purpose, one would need a longer time series, a higher and more evenly distributed number of station data and further reduced uncertainties.

6.2 SOMO35

6.2.1 Concentration map

Figure 6.6 presents the combined final map for SOMO35 as result of combining the separate rural and urban interpolated map following the procedure as described in De Smet et al. (2011) and Horálek et al. (2007). SOMO35 is not subject to one of the EU air quality directives and there are no limit or target values defined.

As one can observe in a few areas of the map, the high or low measurement values do not seem to influence the interpolation results despite their clustering. The main reason is that the map presented here is an aggregation of 1x1 km values to 10x10 km resolution and this aggregation smooths out the values one would more likely be able to distinguish in the higher resolution map, especially in the case of urban stations representing the urban areas. Another less prominent reason is the smoothing effect kriging has in general.

The supplementary data used in the regression models are the same as for 26th highest daily maximum 8-hour mean, i.e. EMEP model output, altitude and surface solar radiation for rural areas and EMEP model output, wind speed and surface solar radiation for urban areas.

Table 6.5 presents the estimated parameters of the linear regression models and of the residual kriging, including the statistical indicators of both the regression and the kriging. The fit of the regression is expressed by the adjusted R^2 and standard error. The adjusted R^2 in 2012 for the rural areas is 0.66 and for the urban areas 0.57. This is better fit than in all the previous years, see Horálek et al. (2014a) and references cited therein). RMSE and bias are the cross-validation indicators showing the quality of the resulting map. Section 6.2.3 discusses in more detail the RMSE analysis and comparison with results of 2005 – 2011.

Table 6.5 Parameters of the linear regression models (Eq. 2.2) and of the ordinary kriging (OK) variograms (nugget, sill, range) – and their statistics – of ozone indicator SOMO35 for 2012 in the rural (left) and urban (right) areas as used for final mapping.

linear regr. model + OK on its residuals	**rural areas parameter values**	**urban areas parameter values**
c (constant)	-1770	-528
a1 (EMEP model 2012)	0.64	0.58
a2 (altitude GTOPO)	1.44	
a3 (wind speed 2012)		-126.22
a4 (s. solar radiation 2012)	263.12	147.75
adjusted R^2	**0.66**	**0.57**
standard error [μg.m^{-3}.d]	**1671**	**1550**
nugget	1.7E+06	1.1E+06
sill	2.5E+06	1.6E+06
range [km]	450	90
RMSE [μg.m^{-3}.d]	**1633**	**1362**
relative RMSE [%]	**29.2**	**31.7**
bias (MPE) [μg.m^{-3}.d]	**-9**	**-1**

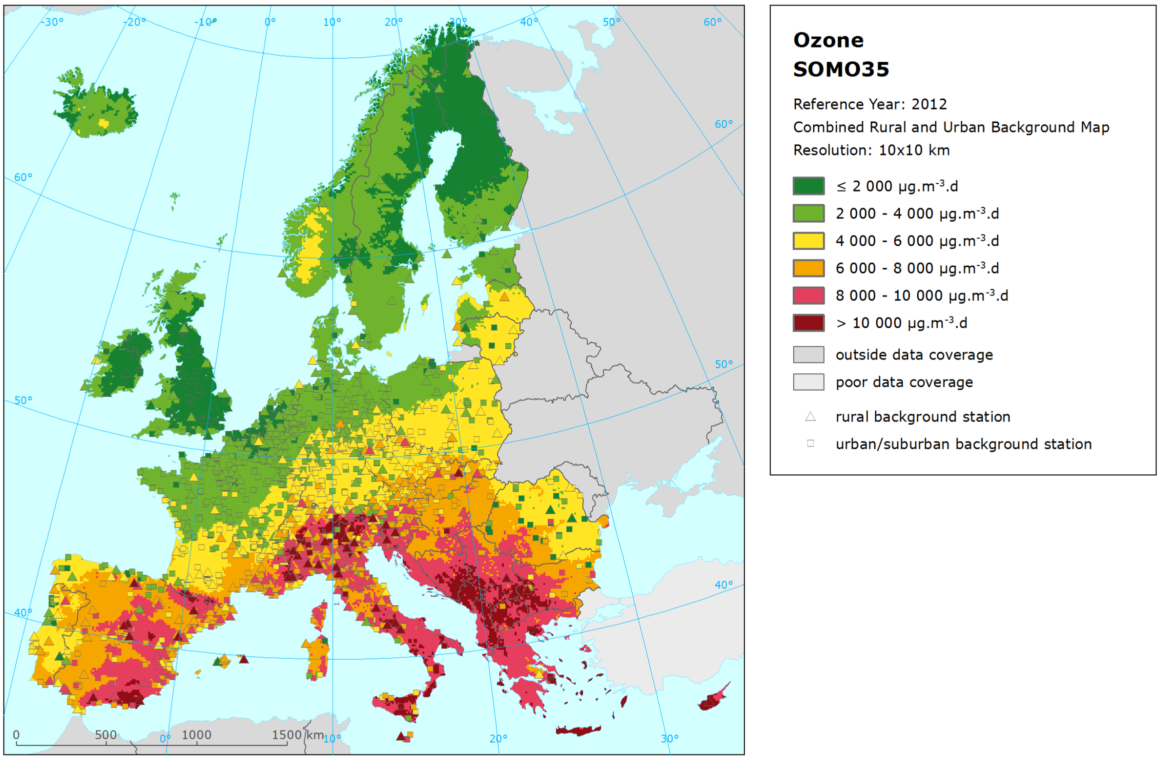

Figure 6.6 Combined rural and urban concentration map of ozone indicator SOMO35 in μg.m^{-3}.days for the year 2012. Resolution: 10x10 km.

The concentration map presented in Figure 6.6 is spatially aggregated from 1x1 km to 10x10 km resolution. As a result, the urban areas are not properly resolved in this map, due to the smoothing effect of this aggregation. Section 6.2.3 discusses the level of the representation of the urban areas in this final combined aggregated 10x10 km map. For better visualising the actual urban concentration levels at the actual urbanised areas, i.e. without the influence of the dominating pattern of extended rural areas, a separate 1x1 km urban background map is presented in Annex 1, Figure A1.5.

Figure 6.7 presents the inter-annual difference between 2012 and 2011 for SOMO35. Red areas show an increase of ozone concentration, while blue areas show a decrease. A considerable increase is observed in the eastern part of Spain, central and southern Italy, the Baltic States and south-eastern Europe, especially in the Balkan region, Hungary, Romania and Bulgaria.

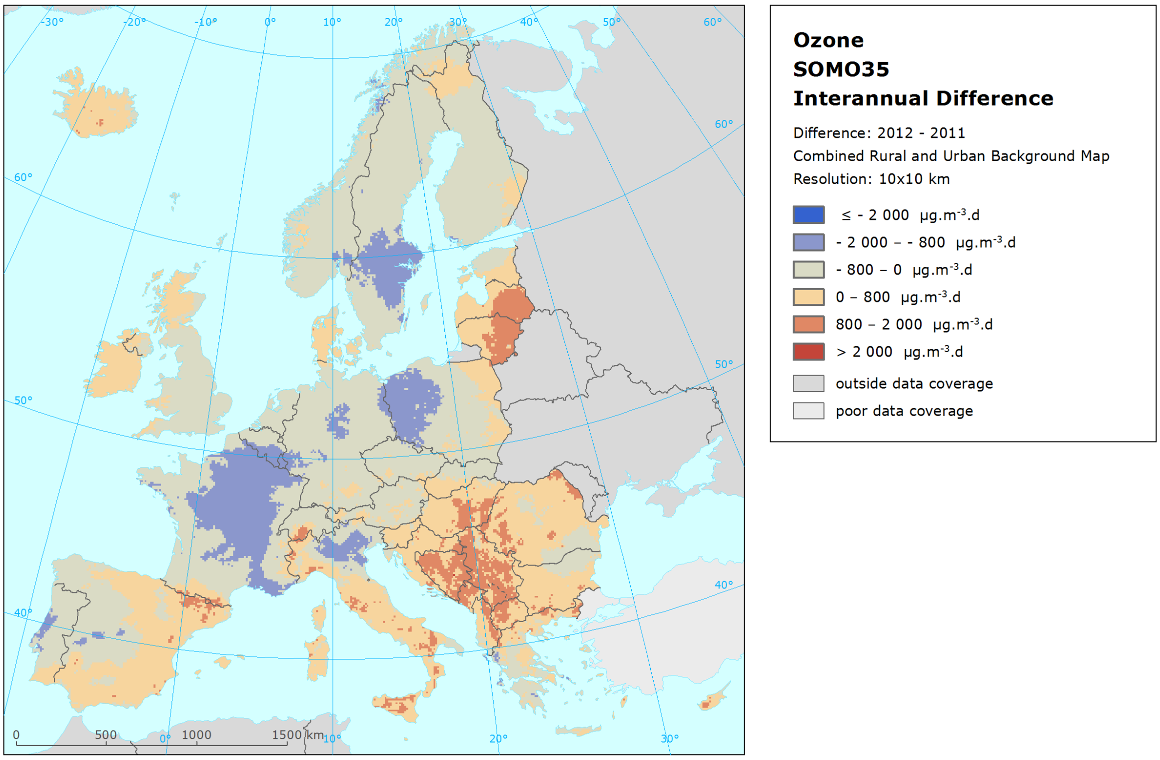

Figure 6.7 Inter-annual difference between mapped concentrations for 2012 and 2011 – ozone, SOMO35. Units: µg.m^{-3}.days.

6.2.2 Population exposure

Table 6.6 gives for SOMO35 the population frequency distribution for a limited number of exposure classes, as well as the population-weighted concentration for individual countries and for Europe as a whole. In the Table 6.7, the evolution of population exposure in the last eight years is presented.

It has been estimated that in 2012 about 24 % of the European population lived in areas with SOMO35 values above 6 000 µg.m^{-3}.d [(*)]. This is similar to that of 2011. In 2012, the northern and north-western European countries show no people living in areas above 6 000 µg.m^{-3}.d (Figure 6.6), similarly to that of the years 2011 and 2010. The other areas mostly show increases of different extents and ranges with the result that most of the southern and south-eastern regions showing exposures above or well above 6 000 µg.m^{-3}.d, especially in the Alpine region, Balkan region, southern Italy and central and southern Spain, and with the exception of Portugal.

[(*)] Note that the 6 mg.m^{-3}.d does not represent a health-related legally binding 'threshold'. In this and previous papers it concerns a somewhat arbitrarily chosen threshold to facilitate the discussion of the observed distributions of SOMO35 levels in their spatial and temporal context. This choice is motivated by a comparison of the 26th highest daily max. 8-hour means versus the SOMO35 of the ozone concentration measurements at all background stations. There is no simple relation between the two indicators, however it seems that the target value of the 26th highest daily maximum 8-hour mean, being 120 µg.m^{-3}, is related approximately with SOMO35 in the range 6 000 - 8 000 µg.m^{-3}.

We observe in 2012, compared to 2011, a slight European overall increase in population exposed to ozone levels above 10 000 μg.m^{-3}.d,where the considerable increase in south-eastern Europe is compensated by the reductions observed in north-western Europe, such that it leads to an overall increase of just 0.9 % in 2012.

Table 6.6 Population exposure and population-weighted concentration – ozone, SOMO35, year 2012.

Country		Population	Ozone, SOMO35, exposed population [%]						Population-weighted conc.
			< 2000	2000 - 4000	4000 - 6000	6000 - 8000	8000 - 10000	> 10000	
		[inhbs.1000]	μg.m^{-3}.d	μg.m^{-3}.d	μg.m^{-3}.d	μg.m^{-3}.d	μg.m^{-3}.d	μg.m^{-3}.d	[μg.m^{-3}.d]
Albania	AL	2 865				17.9	69.9	12.2	8 760
Andorra	AD	78				79.5	9.8	10.7	8 058
Austria	AT	8 408		13.9	65.4	17.5	3.2	0.1	5 419
Belgium	BE	11 095	48.4	51.6					2 050
Bosnia & Herzegovina	BA	3 839			14.0	58.1	23.5	4.3	7 322
Bulgaria	BG	7 327		8.3	53.1	26.9	9.7	2.0	5 960
Croatia	HR	4 276			7.6	69.1	22.7	0.6	7 143
Cyprus	CY	862				47.8	38.3	13.9	8 369
Czech Republic	CZ	10 505		11.1	84.9	4.0			4 806
Denmark	DK	5 581	0.4	99.0	0.6				2 662
Estonia	EE	1 325	51.8	47.7	0.5				2 310
Finland	FI	5 401	81.3	18.7					1 650
France	FR	63 379	8.0	60.3	19.4	11.8	0.5	0.0	3 635
Germany	DE	80 328	0.0	75.7	24.2	0.1	0.0		3 357
Greece	GR	11 123			0.2	6.1	74.7	19.0	9 378
Hungary	HU	9 932		1.6	29.7	65.4	3.2		6 342
Iceland	IS	320	93.2	6.8					1 242
Ireland	IE	4 583	84.9	15.1	0.0				1 479
Italy	IT	59 394			16.4	57.3	24.2	2.1	7 328
Latvia	LV	2 045	2.5	76.7	20.8				3 103
Liechtenstein	LI	36			88.5	11.3	0.2		5 132
Lithuania	LT	3 004		69.6	30.4				3 358
Luxembourg	LU	525		100.0					2 561
Macedonia, FYR of	MK	2 060				24.1	65.7	10.2	8 472
Malta	MT	418				44.7	52.4	2.9	8 022
Monaco	MC	37				99.9	0.1		6 979
Montenegro	ME	621				34.6	41.0	24.4	8 584
Netherlands	NL	16 730	52.4	47.6					1 949
Norway	NO	4 986	46.3	53.1	0.6				2 128
Poland	PL	38 538	0.6	45.5	53.3	0.6	0.0		4 045
Portugal	PT	10 542		47.4	43.1	9.5			4 240
Romania	RO	20 096	4.7	55.8	28.8	9.1	1.6		3 967
San Marino	SM	32			84.7	4.3	11.0		6 048
Serbia (incl. Kosovo)	RS	9 015		0.1	44.6	29.0	22.8	3.5	6 844
Slovakia	SK	5 404			45.2	54.7	0.2		6 103
Slovenia	SI	2 055			15.5	56.5	27.8	0.2	7 092
Spain	ES	46 818		12.8	39.0	40.0	7.5	0.6	5 850
Sweden	SE	9 483	47.8	51.9	0.3				2 233
Switzerland	CH	7 955		0.1	89.1	6.4	3.9	0.5	4 990
United Kingdom	UK	63 495	94.8	5.1	0.1	0.0			1 183
Total		**534 518**	**17.4**	**33.9**	**24.1**	**16.4**	**7.1**	**1.0**	**4 279**
			75.5			**24.5**			
EU-28		**502 673**	**18.1**	**35.7**	**23.3**	**16.0**	**6.0**	**0.8**	**4 154**
			77.2			**22.8**			

Note1: Turkey is not included in the calculation due to lacking air quality data.
Note2: The percentage value "0.0" indicates an exposed population exists, but is small and estimated less than 0.05 %. Empty cells mean: no population in exposure.

Table 6.7 Evolution of percentage population living in above 6000 µg.m^{-3} (left) and population-weighted concentration (right) in the years 2005-2012 – ozone, SOMO35. Resolution: 1x1 km.

Country		Population above 6000 µg.m^{-3}.d [%]									Population-weighted conc. [µg.m^{-3}.d]								
		2005	2006	2007	2008	2009	2010	2011	2012	diff. '12 - '11	2005	2006	2007	2008	2009	2010	2011	2012	diff. '12 - '11
Albania	AL	71.9	75.3	95.8	100	97.6	32.1	99.3	100	0.7	7911	7193	7817	7668	6754	5617	7769	8760	991
Andorra	AD	100	29.3	100	29.6	100	100	100	100	0	7520	6587	7121	6319	7186	7282	7891	8058	167
Austria	AT	40.8	40.1	56.7	12.5	13.4	12.1	22.0	20.7	-1.2	5946	6237	5874	5099	5050	4969	5452	5419	-33
Belgium	BE	0	0.3	0	0	0	0	0	0	0	2775	4017	2235	2520	2599	2401	2714	2050	-664
Bosnia-Herzegovina	BA	38.0	55.5	67.2	37.4	33.8	29.0	38.0	86.0	48.0	6714	6571	6938	5972	5536	4879	5702	7322	1621
Bulgaria	BG	31.4	28.2	39.2	47.7	32.7	8.4	29.6	38.6	9.0	5311	4896	6064	5797	5686	4377	5215	5960	745
Croatia	HR	45.1	85.7	83.2	35.8	32.5	28.6	48.6	92.4	43.8	6324	6928	6756	5899	5491	5419	6470	7143	673
Cyprus	CY	63.4	25.6	98.1	100.0	100	100	90.4	100	9.6	7155	5759	7739	8027	8788	7374	8773	8369	-404
Czech Republic	CZ	37.3	47.3	11.8	1.7	0.8	0.2	8.5	4.0	-4.5	5845	6097	5123	4576	4487	4160	4743	4806	63
Denmark	DK	0	0.0	0	0	0	0	0	0	0	2519	3578	2440	3080	2440	2245	2752	2662	-89
Estonia	EE	0	0	0	0	0	0	0	0	0	2437	3594	2061	2363	1762	2646	2516	2310	-206
Finland	FI	0	0.0	0	0	0	0	0	0	0	2275	3141	1332	1938	1623	1925	2052	1650	-402
France	FR	18.0	18.3	12.0	4.7	13.2	13.4	14.6	12.3	-2.3	4591	4972	3686	3563	4025	4139	4439	3635	-804
Germany	DE	2.5	8.2	1.1	0.5	0.4	0.3	0.4	0.1	-0.2	3940	4860	3648	3822	3507	3652	3668	3357	-311
Greece	GR	72.3	74.6	98.0	99.9	98.8	86.4	98.5	99.8	1.3	8321	6657	8330	8969	8330	7483	9182	9378	196
Hungary	HU	34.2	36.3	87.2	25.5	89.9	0.9	33.7	68.6	34.9	5751	5738	6547	5751	6631	4408	5828	6342	513
Iceland	IS	0	0	0	0	0	0	0	0	0	1329	2265	1168	2224	833	775	1094	1242	149
Ireland	IE	0	0	0	0	0	0	0	0	0	1701	2453	1412	2096	1487	1419	1353	1479	127
Italy	IT	93.7	96.0	86.7	66.1	75.3	61.7	89.9	83.6	-6.2	7634	8205	7506	6386	6986	6302	7532	7328	-204
Latvia	LV	0	0	0	0	0	0	0	0	0	2391	3734	2262	2347	1837	2304	2708	3103	394
Liechtenstein	LI	1.6	51.4	9.1	6.4	12.2	10.8	12.2	11.5	-0.7	5233	6258	4826	4930	5271	5244	5128	5132	5
Lithuania	LT	0.0	0.0	0	0	0	0	0	0	0	3671	4535	2744	3059	2291	2608	3131	3358	228
Luxembourg	LU	0.0	1.2	0	0	0	0	0	0	0	4769	5090	3424	3557	3500	3505	3527	2561	-967
Macedonia, FYR of	MK	33.9	32.7	35.6	100	41.5	13.6	89.9	100	10.1	7069	6297	6690	7133	6229	5081	7110	8472	1362
Malta	MT	100	100	100	100	100	100	97.1	100	2.9	6971	7797	7209	6582	6634	6722	7127	8022	896
Monaco	MC		100	100	100	100	100	100	100	0		8903	8381	7246	8325	8028	8354	6979	-1375
Montenegro	ME	38.8	35.5	71.8	100	37.1	33.1	60.2	100	39.8	7608	6554	7379	7120	6237	5653	6970	8584	1614
Netherlands	NL	0	0	0	0	0	0	0	0	0	1901	3245	1816	2104	1922	1916	2283	1949	-335
Norway	NO	0.5	2.9	0.0	0	0	0	0	0	0	2580	3496	1705	2514	2000	1803	2395	2128	-266
Poland	PL	6.1	27.3	1.4	0.7	0.5	0.0	1.8	0.6	-1.2	4784	5416	4179	3951	3747	3278	4065	4045	-20
Portugal	PT	32.2	24.8	14.8	8.6	28.9	32.4	17.4	9.5	-7.9	5510	5257	4863	3851	5003	5133	4552	4240	-312
Romania	RO	29.4	19.5	41.4	17.9	28.3	1.1	9.0	10.7	1.7	5238	4798	5882	5039	5044	3033	3276	3967	691
San Marino	SM	100	22.9	100	14.1	15.3	11.6	18.4	15.3	-3.1	7540	6321	7296	5863	5860	5331	6220	6048	-173
Serbia (incl. Kosovo)	RS	32.0	27.1	65.1	74.9	60.6	9.4	36.8	55.3	18.5	5947	5239	6768	6378	6118	4001	5793	6844	1051
Slovakia	SK	55.6	51.9	57.8	19.5	75.6	6.2	45.9	54.8	8.9	6141	6261	6098	5455	6348	4748	6051	6103	52
Slovenia	SI	49.7	98.5	68.1	37.2	36.6	37.5	82.3	84.5	2.3	6242	7480	6671	5761	5775	5998	7062	7092	30
Spain	ES	62.0	50.6	61.0	32.6	57.7	50.0	46.7	48.1	1.5	6139	5813	5992	5110	5983	6088	5858	5850	-7
Sweden	SE	0.0	0.0	0	0	0	0	0	0	0	2682	3635	1795	2387	2100	2025	2628	2233	-395
Switzerland	CH	26.2	40.5	12.7	8.6	14.3	12.9	14.3	10.9	-3.4	5740	6321	5114	4619	5139	5127	5435	4990	-444
United Kingdom	UK	0	0.0	0	0	0	0	0	0	0	1551	2676	1174	2044	1433	1072	1471	1183	-288
Total		**27.0**	**29.5**	**28.1**	**19.6**	**24.6**	**16.6**	**23.6**	**24.5**	**1.0**	**4706**	**5167**	**4411**	**4275**	**4275**	**3917**	**4414**	**4279**	**-135**
EU28		**26.5**	**29.0**	**26.9**	**17.4**	**23.6**	**16.7**	**23.6**	**22.8**	**-0.8**	**4613**	**5128**	**4319**	**4178**	**4208**	**3888**	**4339**	**4154**	**-185**

In 2012 the total European population-weighted ozone concentration, in terms of SOMO35, was estimated to be 4279 µg.m^{-3}.d, which is less than in 2011, more than in 2010 and the same as in 2009 and 2008 and as such not an exceptional value.

6.2.3 Uncertainties

Uncertainty estimated by cross-validation

The basic uncertainty analysis is given by the cross-validation. In Table 6.5, the absolute mean uncertainty (RMSE) in 2012 was 1633 µg.m^{-3}.d for the rural areas and 1362 µg.m^{-3}.d for the urban areas; slightly less than in 2011, but not exceptional compared to the years 2011 – 2007 (Horálek et al, 2014a and references cited therein). The relative mean uncertainty of the 2012 map of SOMO35 is 29.2 % for rural and 31.7 % for urban areas, which is for the urban area slightly less than in the years 2011 – 2005 and for the rural areas amidst of those of 2011 – 2005 (Horálek et al., 2014a). Table 7.7 summarises both the absolute and the relative uncertainties over these past eight years.

Figure 6.8 shows the cross-validation scatter plots for interpolated values at both rural and urban areas. R^2 for rural areas and urban areas in 2012 indicates that, respectively, about 68 % and 67 % of the variability is attributable to the interpolation. The corresponding values for the maps of the years 2011 – 2005 (see Table 7.7) illustrate the best fit in the year 2012 for rural areas and one of the two best fits for the urban areas.

The scatter plots show again that in areas with high concentrations the interpolation methods tend to deliver underestimated predictions, although some overestimation or lower values of urban areas is also likely. For example, in urban areas (Figure 6.7, right panel) an observed value of 10 000 µg.m^{-3}.d is estimated in the interpolation as about 8 200 µg.m^{-3}.d. That is 18 % too low, leading in general to considerable underestimations at high SOMO35 values. Vice versa at low values an overestimation will occur, e.g. at a measured 2000 µg.m^{-3}.d the interpolation will predict some 2 700 µg.m^{-3}.d, which is about 37 % too high.

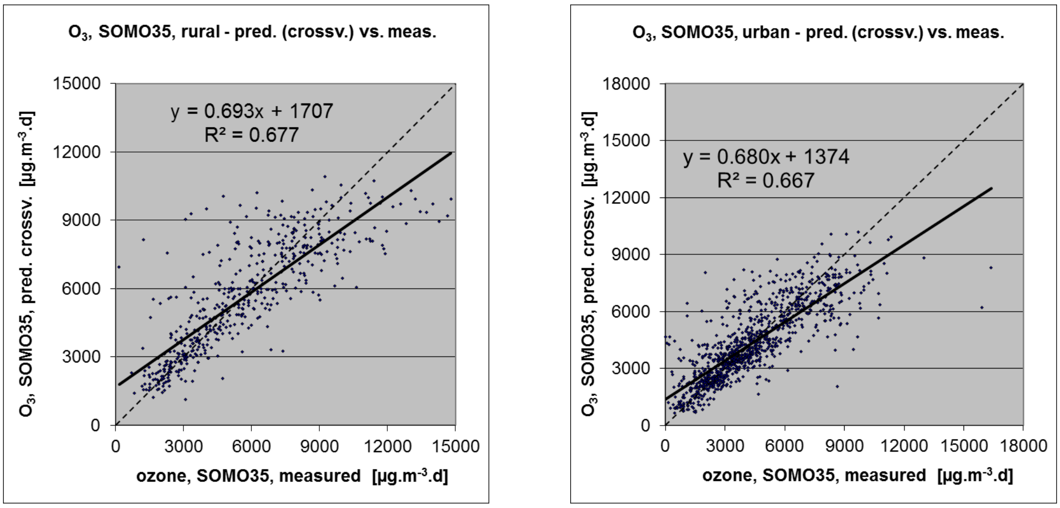

Figure 6.8 Correlation between cross-validation predicted values (y-axis) and measurements (x-axis) for the ozone indicator SOMO35 for rural (left) and urban (right) areas in 2012.

Comparison of point measurement values with the predicted grid value

Additional to the above point observation – point prediction cross-validation, a simple comparison was made between the point measurements and interpolated predicted grid values averaged in on a grid of 10x10 km resolution the separate rural and urban background maps. This point-grid comparison indicates to what extent the predicted value of a grid cell represents the corresponding measured values at stations located in that cell.

The comparison has been executed primarily for the separate rural and separate urban background maps at 10x10 km resolution. (One can directly relate this comparison result to the cross-validation results of Figure 6.8.)

Next to this, the comparison has been done also for the final combined maps at 1x1 km resolution and for the spatial aggregated final maps at 10x10 km resolution. Figure 6.9 shows the scatterplots for these comparisons.

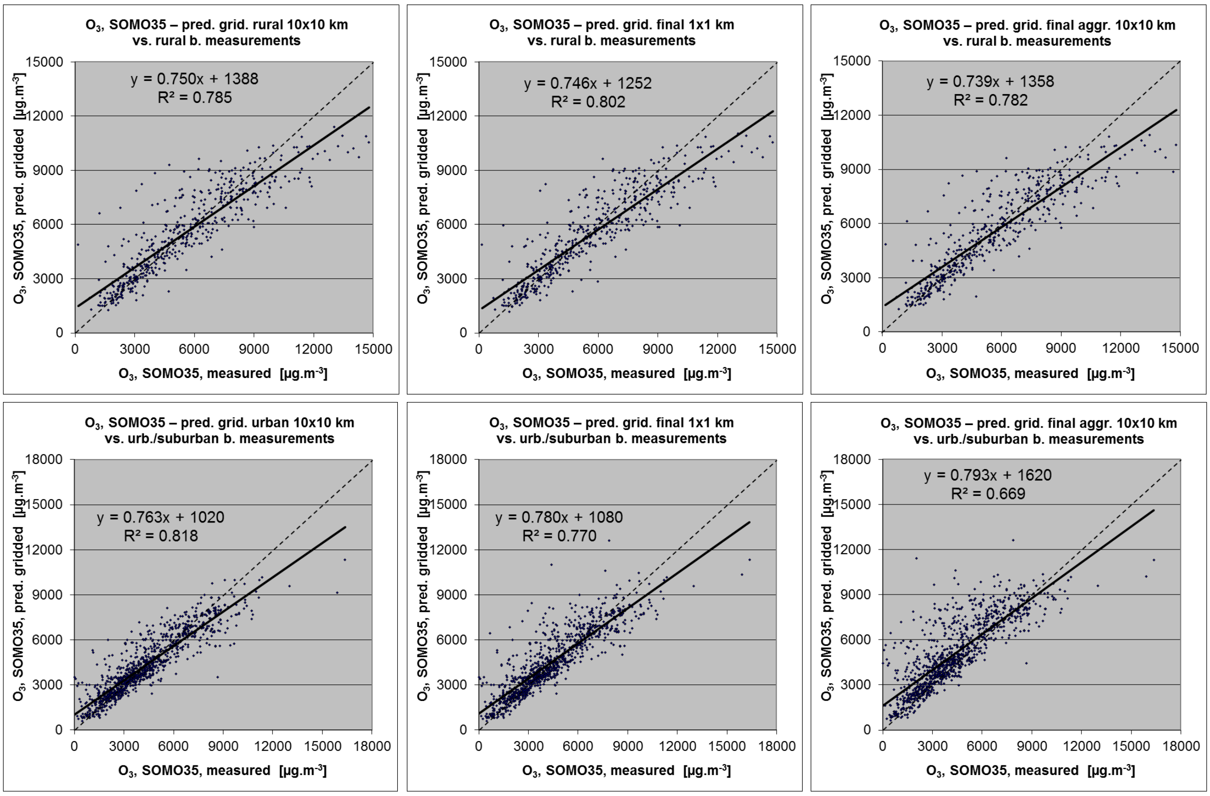

Figure 6.9 Correlation between predicted grid values from rural 10x10 km (upper left), urban 10x10 km (bottom left), final combined 1x1 km (upper and bottom middle) and final combined spatially aggregated 10x10 km (upper and bottom right) map (y-axis) versus measurements from rural (top), resp. urban/suburban (bottom) background stations (x-axis) for the ozone indicator SOMO35 for 2012.

The results of the point observation – point prediction cross-validation of Figure 6.8 and those of the point-grid validation for the separate rural and the separate urban background map, and for the final combined maps at both resolutions (Figure 6.4), are summarised in Table 6.8.

By the comparing the scatterplots and the statistical indicators for the separate rural and separate urban background map with the final combined maps in both resolutions, one can evaluate the level of representation of the rural resp. urban background areas in the final combined maps. The rural air quality is fairly well represented in both the 1x1 km and the aggregated 10x10 km final combined map. The urban air quality is quite well represented in the final combined 1x1 km map, but not in the aggregated final combined 10x10 km map, as one can deduce from the higher RMSE, the bias being further from zero and the lower R^2. Therefore, we present in Figure A1.5 of Annex 1 the 1x1 km urban background map in addition to the 10x10 km final combined map of Figure 6.6.

Table 6.8 shows a better correlated relationship (i.e. lower RMSE, higher R^2, smaller intercept, slope closer to 1) between station measurements and the interpolated values of the corresponding grid cells at both rural and urban background map areas than it does for the point cross-validation predictions. This is because the simple comparison between point measurements and the gridded interpolated values shows the uncertainty of predictions where there are actual station locations, while the point cross-validation prediction simulates the behaviour of the interpolation at point positions assuming no actual measurements would exist at these points within the area covered by measurements. The uncertainty at measurement locations is caused partly by the smoothing effect of the interpolation and partly by the spatial averaging of the values into 10x10 km grid cells. The degree of smoothing leading to underestimation in areas with high values is weaker when measurements exist, than when no measurement exists. For example, in urban areas the predicted interpolation grid value in the separate urban background map will be about 8 700 µg.m^{-3}.d at a corresponding station point with an observed value of 10 000 µg.m^{-3}.d. This is an underestimation of about 13 %. It is less than the prediction underestimation of 18 % at the same point location, when leaving out this one actual measurement point and one does the interpolation without the station (see the previous subsection).

Table 6.8 Statistical indicators RMSE, bias, coefficient of determination R^2 and linear regression equation from the scatter plots for the predicted point values based on cross-validation and the predicted grid values from separate (rural resp. urban) 10x10 km, final combined 1x1 km and final combined spatially aggregated 10x10 km map versus the measured point values for rural (left) and urban (right) background stations for the ozone indicator SOMO35 of 2012.

	rural backgr. stations				urb./suburban backgr. stations			
	RMSE	bias	R^2	equation	RMSE	bias	R^2	equation
cross-valid. prediction, separate (r or ub) map	1633	-9	0.677	y = 0.693x + 1707	1362	-1	0.667	y = 0.680x + 1374
grid prediction, 10x10 km separate (r or ub) map	1336	-6	0.785	y = 0.750x + 1388	1015	3	0.818	y = 0.763x + 1020
grid prediction, 1x1 km final merged map	1302	-168	0.802	y = 0.746x + 1252	1139	136	0.770	y = 0.780x + 1080
grid prediction, aggr. 10x10 km final merged map	1351	-102	0.782	y = 0.739x + 1358	1583	734	0.669	y = 0.793x + 1620

No Limit Value or Target Value is set for the WHO recommended ozone health indicator SOMO35, therefore no probability of exceedance map has been prepared.

6.3 AOT40 for crops and for forests

The ecosystem based accumulative ozone indicators described in this section are specifically prepared for calculation of EEA Core Set Indicator 005 (CSI005, http://themes.eea.europa.eu/indicators). For the estimation of the vegetation and forested area exposure to accumulated ozone the maps in this section are created on a grid of 2x2 km resolution, instead of the 10x10 km grid used for the human health indicators. This resolution is selected as a compromise between calculation time and accuracy in the impact assessment done for ozone within CSI005. It serves as a refinement of the exposure frequency distribution outcomes of the overlay with 100x100 m resolution CLC2006 land cover classes.

6.3.1 Concentration maps

The interpolated maps of AOT40 for crops and AOT40 for forests were created for rural areas only, combining AOT40 data derived from rural background station observations with supplementary data sources EMEP model output, altitude and surface solar radiation. The relevant linear regression model is referred to as O.Ear. Note that supplementary data sources are the same as for the human health related ozone indicators.

Table 6.9 presents the estimated parameters of the linear regression models and of the residual kriging, including their statistical indicators of the regression and kriging. The fit of the regression is expressed by adjusted R^2 and the standard error. The adjusted R^2 is 0.67 both for AOT40 for crops and for AOT40 for forests in 2012 is better than in the previous seven years, see Horálek et al. (2014a) and references cited therein. RMSE and bias are the cross-validation indicators, showing the quality of the resulting map. Section 5.3.3 discusses in more detail the RMSE analysis and comparison with results of 2005 – 2011.

Table 6.9 Parameters of the linear regression models (Eq2.1) and of the ordinary kriging (OK) variograms (nugget, sill, range) - and their statistics - of ozone indicators AOT40 for crops (left) and for forests (right) for 2012 in the rural areas as used for final mapping.

linear regr. model + OK on its residuals	**AOT40 for crops**	**AOT40 for forests**
	parameter values	**parameter values**
c (constant)	-6373	-11859
a1 (EMEP model 2012)	0.77	0.62
a2 (altitude GTOPO)	2.45	6.39
a3 (s. solar radiation 2012)	833.0	1604.3
adjusted R^2	**0.67**	**0.67**
standard error [µg.m^{-3}]	**5322**	**9284**
nugget	1.7E+07	4.0E+07
sill	2.5E+07	7.4E+07
range [km]	120	190
RMSE [µg.m^{-3}]	**5062**	**8847**
relative RMSE [%]	**32.9**	**32.8**
bias (MPE) [µg.m^{-3}]	**72**	**33**

Figure 6.10 presents the final map of AOT40 for *crops*. The areas and stations in the map that exceed the target value (TV) of 18 mg.m^{-3}.h are marked in red and dark red. As urban areas are considered not to represent agricultural areas, this map is applicable to rural areas only, and as such it is based on rural background station observations only. The map was compared to the one of 2011 and in general a clear increase in the extent of areas with the highest AOT40 levels (red and dark red) was found specifically in the southern and south-eastern regions of Europe. Decreases are observed in the extent of areas exposed to levels just below the target value (a shift from yellow to orange), especially France, northern Germany and northern Poland.

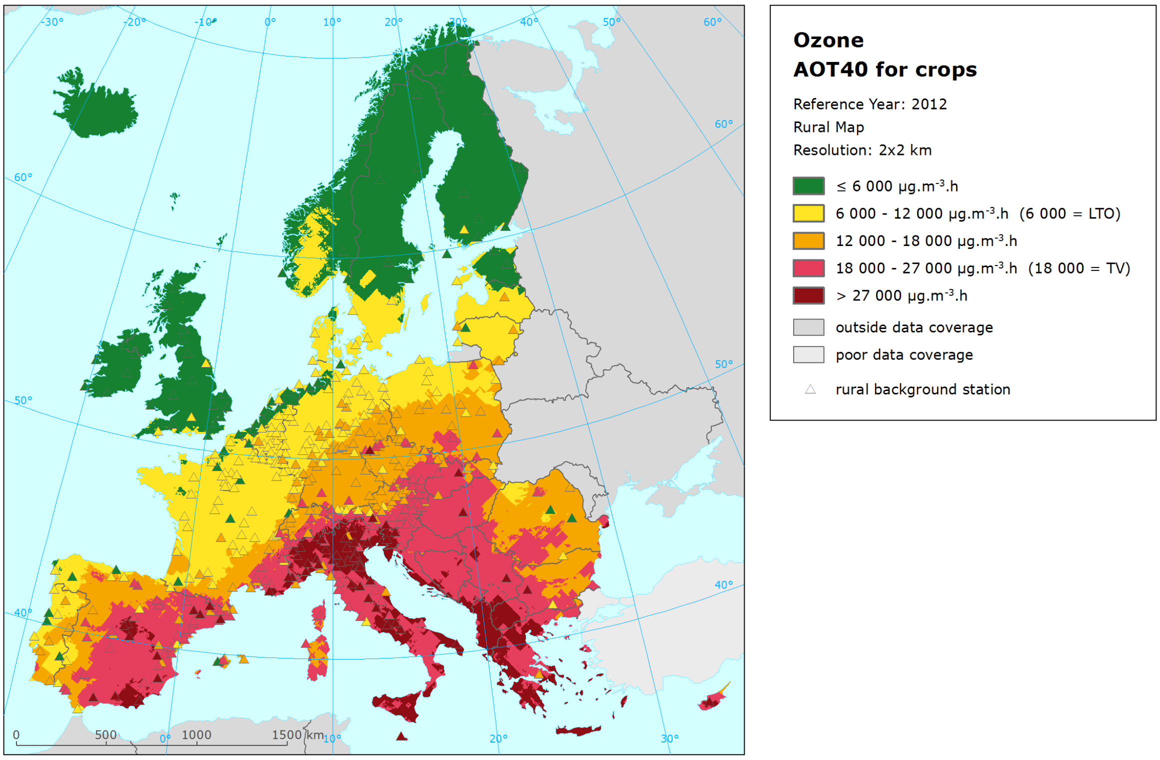

Figure 6.10 Rural concentration map of ozone vegetation indicator AOT40 for crops for the year 2012. Units: µg.m^{-3}.hours. Resolution: 2x2km.

Figure 6.11 presents the inter-annual difference between 2012 and 2011 for AOT40 for crops. Red areas show an increase of ozone concentration, while blue areas show a decrease. The highest decreases are observed in Portugal, and the range of France, Germany, Switzerland, western Poland, Sweden, Finland and Estonia. Contrary to that, considerable increases are observed in eastern Spain, Italy, the Alps and the whole region of south-eastern Europe with elevated concentrations well above the target value of 18 000 µg.m^{-3}.h.

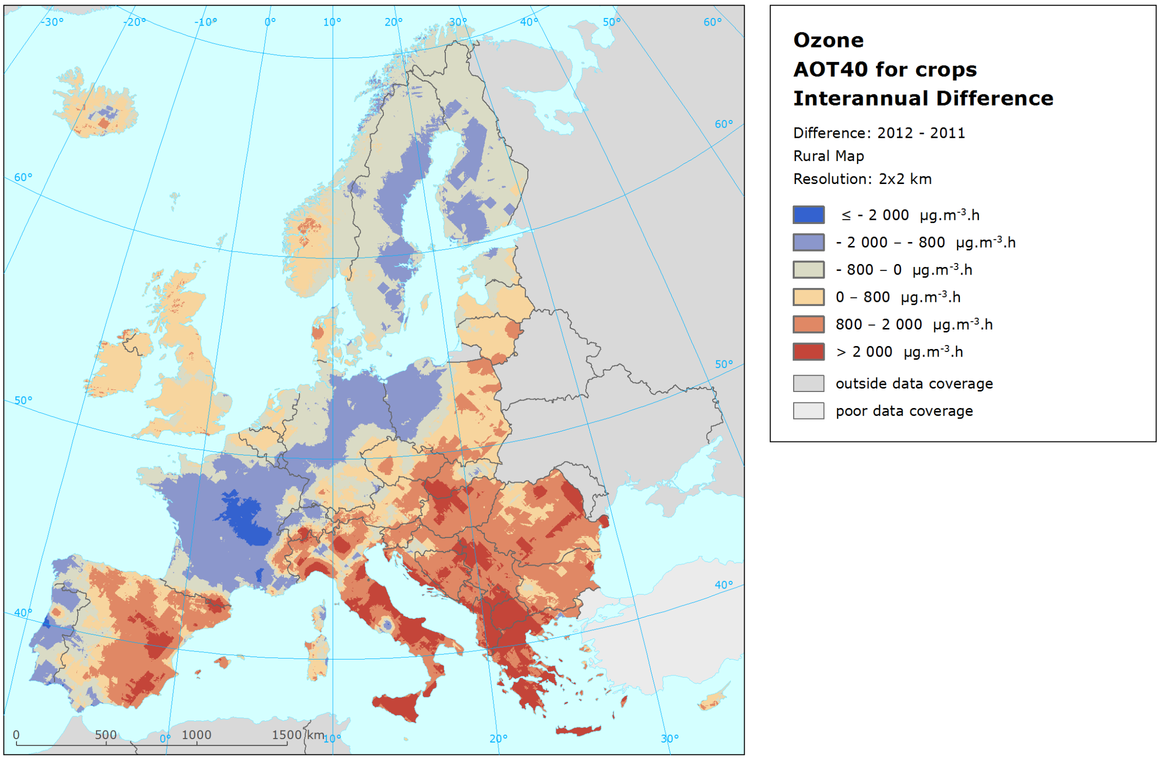

Figure 6.11 Inter-annual difference between mapped concentrations for 2012 and 2011 – ozone, AOT40 for crops. Units: µg.m^{-3}.hours.

Figure 6.12 presents the final map of AOT40 for forests. Like Figure 6.10, it concerns a map for rural areas as urban areas are considered as not forested. Therefore, the map is based on rural background station observations only, representing an indicator for vegetation exposure to ozone. For AOT40 for forests there is no TV defined.

Figure 6.13 shows the inter-annual difference between 2012 and 2011 for AOT40 for forests. Again, the main increase is visible in Eastern Europe (Latvia, Lithuania, East Poland), Central Europe (Slovakia, Hungary), the central and eastern part of Spain, large parts of Italy, and south-eastern Europe, specifically the Balkan countries, Romania, Bulgaria, Greece and Cyprus. The decrease is visible particularly in Portugal, and the range of France, Germany, Switzerland, Benelux, western Poland, Sweden and Finland.

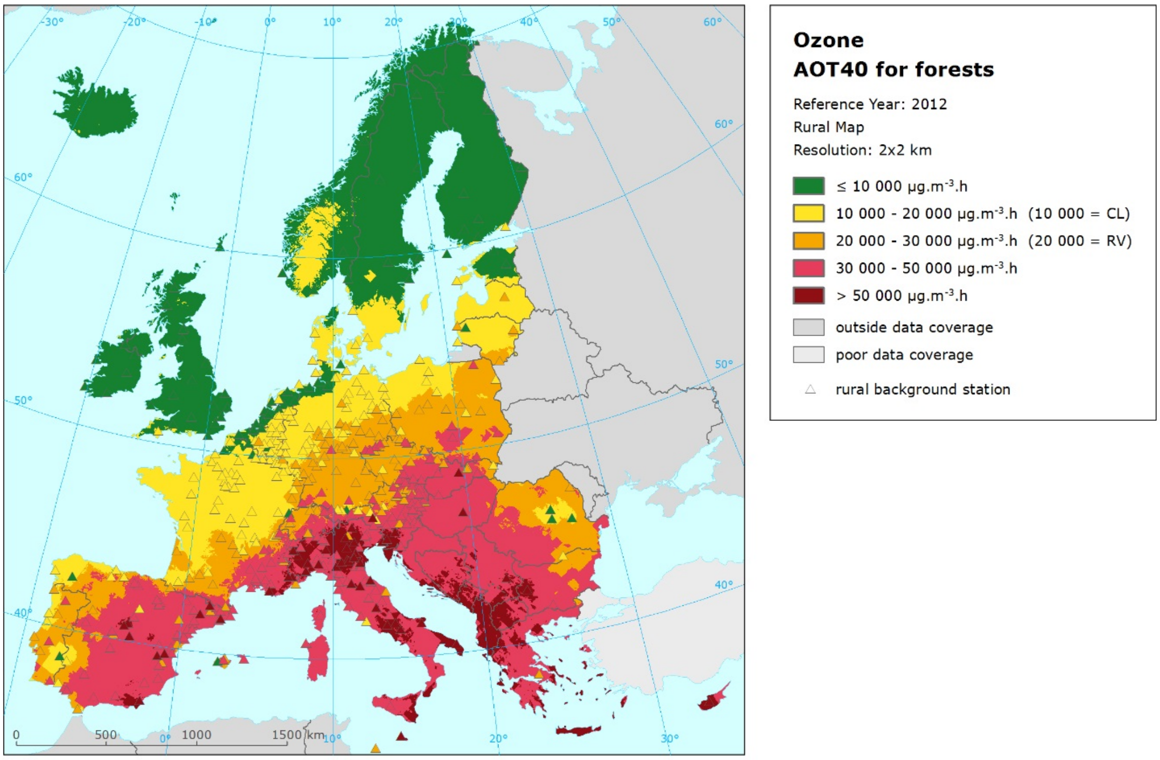

Figure 6.12 Rural concentration map of ozone vegetation indicator AOT40 for forests for the year 2012. Units: µg.m^{-3}.hours. Resolution: 2x2km.

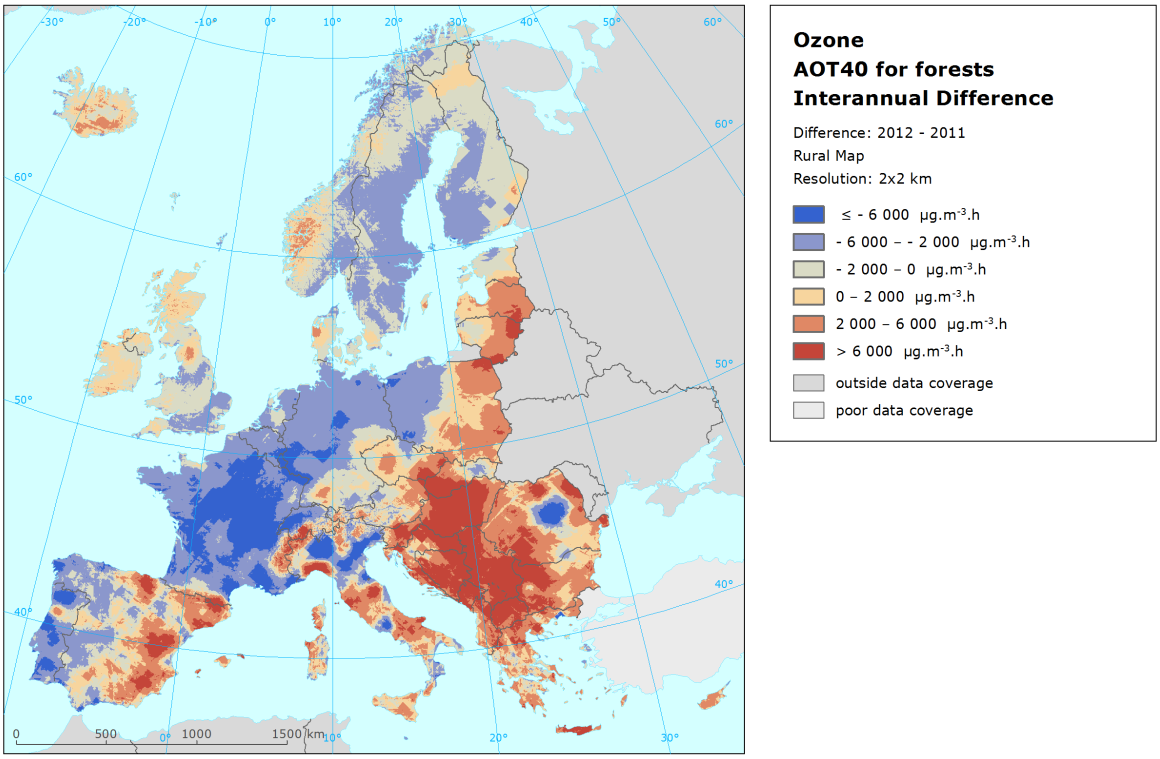

Figure 6.13 Inter-annual difference between mapped concentrations for 2012 and 2011 – ozone, AOT40 for crops. Units: µg.m^{-3}.hours. Resolution: 2x2km.

6.3.2 Vegetation exposure

Agricultural crops

The rural map with ozone indicator AOT40 for vegetation, i.e. agricultural crops, as given in Figure 6.10, has been combined with the land cover CLC2006 map. Following a similar procedure as described in Horálek et al. (2007) the exposure of agricultural areas, defined as the Corine Land Cover level-1 class *2 Agricultural areas* (encompassing the level-2 classes *2.1 Arable land, 2.2 Permanent crops, 2.3 Pastures* and *2.4 Heterogeneous agricultural areas)* has been calculated at the country-level.

Table 6.10 gives the absolute and relative agricultural area for each country and for four European regions where the target value (TV) and long-term objective (LTO) for ozone are exceeded. The frequency distribution of the agricultural area per country over the exposure classes is presented as well.

The table indicates the country grouping with corresponding colours of the region; *Northern Europe*: Sweden, Finland, Norway, Estonia, Lithuania, Latvia and Denmark. *North-western Europe*: United Kingdom, Ireland, Iceland, the Netherlands, Belgium, Luxembourg and France north of 45 degrees latitude. *Central and Eastern Europe*: Germany, Poland, Czech Republic, Slovakia, Hungary, Austria, Liechtenstein, Bulgaria and Romania. *Southern Europe*: Albania, Bosnia-Herzegovina, France south of 45 degrees latitude, Portugal, Spain, Italy, San Marino, Slovenia, Croatia, Greece, Cyprus, F.Y.R. of Macedonia, Montenegro, Serbia (including Kosovo) and Malta.

Table 6.10 illustrates that in 2012, some 30 % of all European agricultural land was exposed to ozone exceeding the target value (TV) of 18 $mg.m^{-3}.h$. This is an increase in the total area with agricultural crops above the TV (and as such considered to suffer from adverse effects to ozone exposure) compared to 2011 (19 %), 2010 (21 %) and 2009 (26 %). It is lower than 2008 (38 %), 2007 (36 %) and well below that of 2006 (70 %) (Table 6.12). It is also below that of 2005 (49%) (Horálek et al., 2008). Considering the long-term objective (LTO, 6 $mg.m^{-3}.h$) the area in excess (about 86 %), which is lower than in 2011 (88 %), 2008 (96 %) and 2006 (98 %), and higher than in 2010 (85 %), 2009 (81%) and 2007 (78 %). Like in 2011 and 2010, only the countries Ireland and Iceland did have ozone levels not being in excess of the LTO. In many countries of southern Europe, more than half of their total agricultural area experienced exposures above the less stringent TV.

Table 6.12 (left) presents for comparison the percentages of area in exceedance of the target value for the years 2005 – 2012. In southern Europe, about 70 % of the total agricultural area exceeded the target value in 2012. This is considerably more than in years 2007 – 2011 with 54 to 57 % but still substantially below the amount of 2006 (94 %). In northern Europe for the years 2005 and 2007 – 2012, no area was mapped in excess of the target value; only in 2006 almost 4 % of its area was in excess. In the north-western region the area exceeding the target value is still low with its 0.1 %, comparable to the levels of most of its previous years. For the central and eastern region the total area where ozone exceeds the target value increased considerably to some 21 % comparable to the levels of 2009 (17 %), which means that a tendency of decreasing area in exceedance has not been continued into 2012.

Compared to 2006, the frequency distribution of agricultural areas over the exposure classes showed a clear shift towards lower exposures in 2007 leading to a decreased total area exceeded, towards a distribution more similar to that of 2005 (Horálek et al., 2008). In 2008, this tendency continued with an approximately similar area percentage in excess of the TV. However, a shift in area percentages with lower exposure levels in 2007 to somewhat higher levels in 2008 (but still below the target value) also occurred. Compared to 2007 – 2008, we observed in 2009 – 2010 an increased area with lower exposure level, leading to a lower TV exceedance. In 2011 this tendency seems to continue for most regions except for the southern European region where the areas with more elevated levels or areas in exceedances of the TV continue to exist or extended. In 2012 this evolution seems to be continued rather unaltered.

Table 6.10 Agricultural area exposure and exceedance (Long Term Objective, LTO and Target Value, TV) for ozone, AOT40 for crops, year 2012.

Country	Agricultural Area, 2012					Percentage of agricultural area, 2012 [%]				
	total area	> LTO (6 mg.m^{-3}.h)		> TV (18 mg.m^{-3}.h)		< 6	6 - 12	12 - 18	18 - 27	> 27
	[km^2]	[km^2]	[%]	[km^2]	[%]	mg.m^{-3}.h	mg.m^{-3}.h	mg.m^{-3}.h	mg.m^{-3}.h	mg.m^{-3}.h
Albania	7877	7877	100	7877	100				13.5	86.5
Austria	27222	27222	100	16184	59.5		0.1	40.4	59.4	0.1
Belgium	17597	14881	84.6		0	15.4	84.6			
Bosnia-Herzegovina	18840	18840	100	18836	99.98			0.0	96.0	4.0
Bulgaria	57402	57402	100	17947	31.3			68.7	31.2	0.1
Croatia	22502	22502	100	22419	99.6			0.4	84.6	15.0
Cyprus	4290	4290	100	3776	88.0			12.0	73.3	14.7
Czech Republic	45117	45117	100	11148	24.7			75.3	24.7	
Denmark (no Faroes)	32042	29684	92.6		0	7.4	92.5	0.2		
Estonia	14644	2418	16.5		0	83.5	16.5			
Finland	29023	562	1.9		0	98.1	1.9			
France	327710	323600	98.7	12327	3.8	1.3	84.6	10.3	3.5	0.2
Germany	212177	203824	96.1	708	0.3	3.9	54.7	41.0	0.3	
Greece (CLC2000)	51574	51574	100	49859	96.7			3.3	46.8	49.9
Hungary	62219	62219	100	55398	89.0		0.7	10.3	89.0	
Iceland	2378					100				
Ireland	46141					100				
Italy	156491	156491	100	151353	96.7			3.3	45.9	50.8
Latvia	28253	26017	92.1			7.9	92.1	0.0		
Liechtenstein	41	41	100	2.6	6.5			93.5	6.5	
Lithuania	39815	39815	100				97.9	2.1		
Luxembourg	1389	1389	100				100			
Macedonia, FYR of	9316	9316	100	9316	100				44.4	55.6
Malta	124	124	100	124	100				18.5	81.5
Monaco	0.00									
Montenegro	2297	2297	100	2297	100				75.4	24.6
Netherlands	24238	13508	55.7			44.3	55.7			
Norway	15673	1292	8.2			91.8	8.2			
Poland	195798	195697	99.9	7890	4.0	0.1	34.8	61.1	4.0	
Portugal	41909	41780	99.7	438	1.0	0.3	65.7	32.9	1.0	
Romania	135293	135293	100	30169	22.3		6.8	70.9	22.3	0.0
San Marino	42	42	100	42	100					100
Serbia (incl. Kosovo)	48639	48639	100	47800	98.3			1.7	92.0	6.3
Slovakia	23660	23660	100	17645	74.6		1.1	24.3	74.6	
Slovenia	7104	7104	100	7104	100				78.2	21.8
Spain	251578	251182	99.8	153376	61.0	0.2	8.1	30.8	57.5	3.5
Sweden	38647	16052	41.5			58.5	41.5	0.0		
Switzerland	11806	11806	100	1711	14.5		5.7	79.8	13.8	0.7
United Kingd.(& Man)	138874	3665	2.6			97.4	2.6			
Total	**2149740**	**1857221**	**86.4**	**645747**	**30.0**	**13.6**	**31.1**	**25.3**	**23.7**	**6.4**
EU-28	**2032832**	**1757071**	**86.4**	**557865**	**27.4**	**13.6**	**32.8**	**26.2**	**21.5**	**5.9**
France over 45N	259931	255820	98.4	378	0.1	1.6	93.8	4.5	0.1	0.0
France below 45N	67779	67779	100	11950	17.6	89.0	11.0			
Kosovo	4438	4438	100	4438	100				74.3	25.7
Serbia (excl. Kosovo)	44201	44201	100	43362	98.1			1.9	93.7	4.4

Northern	198097	115840	58.5	0	0
North-western	490547	289263	59.0	378	0.1
Central & Eastern	770734	762281	98.9	158803	20.6
Southern	690362	689837	99.9	486567	70.5
Total	**2149740**	**1857221**	**86.4**	**645747**	**30.0**

Note1: Countries not included due to lack of land cover data: Andorra, Turkey.
Note2: The percentage value "0.0" indicates an exposed agricultural area exists, but is small and estimated less than 0.05 %.
Empty cells mean: no agricultural area in exposure.

Forests

The rural map with ozone indicator AOT40 for forests, as given in Figure 6.9, was combined with the land cover CLC2000 map as done for crops. Following a similar procedure as described in Horálek et al. (2007) the exposure of forest areas, defined as CORINE Land Cover level-2 class *3.1 Forests* has been calculated at the country-level.

Table 6.11 gives the absolute and relative forest area where the *Reporting Value* (RV of 20 $mg.m^{-3}.h$, as Annex III of the ozone directive defines it) in combination with the *Critical Level* (*CL* of 10 $mg.m^{-3}.h$, as defined in the UNECE Mapping Manual) are exceeded. This is done for each country, for four European regions and for Europe as a whole. The table presents the frequency distribution of the forest area per country and over the exposure classes. The Reporting Value of the ozone directive was exceeded in 2012 at some 47 % of the total European forest area. Table 6.12 (right) presents for comparison the percentages of area that exceed the Reporting Value for the years 2006 – 2012. The area above the RV for 2012 is some 6 % lower than in 2011 (53 %) and also somewhat lower than the earlier mapping years 2010 – 2007 (48 – 50 %), while in 2006 it was almost 70 % (and in 2005 about 60 %, see Horálek et al., 2008). This means that the area of forest exposed to levels above the accumulated ozone RV diminished and stabilised around 50 % in the period from 2007 to 2012, which is an area of around 20 percent points below that of 2006 and 10 percent points below that of 2005.

In 2006 about all of the European forest areas were exposed to exceedances of the Critical Level (CL) of 10 $mg.m^{-3}.h$ (while in 2005 it was the case for three-quarters of the forest areas). This extensive portion shrank in 2007 to 62 %, but in 2008 it increased to 80 %. In 2009 – 2012, the area reduced to a rather stable level ranging between 63 – 69 %, with 65 % in 2012 (Table 6.11).

Like in 2010 and 2011, in 2012 almost all European countries had their forests exposed to accumulated ozone concentrations above the CL and many of those had forest areas experiencing exposures in excess of the less stringent RV. About the same set of countries do show in 2012 no RV exceedances like in 2010 - 2011, of which for some the area with concentrations above the CL has increased and for other it decreased. As in previous years, in 2012 the southern European region continued to have AOT40 levels such that all forested areas were exposed to exceedances of the CL and approximately all of the RV. In 2012, about all forests of central and eastern regions are above the CL, of which some 81 % also above the RV.

The central and eastern regions show, for the period of 2005 – 2012, a continued (close to) 100 % exceedance of the CL. The area with exceedances of the RV (Table 6.12) showed a peak of almost 100 % in 2006, followed by a reduction to about 86 % in 2007 and a subsequent increase of about 10 % in 2008 to 95 % (which comes close to the 96 % of 2005, see Horálek et al., 2008). In 2009, the area in excess of the RV was 88 %. In 2010 it is 76 % and in 2011 it increases to 90% with a decrease to some 82 % in 2012.

In the north-western region, the area exceeding the CL increased from 84 % in 2005 to practically the whole area (98 %) in 2006. In 2007, it dropped again to 78 %, but in 2008 it increased to almost all forested area (94 %). From 2009 to 2012 the percentages fluctuate between 80 – 82 % (Table 6.11), i.e. close to the excess of 2007. Concerning the north-western European forested area above the RV, there was a prominent drop from 80% in 2006 to 28% in 2007 (after an increase from 69% in 2005) that continued in 2008 to 23 %, but increased again in 2009 to 30 % and to 60 % in 2010 and 2011. In 2012, it dropped to 20 %. Specifically in the northern region of Europe, the area in exceedance peaked considerably in 2006: the area above the CL enlarged from 40 % in 2005 to 100 % in 2006 and reduced thereafter to 12 % in 2007 and increased in 2008 to 51 %. In 2009, some 23 % of the northern European forest area exceeded the CL. In 2010, it was about 13 %, which increased in 2011 back to some 25 % and in 2012 again downward back to some 17 % (Table 6.11). The RV (Table 6.12) decreases in northern Europe from 23 % in 2006 (after an increase from none in 2005) to about none in 2007 – 2012.

Table 6.11 Forested area exposure and exceedance (critical level, CL and reporting value, RV) for ozone, AOT40 for forests, year 2012.

Country	Forested area, 2012					Percentage of forested area, 2012 [%]				
	total area	> CL (10 $mg.m^{-3}.h$)		> RV (20 $mg.m^{-3}.h$)		< 10	10 - 20	20 - 30	30 - 50	> 50
	[km^2]	[km^2]	[%]	[km^2]	[%]	$mg.m^{-3}.h$	$mg.m^{-3}.h$	$mg.m^{-3}.h$	$mg.m^{-3}.h$	$mg.m^{-3}.h$
Albania	7589	7589	100	7589	100				2.4	97.6
Austria	37223	37223	100	37136	100		0.2	28.3	71.1	0.3
Belgium	6092	5966	97.9			2.1	97.9			
Bosnia-Herzegovina	22806	22806	100	22806	100				80.9	19.1
Bulgaria	34635	34635	100	34635	100			10.0	79.9	10.1
Croatia	20094	20094	100	20094	100				77.7	22.3
Cyprus	1535	1535	100	1535	100				9.6	90.4
Czech Republic	26092	26092	100	26092	100			63.9	36.1	
Denmark (no Faroes)	3731	3359	90.0	8	0.2	10.0	89.8	0.2		
Estonia	20559	7494	36.5			63.5	36.5			
Finland	194003	969	0.5			99.5	0.5			
France	141881	141466	100	72417	51.0	0.3	48.7	28.8	20.7	1.5
Germany	104143	102889	99	62049	59.6	1.2	39.2	57.1	2.4	
Greece (CLC2000)	23561	23561	100	23561	100			0.1	71.5	28.4
Hungary	17520	17520	100	17520	100			2.4	97.5	0.0
Iceland	318	0	0			100.0				
Ireland	2835	4	0			99.9	0.1			
Italy	78246	78246	100	78246	100				66.9	33.1
Latvia	26158	26158	100.0	2	0.0		100.0	0.0		
Liechtenstein	85	85	100	85	100			20.3	79.7	
Lithuania	18728	18728	100	4616	24.6		75.4	24.6		
Luxembourg	931	931	100				100.0			
Macedonia, FYR of	8232	8232	100	8232	100				26.7	73.3
Malta	2	2	100	2	100					100.0
Monaco	0.44	0.44	100	0.44	100				100.0	
Montenegro	5736	5736	100	5736	100				41.6	58.4
Netherlands	3100	2237	72.2			27.8	72.2			
Norway	103846	15392	14.8			85.2	14.8			
Poland	93919	93919	100	66957	71.3		28.7	59.3	12.0	
Portugal	20132	20132	100	14414	71.6		28.4	68.4	3.2	
Romania	69989	69989	100	62201	88.9		11.1	44.4	44.5	
San Marino	6	6	100	6	100				100.0	
Serbia (incl. Kosovo)	26875	26875	100	26875	100				78.5	21.5
Slovakia	19683	19683	100	19683	100			13.8	86.2	
Slovenia	11471	11471	100	11471	100				53.6	46.4
Spain	90274	90265	100	80759	89.5	0.0	10.5	19.1	68.2	2.2
Sweden	243521	33330	13.7			86.3	13.7			
Switzerland	12530	12530	100	12391	99		1.1	50.6	44.8	3.5
United Kingd. (& Man)	20056	298	1.5			89.0	11.0			
Total	**1518137**	**987446**	**65.0**	**717117**	**47.2**	**35.0**	**17.8**	**17.3**	**24.7**	**5.2**
EU-28	**1330115**	**888196**	**66.8**	**633398**	**47.6**	**33.2**	**19.2**	**19.3**	**24.5**	**3.9**
France over 45N	88005	87590	99.5	24182	27.5	0.5	72.1	23.7	3.8	0.0
France below 45N	53876	53876	100.0	48235	89.5	89.0	11.0			
Kosovo	4292	4292	100	4292	100				56.9	43.1
Serbia (excl.Kosovo)	22583	22583	100	22583	100				82.7	17.3

Northern	610546	105429	17.3	4625	0.8
North-western	121336	97026	80.0	24182	19.9
Central & Eastern	415821	414566	99.7	338750	81.5
Southern	370434	370425	100.0	349560	94.4
Total	**1518137**	**987446**	**65.0**	**717117**	**47.2**

Note1: Countries not included due to lack of land cover data: Andorra, Turkey.
Note2: The percentage value "0.0" indicates an exposed forested area exists, but is small and estimated less than 0.05 %.
Empty cells mean: no forested area in exposure.

Table 6.12 Evolution of percentage agricultural area above target value for AOT40 for crops (left) and percentage forested area above reporting value for AOT40 for forests (right) in the years 2005-2012.

Country		AOT40 for crops									AOT40 for forests								
		Agricultural area above TV [%]									Forested area above RV [%]								
		2005	2006	2007	2008	2009	2010	2011	2012	diff. '12 - '11	2005	2006	2007	2008	2009	2010	2011	2012	diff. '12 - '11
Albania	AL	100	100	100	87.3	100	4.0	100	100	0	100	100	100	100	100	100	100	100	0
Austria	AT	98.6	100	81.8	67.3	4.0	40.9	32.5	59.5	26.9	100	100	100	100	100	99.7	99.7	99.8	0.1
Belgium	BE	6.4	98.0	0	0	0	0	0	0	0	74.3	99.8	7.9	0	0	33.7	35.8	0	-35.8
Bosnia-Herzegovina	BA	78.1	62.7	100	80.0	90.3	46.2	51.2	99.98	48.8	100	100	100	100	100	100	100	100	0
Bulgaria	BG	99.0	44.5	99.6	2.4	64.4	4.6	10.5	31.3	20.8	100	100	100	100	100	98.1	100	100	0
Croatia	HR	74.1	82.2	100	95.8	85.5	62.0	68.6	99.6	31.0	100	100	100	100	100	100	100	100	0
Cyprus	CY	100	99.0	100	0.0	100	87.2	90.6	88.0	-2.6	100	100	100	100	100	100	100	100	0
Czech Republic	CZ	81.4	100	83.0	99.0	0.0	8.0	4.8	24.7	19.9	100	100	100	100	100	96.4	99.7	100	0.3
Denmark	DK	0	5.3	0	0	0	0	0	0	0	5.9	91.7	0.9	1.7	1.7	0	0.9	0.2	-0.7
Estonia	EE	0	0	0	0	0	0	0	0	0	0.0	52.6	0	0	0	0	0	0	0.0
Finland	FI	0	0	0	0	0	0	0	0	0	0.0	2.1	0	0	0	0	0	0	0.0
France	FR	33.7	78.0	3.4	10.2	10.2	11.9	6.5	3.8	-2.8	92.6	97.0	50.9	48.0	52.2	85.3	85.3	51.0	-34.2
Germany	DE	33.9	94.7	3.6	62	0.0	24.4	0.3	0.3	0.0	88.6	99.8	76.9	92.8	81.0	84.0	85.1	59.6	-25.6
Greece	GR	100	95.2	97.4	79.0	95.2	44.1	77.6	96.7	19.1	100	100	100	100	100	100	100	100	0
Hungary	HU	75.2	93.4	100	82.8	83.6	7.2	15.3	89.0	73.8	100	100	100	100	100	92.6	99.95	100	0.0
Iceland	IS	*no data*		0	0	0	0	0	0	0	*no data*		0	0	0	0	0.0	0	0
Ireland	IE	0	0	0	0	0	0	0	0	0	0	0	0	0	0	0	0.0	0	0
Italy	IT	99.7	100.0	84.0	83.8	91.2	67.9	80.7	96.7	16.0	100	100	100	100	100	100	100	100	0
Latvia	LV	0	0	0	0	0	0	0	0	0	0.0	39.9	0	0	0	0	0.2	0.0	-0.2
Liechtenstein	LI	100	100	7.7	100	0	100	100.0	6.5	-93.5	100	100	100	100	100	100	100	100	0
Lithuania	LT	0	0	0	0	0	0	0	0	0	0.3	55.1	0	0	0	0	0	24.6	24.2
Luxembourg	LU	95.6	100	0	0	0	26.8	0	0	0	100	100	64.8	7.4	100	94.9	82.0	0	-82.0
Macedonia, FYR of	MK	100	100	100	99.8	100	1.3	72.1	100	27.9	100	100	100	100	100	100	100	100	0
Malta	MT	100	99	99.1	100	100	100	100	100	0	100	100	100	100	100	100	100	100	0
Monaco	MC		100	92.3	0	100	100	0	0	0		100	100	100	100	100	100	100	0
Montenegro	ME	*no data*		100	94.2	100	26.4	83.3	100	16.7	*no data*		100	100	100	100	100	100	0
Netherlands	NL	0	53.3	0	0	0	0	0	0	0	0	87.7	0	0	0	0	0	0	0
Norway	NO	*no data*		0	0	0	0	0	0	0	*no data*		0.2	0.0	0	0	0	4.0	4.0
Poland	PL	6.0	94.4	21.2	38.9	0	0	0.6	4.0	3.4	96	100	65.3	81.7	70.0	27.3	73.2	71.3	-1.9
Portugal	PT	98.7	87.7	0	2	0	41.5	4.2	1.0	-3.1	100	100	91.1	89.1	95.7	99.7	89.1	71.6	-17.5
Romania	RO	49.4	10.4	97.0	9.9	21.5	0	0.0	22.3	22.3	100.0	98.8	100	99.6	100	80.8	96.0	88.9	-7.1
San Marino	SM	100	100	100	100	100	100	100	100	0	100	100	100	100	100	100	100	100	0
Serbia (inc.Kosovo)	RS	*no data*		100	67.4	100	2.9	24.1	2.9	-21.2	*no data*		100	100	100	100	100	100	0
Slovakia	SK	76.4	99.1	99.7	78.7	58.4	0.2	25.4	74.6	49.2	100	100	100	100	100	90.8	99.8	100	0.2
Slovenia	SI	86.6	100	100	95.6	73.1	100	100	100	0	100	100	100	100	100	100	100	100	0
Spain	ES	98.7	93.3	27.2	58.5	35.1	60.7	48.4	61.0	12.6	100.0	99.4	94.3	89.8	88.4	93.3	93.1	89.5	-3.6
Sweden	SE	0	12.6	0	0	0	0	0	0	0	0.2	31.2	0.0	0	0	0	0	0	0
Switzerland	CH	*no data*			67.4	10.0	98.1	29.2	14.5	-14.7	*no data*			100	99.9	100	100	98.9	-1.1
United Kingdom	UK	0	14.4	0	0	0	0	0	0	0	0.0	11.0	0	0	0	0	0	0	0
Total		**48.5**	**69.1**	**35.7**	**37.8**	**26.0**	**21.3**	**19.2**	**30.0**	**10.8**	**59.1**	**69.4**	**48.4**	**50.2**	**49.2**	**49.3**	**53.0**	**47.2**	**-5.8**
EU-28		**47.8**	**68.9**	**33.3**	**36.3**	**23.3**	**21.4**	**18.3**	**27.4**	**9.1**	**57.9**	**68.5**	**49.4**	**51.0**	**49.9**	**49.9**	**54.2**	**47.6**	**-6.6**
Northern		0	3.6	0	0	0	0	0	0	0	0.2	22.9	0.0	0	0.0	0	0.0	0.8	0.7
North-western		11.2	49.4	0.1	2.0	2.0	33.0	1.1	0.1	-1.0	69.3	79.8	27.8	23.3	29.9	59.7	59.6	19.9	-39.7
Central & eastern		44.1	76.8	50.3	47.2	17.4	11.0	4.9	20.6	15.7	96.1	99.7	86.1	94.0	88.5	75.4	89.5	81.5	-8.0
Southern		96.2	93.9	55.3	63.5	60.4	56.8	53.6	70.5	16.9	100.0	99.7	94.2	93.1	92.8	97.8	97.2	94.4	-2.8

Note: Lack of land cover data in 2006: CH, IS, ME, NO, RS; in 2007: CH.

In comparison with 2006, the frequency distribution of the whole European forested area over the exposure classes shows for 2007 a clear shift to lower exposures. In 2008 a shift was observed of areas exposed in 2007 to the highest exposure class to its neighbouring lower class interval and for the areas exposed in 2007 to the lowest exposure class to its neighbouring higher class interval. In 2009 and 2010 the distribution showed similarity with that of 2007. In 2011 a light shift to the higher classes is observed, most prominently in the central and eastern European regions. In 2012 the overall distribution looks very familiar to that of the years 2009.

The total area with AOT40 levels below the CL diminished by 18 % in 2008 (20 %) compared to 2007 (38 %) but increased again in 2009 up to 33 % and in 2010 to 37 %. In 2011 it is with 32% about the same as in 2009. In 2012 it is with 35 % in the same range as in the years 2008 and 2009 – 2011 with percentages between 33 – 38 %. The total forested area exposed to levels below the RV fluctuated in the period 2007 – 2012 around a value of some 50 %.

6.3.3 Uncertainties

Uncertainty estimated by cross-validation

In Table 6.9 the absolute mean uncertainty (RMSE) obtained by cross-validation is 5062 $\mu g.m^{-3}.h$ for the AOT40 for crops and 8847 $\mu g.m^{-3}.h$ for the AOT40 for forests. It indicates that the year 2012 has lower absolute mean uncertainties for the crops than in its previous seven years, see Horálek et al (2014a). For forests, it is higher than the values in 2010 and 2008, and lower than the values those of 2011, 2009 and 2007 – 2005. The relative mean uncertainties of the 2012 maps are for both vegetation indicator type some 33 %. . For crops, that is higher than in 2010 (31%), 2008 (31 %) and 2006 (30 %), while lower than in 2011 (35 %), 2009 (38 %), 2007 (40 %) and 2005 (41 %). For forests, the relative RMSE is the same as in 2011, more than in 2010 and less than in the period 2009 – 2005. Table 7.7 summarises both the absolute and the relative uncertainties over these past eight years.

Figure 6.14 shows the cross-validation scatter plots of the AOT40 for both crops and forests. R^2 indicates that for both indicators about 70 % of the variability is attributable to the interpolation. The corresponding values for the previous seven years one find in Table 7.7 and demonstrate a somewhat increased level of interpolation performance in the period 2012 – 2009 compared to its previous years.

The cross-validation scatter plots show again that in areas with higher accumulated ozone concentrations the interpolation methods tend to deliver underestimated predicted values. For example, in agricultural areas (Figure 6.12, left panel) an observed value of 30 000 $\mu g.m^{-3}.h$ is estimated in the interpolation as about 26 000 $\mu g.m^{-3}.h$, i.e. an underestimation of about 13 %. In addition, an overestimation at the lower end of predicted values occurred. One could reduce this under- and overestimation by extending the number of measurement stations and by optimising the spatial distribution of those stations, specifically in areas with elevated values.

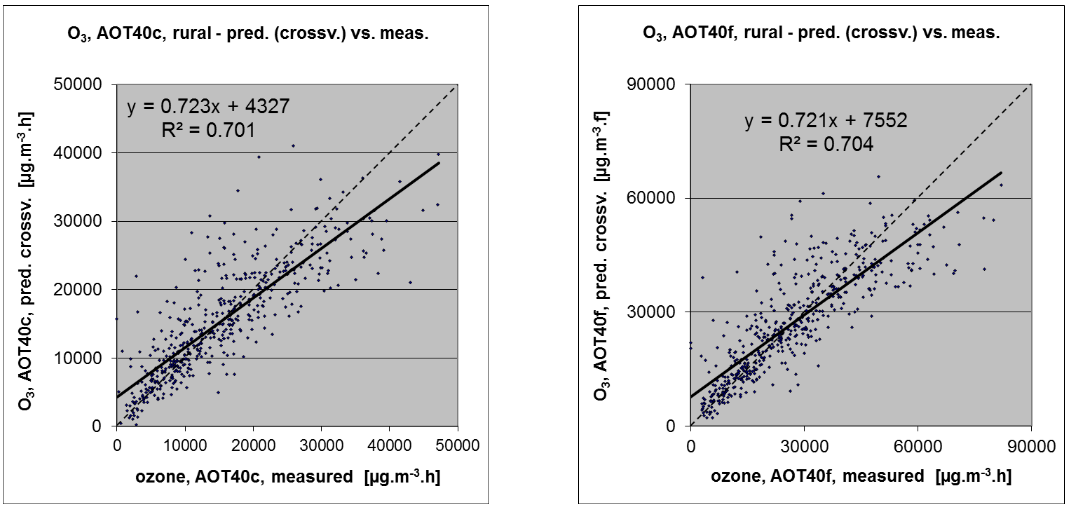

Figure 6.14 Correlation between cross-validation predicted values (y-axis) and measurements (x-axis) for the ozone indicators AOT40 for crops (left) and AOT40 for forests (right) for rural areas in 2012.

Comparison of point measurement values with the predicted grid value

In addition to the above point observation – point prediction cross-validation, a simple comparison was made between the point measurements and interpolated predicted grid values on the grid of 2x2 km resolution. The results of the cross-validation compared to the gridded validation are summarised in Table 6.13. The table shows for both receptors a better correlation between the station measurements and the averaged interpolated predicted values of the corresponding grid cells, case ii), than it does at the point cross-validation predictions, case i), of Figure 6.14. Case ii) represents the uncertainty of the predicted gridded interpolation map at the actual station locations (points) themselves, whereas the point cross-validation prediction of case i) simulates the behaviour of the interpolation at point positions assuming no actual measurements would exist at these points within the area covered by measurements. The uncertainty at measurement locations has partly its cause in the smoothing effect of interpolation and partly in the spatial averaging of the values in the 2x2 km grid cells. In such situations, the degree of smoothing leading to underestimation at areas with high values appears to be smaller than when there would be no measurement present in such areas. For example, in agricultural areas a predicted interpolation grid value will be about 27 000 µg.m^{-3}.h at a corresponding station point with an observed value of 30 000 µg.m^{-3}.h. This is an underestimation of about 9 %. %. Nevertheless, it is less than the prediction underestimation of 13 % at the same point location, when leaving out this one actual measurement point from the interpolation (see the previous subsection).

Table 6.13 Statistical indicators RMSE, bias, coefficient of determination R^2 and linear regression equation from the scatter plots for (i) the predicted point values based on cross-validation and (ii) aggregation into 2x2 km grid cells versus the measured point values for ozone indicators AOT40 for crops (left) and AOT40 for forests (right) for rural areas in 2012.

	AOT40 for crops				AOT40 for forests			
	RMSE	bias	R^2	equation	RMSE	bias	R^2	equation
(i) cross-validation prediction, rural map	8847	33	0.701	y = 0.723x + 4327	5062	72	0.704	y = 0.721x + 7552
(ii) grid prediction, 2x2 km rural map	3559	41	0.854	y = 0.806x + 3019	5664	18	0.882	y = 0.823x + 4782

The AOT40 for crops with a target value of 18 000 µg.m^{-3}.h would allow us to prepare a probability of exceedance map. However, we limited the preparation of such maps to the human health related indicators, thus not involving the accumulative ozone indicators used in the EEA CSI005 (itself not demanding such maps).

7 Concluding exposure and uncertainty estimates

Mapping and exposure results

This paper presents the interpolated maps for 2012 on the PM_{10}, $PM_{2.5}$ and ozone human health related air pollution indicators, together with their frequency distribution of the estimated population exposures and exceedances. It concerns the annual average and the 36th highest daily mean for PM_{10}, annual average for $PM_{2.5}$, and the 26th highest daily maximum 8-hour value and the SOMO35 for ozone. Interpolated maps on the vegetation/ecosystem based ozone indicators AOT40 for crops and AOT40 for forests are additionally presented, including their frequency distribution of estimated land area exposures and exceedances. A mapping approach similar to previous years (De Smet et al. 2011 and references cited therein, Denby et al. 2011c) on observational data was used. For the third time, inter-annual difference maps are presented.

Human health PM_{10} indicators

Table 7.1 summarises for both *human health PM_{10} indicators* the average concentration the European inhabitant is exposed to, i.e. the population-weighted concentration and the number of Europeans exposed to PM_{10} concentrations above their limit values (LV) for the years 2005 to 2012. The table presents the results obtained from both the 10x10 km resolution fields, as used in previous data years up to 2007 and the 1x1 km resolution grid as tested with the 2006 data in Horálek et al (2010), recomputed for 2007 and implemented fully on the 2008 data and onwards. This indicates that the underestimated predictions of PM_{10} values caused by merging rural and urban predictions at 10x10 km resolution have been resolved better when using the higher 1x1 km grid resolution. In other words, an increased merging resolution contributes to a quantitatively better population exposure estimate due to better-resolved spatially smaller urbanised patterns in the map.

Table 7.1 Percentage of the total European population exposed to PM_{10} concentrations above the limit values (LV) and the population-weighted concentration for the human health PM_{10} indicators annual average and 36th highest daily average for 2005 to 2012.

PM10			2005	2006	2007	2008	2009	2010	2011	2012
Annual average										
Population-weighted concentration	(µg.m^{-3})	10x10 merger	26.3	27.1	25.3					
		1x1 merger	28.0	28.5	26.2	24.8	24.6	24.3	22.1	22.7
Population exposed > LV (40 µg.m^{-3})	(% of total)	10x10 merger	9.3	7.7	5.7					
		1x1 merger	13.3	10.3	6.8	5.8	6.0	5.2	2.5	3.4
36th max. daily average										
Population-weighted concentration	(µg.m^{-3})	10x10 merger	43.8	45.4	42.4					
		1x1 merger	46.8	47.8	44.1	41.3	41.2	41.9	39.0	39.7
Population exposed > LV (50 µg.m^{-3})	(% of total)	10x10 merger	28.1	28.5	22.0					
		1x1 merger	34.3	35.7	26.2	19.4	16.5	20.6	15.8	16.5

The population exposed to *annual mean* concentrations of PM_{10} above the limit value of 40 µg.m^{-3} is at least 3.4 % of the total population in 2012, somewhat more than in 2011. Furthermore, it is estimated that European inhabitants living in background (neither hot-spot nor industrial) areas – without regard to urban or rural – are exposed on average to the annual mean PM_{10} concentration of about 23 µg.m^{-3}. In comparison with the previous seven years, the number of people living in the areas above the LV tends not to go down further. However, it is not possible to talk about a trend when taking into account (i) the meteorologically induced variations and (ii) the uncertainties involved in the interpolation and (iii) station densities and their spatial distributions over the European regions. Longer time series, reduced uncertainties and improved spatial coverages will be needed before any conclusions on a possible trend can be drawn. Next to this, we should bear in mind that different trends in various parts of Europe may take place. Moreover, if we do a trend-like analysis it should be based on pop-weighted concentrations as this is more robust than the fraction exposed.

In 2012 at least some 16 % of the European population lived in areas where the PM_{10} limit value of 50 µg.m^{-3} for the *36th highest daily mean* is exceeded, being almost 1 % higher than in 2011,. When comparison this quantity with those of the previous years of the given limited time series, one may conclude that it fits within the fluctuation of the past five years. The overall European population-weighted concentration of the 36th highest daily mean for the background areas is estimated to be at least 39 µg.m^{-3}, which fits in the range we observed over the past five years.

Comparing the observed (and also predicted) exceedances for both PM_{10} indicators, one may conclude that the daily limit value is more stringent throughout the years.

Human health $PM_{2.5}$ indicator

Table 7.2 summarises for *human health $PM_{2.5}$ indicator* (annual average) the population-weighted concentration and the number of Europeans exposed to $PM_{2.5}$ concentrations above its target value (TV) for the years 2007 to 2012 (without 2009, for which nor the map nor the population exposure were prepared).

Table 7.2 Percentage of the total European population exposed to $PM_{2.5}$ concentrations above the target value (TV) and the population-weighted concentration for the human health $PM_{2.5}$ indicator annual average for 2007 to 2012.

PM2.5			2007	2008	2009	2010	2011	2012
Annual average								
Population-weighted concentration	(µg.m^{-3})	10x10 merger	15.5	15.6	not mapped			
		1x1 merger	16.3	16.3		16.8	15.9	15.6
Population exposed > TV (25 µg.m^{-3})	(% of total)	10x10 merger	6.2	6.2	not mapped			
		1x1 merger	7.8	7.6		8.3	6.2	9.0

The proportion exposed to annual mean concentrations of $PM_{2.5}$ above the target value of 25 µg.m^{-3} is at least 18 % of the total population in 2012, which is bout three time higher than in all the previous years of the limited time series considered. Furthermore, it is estimated that European inhabitants living in background (neither hot-spot nor industrial) areas – without regard to urban or rural – are exposed on average to the annual mean $PM_{2.5}$ concentration of about 16 µg.m^{-3}. In comparison with the previous years, the number of people living in the areas above the TV seems to decrease just slightly.

Health related ozone indicators

Table 7.3 summarises the levels of both *human health ozone indicators* that European inhabitants are exposed to, i.e. population-weighted concentrations. Furthermore, it presents the number of Europeans exposed to concentrations above the target value (TV) of the 26th highest daily maximum 8-hour mean and above a level of 6 mg.m^{-3}.d for the SOMO35 for the years 2005 to 2012.

Table 7.3 Percentage of the total European population exposed to ozone concentrations above the target value (TV) for the 26th highest daily maximum 8-hour average and an indicative chosen threshold for SOMO35, including their population-weighted concentrations for2005 to 2012.

Ozone			2005	2006	2007	2008	2009	2010	2011	2012
26th highest daily max. 8-hr average										
Population-weighted concentration	(µg.m^{-3})	10x10 merger	112.9	119.6	112.1					
		1x1 merger	112.1	118.2	110.7	109.8	108.1	106.8	108.9	107.9
Population exposed > TV (120 µg.m^{-3}.h)	(% of total)	10x10 merger	37.8	55.5	33.5					
		1x1 merger	31.6	51.4	27.1	15.0	16.0	16.3	16.5	20.7
SOMO35										
Population-weighted concentration	(µg.m^{-3})	10x10 merger	5047	5485	4679					
		1x1 merger	4706	5167	4411	4275	4275	3917	4414	4279
Population exposed > 6 mg.m^{-3}.d	(% of total)	10x10 merger	33.9	37.4	32.6					
		1x1 merger	27.0	29.5	28.1	19.6	24.6	16.6	23.6	24.5

The table presents the results obtained with the merging resolution of 10x10 km, as used at previous data years up to 2007, and the 1x1 km merging resolution as tested on the 2006 data in Horálek et al (2010) and implemented fully on the 2008 data and onwards. It provides an indication that the underestimation of ozone values when merged with the 10x10 km grid resolution has been resolved better when using a higher 1x1 km grid resolution. In other words, an increased merging resolution contributes to a quantitatively better population exposure estimate due to better-resolved spatially smaller urbanised patterns in the map.

For the ozone indicator *26th highest daily maximum 8-hour mean* it is estimated that at least 20 % of the population lived in 2012 in areas above the ozone target value (TV) of 120 $\mu g.m^{-3}$, which is higher than in its four previous years. The overall European population-weighted ozone concentration in terms of the 26th highest daily maximum 8-hour mean in the background areas is estimated at almost 108 $\mu g.m^{-3}$, which is within the range of values of the four earlier years of the recorded time series. Examining the time series 2005 – 2012, one could conclude that 2006 is an exceptional year with elevated ozone concentrations, leading to increased exposure levels compared to the other eight years. Additionally, the population exposed to ozone level above the target value is in the period 2008 – 2012 lower than in the preceding period of 2007 – 2005.

A similar tendency is observed for the *SOMO35*: In 2006 – 2007 almost one-third of the population lived in areas where a level of 6 $mg.m^{-3}.d$[(*)] was exceeded, with the highest level in 2006. In the period of 2008 – 2012 it fluctuates between about one-fifth to a quarter of the population. The population-weighted SOMO35 concentrations shows a quite similar kind of pattern over time.

(*) Note that the 6 $mg.m^{-3}.d$ does not represent a health-related legally binding 'threshold'. In this and previous papers it concerns a somewhat arbitrarily chosen threshold to facilitate the discussion of the observed distributions of SOMO35 levels in their spatial and temporal context. For motivation of this choice, see Section 6.2.2.

Agricultural and forest ozone indicators

Exposure indicators describing the *agricultural and forest areas exposed to accumulated ozone* concentrations above defined thresholds are summarised in Table 7.4. Those thresholds are the target value (TV) of 18 $mg.m^{-3}.h$ and the long-term objective (LTO) of 6 $mg.m^{-3}.h$ for the AOT40 for crops, and the Reporting Value (RV) of 20 $mg.m^{-3}.h$ and the Critical Level (CL) of 10 $mg.m^{-3}.h$ for the AOT40 for forests.

Table 7.4 Percentages of the total European agricultural and forest area exposed to ozone concentrations above their thresholds: target value (TV) and long-term objective (LTO) for AOT40 for crops, and Critical Level (CL) and Reporting Value (RV) for AOT40 for forests for2005 to 2012.

Ozone		2005	2006	2007	2008	2009	2010	2011	2012
AOT40 for crops									
Agricultural area % > TV (18 $mg.m^{-3}.h$)	(% of total)	48.5	69.1	35.7	37.8	26.0	21.3	19.2	13.6
Agricultural area % > LTO (6 $mg.m^{-3}.h$)	(% of total)	88.8	97.6	77.5	95.5	81.0	85.4	87.9	86.4
AOT40 for forests									
Forest area exposed > RV (20 $mg.m^{-3}.h$)	(% of total)	59.1	69.4	48.4	50.2	49.2	49.3	53.0	47.2
Forest area exposed > CL (10 $mg.m^{-3}.h$)	(% of total)	76.4	99.8	62.1	79.6	67.4	63.4	68.6	65.0

In 2012, at least 13 % of all agricultural land (*crops*) was exposed to accumulated ozone concentrations (AOT40) exceeding the target value (TV) and 86 % was exposed to levels in excess of the long-term objective (LTO). Compared to the previous seven years one could conclude that 2006 was a year with elevated ozone concentrations, leading to increased exposure levels above the target value. One the one hand, from 2007 and onward the total area exceeding the TV reduced continuously. On the other hand, the percentage of the total area exposed to levels above the LTO is in 2007 lowest compared to all the other years of the time series 2005 – 2012, and in the period 2008 – 2012 it ranges between 81 – 88 %, not demonstrating the same reduction as observed at the TV exceedance.

For the ozone indicator AOT40 for *forests* the level of 20 $mg.m^{-3}.h$ (Reporting Value, RV) was in 2012 exceeded in about 47 % of the European forest area, which is the lowest of the whole time series and clearly below the percentages of the years 2005 and 2006. The forest area exceeding the Critical Level (CL) was in 2012 about 65 %, which is within the range of exceedances between 62 – 67 % as observed for the years 2007 and 2009 – 2012 and well below the exceedances of 2008 and 2005 (with 76 – 80 %), and 2006 when all forest area was exceeded.

The temporal pattern of the AOT40 for forests exceedances shows some similarity with those of the AOT40 for crops, despite their different definitions. This annual variability is, however, heavily dependent on meteorological variability.

Uncertainty results

Next to the creation of European wide interpolated air pollutant maps and exposure tables, we evaluated the uncertainty of the presented concentration maps and maps with estimated probability of threshold exceedance for the human health indicators. As the same method and data sources have been applied over the years 2005 to 2012, a change in uncertainty is in principle related to the data content itself. However, for the 2008 data we implemented for the first time an increased resolution (from a 10x10 km into 1x1 km grid field) at the merging of the separate human health indicator interpolated maps (on 10x10 km grid) into one combined final 1x1 km gridded indicator map. The merging made use of the 1x1 km population density map. (The subsequent exposure estimates however, have been based on the 10x10 km grid fields aggregated from the 1x1 km grids of the merging result). The increased merging resolution should in principle improve the accuracy in the concentration maps, including the subsequent exposure estimates. Denby et al. (2009) discusses a diversity of uncertainty factors potentially involved, including their possible levels of influence. More background information on causes of uncertainties and their assessment can be found in Malherbe et al (2012). The paper recommends options to reduce uncertainties systematically. Horálek et al. (2010) explored specific options to reduce interpolation uncertainty related to the spatial resolutions applied at the different process steps of the mapping method. This paper concludes and justifies the implementation of the increased merging grid as the most significant uncertainty reduction measure, against the least additional computational demands. For further reading on the sub-grid variability and its influence to the exposure estimates, see Denby et al. (2011a).

Table 7.5 summarises the absolute and relative mean interpolation uncertainties, and additionally also R^2 from cross-validation scatterplot for the PM_{10} maps for the eight-year sequence. The higher uncertainty levels for urban areas in the years 2008 – 2012, compared to the years 2005 – 2007, are caused specifically by addition of Turkish urban background stations reported only since 2008.

Table 7.5 Absolute mean uncertainty (RMSE, $\mu g.m^{-3}$), relative mean uncertainty (RMSE relative to mean indicator value, in %) and R^2 from cross-validation scatterplot for the total European rural and urban areas for PM_{10} annual average and the 36^{th} highest daily average for the years 2005 – 2012.

PM10			2005	2006	2007	2008	2009	2010	2011	2012
Annual average										
rural areas	abs. mean uncertainty	RMSE [$\mu g.m^{-3}$]	5.5	5.8	4.6	5.0	4.6	4.5	4.1	3.8
	rel. mean uncertainty	RRMSE [%]	*25.9*	*26.6*	*23.5*	*27.2*	*23.9*	*22.7*	*21.1*	*21.4*
	coeff. of determination	R^2	*0.52*	*0.52*	*0.59*	*0.48*	*0.54*	*0.62*	*0.68*	*0.67*
urban areas	abs. mean uncertainty	RMSE [$\mu g.m^{-3}$]	5.5	6.1	5.0	6.3	6.7	6.6	6.1	6.1
	rel. mean uncertainty	RRMSE [%]	*20.0*	*20.9*	*18.4*	*22.4*	*23.0*	*22.5*	*20.7*	*22.1*
	coeff. of determination	R^2	*0.71*	*0.69*	*0.66*	*0.82*	*0.73*	*0.75*	*0.77*	*0.76*
36^{th} max. daily average										
rural areas	abs. mean uncertainty	RMSE [$\mu g.m^{-3}$]	9.7	9.9	8.0	8.8	8.0	8.6	8.4	7.7
	rel. mean uncertainty	RRMSE [%]	*26.3*	*26.6*	*23.5*	*28.2*	*24.1*	*24.4*	*23.5*	*24.5*
	coeff. of determination	R^2	*0.55*	*0.56*	*0.60*	*0.52*	*0.56*	*0.64*	*0.66*	*0.64*
urban areas	abs. mean uncertainty	RMSE [$\mu g.m^{-3}$]	9.9	11.7	9.1	12.7	13.2	12.2	13.0	11.9
	rel. mean uncertainty	RRMSE [%]	*21.4*	*23.5*	*19.6*	*24.4*	*26.7*	*23.7*	*24.3*	*24.5*
	coeff. of determination	R^2	*0.75*	*0.65*	*0.65*	*0.79*	*0.72*	*0.77*	*0.75*	*0.75*

Table 7.6 presents the uncertainty results for $PM_{2.5}$ maps for the years 2007 – 2012 (excluding the 'non-mapped' year 2009). Both absolute and relative uncertainties show for 2012 worse results than in 2011, quite similar results as in 2010, and better results than in 2007 – 2008.

Table 7.6 Absolute and relative mean uncertainty and R^2 from cross-validation scatterplot for the total European rural and urban areas for $PM_{2.5}$ annual average, for the years 2007 – 2012.

PM2.5			2007	2008	2009	2010	2011	2012
Annual average								
rural areas	abs. mean uncertainty	RMSE [μg.m^{-3}]	3.3	3.5	not mapped	3.4	2.8	3.0
	rel. mean uncertainty	RRMSE [%]	*27.4*	*29.8*		*25.0*	*16.8*	*24.9*
	coeff. of determination	R^2				*0.74*	*0.82*	*0.78*
urban areas	abs. mean uncertainty	RMSE [μg.m^{-3}]	4.1	3.6	not mapped	3.1	3.2	3.3
	rel. mean uncertainty	RRMSE [%]	*23.7*	*20.0*		*16.8*	*16.7*	*18.7*
	coeff. of determination	R^2				*0.81*	*0.80*	*0.78*

The mean interpolation uncertainty of the ozone maps in Table 7.7 at the rural areas decreased slightly for the majority of the indicators in 2012, compared to previous year 2011. The exception is the 26th highest daily maximum 8-hour average with a slight increase in both absolute and relative uncertainties, and the AOT40 for forests with a slight increase in relative uncertainty. For the urban areas, the absolute uncertainties of the 2012 maps show quite similar results like in previous years, while the relative uncertainties show slight increase in comparison with the years 2010 and 2011.

Table 7.7 Absolute and relative mean uncertainty and R^2 from cross-validation scatterplot for the total European areas for ozone the 26th highest daily maximum 8-hour average, SOMO35, AOT40 for crops and for forests, for the years 2005 – 2012.

Ozone			2005	2006	2007	2008	2009	2010	2011	2012
26th highest daily max. 8-hr average										
rural areas	abs. mean uncertainty	RMSE [μg.m^{-3}]	12.3	11.2	8.8	8.7	8.2	8.9	8.4	8.5
	rel. mean uncertainty	RRMSE [%]	*10.3*	*8.9*	*7.5*	*7.6*	*7.2*	*7.7*	*7.2*	*7.4*
	coeff. of determination	R^2	*0.51*	*0.49*	*0.71*	*0.56*	*0.69*	*0.68*	*0.67*	*0.71*
urban areas	abs. mean uncertainty	RMSE [μg.m^{-3}]	10.0	10.2	8.9	8.8	9.3	9.2	9.1	9.1
	rel. mean uncertainty	RRMSE [%]	*8.9*	*8.4*	*7.9*	*7.9*	*8.4*	*8.2*	*8.1*	*8.3*
	coeff. of determination	R^2	*0.50*	*0.53*	*0.66*	*0.61*	*0.64*	*0.71*	*0.66*	*0.70*
SOMO35										
rural areas	abs. mean uncertainty	RMSE [μg.m^{-3}.d]	2 173	2 077	1 801	1 609	1 635	1 608	1 747	1 633
	rel. mean uncertainty	RRMSE [%]	*35.5*	*31.6*	*33.3*	*30.7*	*29.7*	*29.6*	*29.6*	*29.2*
	coeff. of determination	R^2	*0.55*	*0.47*	*0.63*	*0.63*	*0.63*	*0.62*	*0.63*	*0.68*
urban areas	abs. mean uncertainty	RMSE [μg.m^{-3}.d]	1 459	1 472	1 260	1 293	1 475	1 278	1 374	1 362
	rel. mean uncertainty	RRMSE [%]	*32.0*	*29.2*	*29.5*	*31.3*	*33.1*	*29.6*	*29.7*	*31.7*
	coeff. of determination	R^2	*0.58*	*0.49*	*0.67*	*0.54*	*0.62*	*0.65*	*0.66*	*0.67*
AOT40 for crops										
rural areas	abs. mean uncertainty	RMSE [μg.m^{-3}.h]	7 677	7 674	5 876	5 283	5 138	5 198	5 263	5 062
	rel. mean uncertainty	RRMSE [%]	*40.7*	*29.6*	*39.6*	*31.3*	*37.7*	*30.8*	*34.9*	*32.9*
	coeff. of determination	R^2	*0.58*	*0.53*	*0.63*	*0.53*	*0.69*	*0.67*	*0.62*	*0.70*
AOT40 for forests										
rural areas	abs. mean uncertainty	RMSE [μg.m^{-3}.h]	12 474	11 990	10 190	8 750	9 304	8 384	9 341	8 847
	rel. mean uncertainty	RRMSE [%]	*41.5*	*33.6*	*37.1*	*34.0*	*33.9*	*31.4*	*32.7*	*32.8*
	coeff. of determination	R^2	*0.55*	*0.49*	*0.67*	*0.56*	*0.68*	*0.69*	*0.67*	*0.70*

The scatter plots of the interpolation results versus the measurements show that for both the PM_{10} and the ozone indicators, in areas with high values, an underestimation of the predicted values occurs. This also leads to a considerable underestimation at locations without measurements and at areas with the higher concentrations. This effect occurs most prominently for the ozone indicators. We expect that the underestimation would reduce when an improved fit of the linear regression with (other) supplementary data could be obtained. For example, in the near future more contributions from satellite imagery data and interpretation techniques could be expected. An option is to extend the number of measurement stations and/or using additional mobile stations. Another possibility is the use of more advanced chemical transport model. For further reading on this subject, we refer to Denby et al. (2009), Gräler et al. (2013), Schneider et al. (2012), Castell et al (2013) and Horálek et al (2014b).

Probability of exceedance

Maps with the probability of exceedance of Limit Values and Target Value have been prepared for the human health indicators of PM_{10}, $PM_{2.5}$, and ozone, respectively. These probability maps, with a class distribution as defined in Table 4.5, are derived from combining the indicator map and its uncertainty map following the same method throughout the years 2005 to 2011. The differences in the maps between years depend on annual fluctuations in concentration levels, supplementary data and their involved uncertainties (Denby et al. 2009, Gräler et al. 2012, 2013). Some disruption or 'jump' could be expected between the data of 2005 – 2007 and 2008 – 2012. This would be caused by the increased merging resolution applied for the first time on the 2008 data. As Horálek et al. (2010) indicated, it should improve the population exposure estimates, specifically for population living in urban areas (that profit most of this methodological refinement). Nevertheless, as the maps are spatially merged into 10x10 km grid resolution, the influence of the urban pollution into the final map is smaller than was in the methodology used until 2007. Thus, it is needed to bear in mind that the spatial average of a 10x10 km grid cell can show low probability of exceedance even though some smaller (e.g. urban) areas inside such a grid cell would show high probability of exceedance (in case of using a finer grid cell resolution).

In 2012 for the annual average PM_{10}, the patterns in the spatial distribution of the different probability of exceedance (PoE) classes over Europe were somewhat reduced to those of 2011. The Po Valley in Italy shows a considerable reduced probability of exceedance compared to 2011. The region of southern Poland – north-eastern Czech Republic shows in 2012 slightly smaller area with the highest PoE compared to 2011. In south-eastern Europe, only somewhat elevated PoE do show up at a few cities. In comparison with 2011, their number has reduced considerably. In other parts of Europe there exists just little likelihood of exceedance, with the exception of the area around Almería, Spain, where a high likelihood of exceedance appears to exist.

The 36th highest daily means of PM_{10} do show a decrease in the spatial extents and PoE levels throughout south-eastern Europe, in comparison with 2011. The Po Valley in northern Italy has quite a similar PoE pattern to 2010 and has slightly reduced PoE pattern compared to 2011. Throughout the years 2009 – 2012, areas with continued increased PoE levels do occur in southern Poland and north-eastern Czech Republic. The increased levels of PoE area around Almería, southern Spain, has extended in 2012 compared to the years 2009 – 2011.

PoE map for $PM_{2.5}$ shows the highest probability of TV exceedance in the Po Valley in northern Italy, the region of southern Poland – north-eastern Czech Republic, the cities in the central part of Poland, and big cities in south-eastern Europe. In comparison with 2011, the reduction of the areas with elevated levels of PoE took place in all these areas.

In the case of ozone, one can conclude that in the southern and south-eastern Europe, the PoE increased considerably in its level in 2012 compared to 2011. On the Iberian Peninsula we observe in the more eastern part of the Spain some increases of areas with large PoE and further decreases in the more western part of the peninsula. This is in agreement with the inter-annual general decrease of the ozone concentrations in the northwest of Europe and their general increase in the southeast of Europe.

References

AirBase, European air quality database, http://acm.eionet.europa.eu/databases/airbase/index_html

Castell N, Viana M, Minguillón M C, Guerreiro C, Querol X (2013). Real-world application of new sensor technologies for air quality monitoring. ETC/ACM Technical Paper 2013/16. http://acm.eionet.europa.eu/reports/ETCACM_TP_2013_16_new_AQ_SensorTechn

Cressie N (1993). Statistics for spatial data. Wiley series, New York.

Danielson JJ, Gesch DB (2011). Global multi-resolution terrain elevation data 2010 (GMTED2010): U.S. Geological Survey Open-File Report 2011–1073. https://lta.cr.usgs.gov/GMTED2010

Denby B, Schaap M, Segers A, Builtjes P, Horálek J (2008). Comparison of two data assimilation methods for assessing PM_{10} exceedances on the European scale. Atmospheric Environment 42, 7122–7134.

Denby B, De Leeuw F, De Smet P, Horálek J (2009). Sources of uncertainty and their assessment in spatial mapping. ETC/ACC Technical Paper 2008/20. http://acm.eionet.europa.eu/reports/ETCACC_TP_2008_20_spatialAQ_uncertainties

Denby B, Cassiani M, de Smet P, de Leeuw F, Horálek J (2011a). Sub-grid variability and its impact on European wide air quality exposure assessment. Atmospheric Environment 45, 4220-4229.

Denby B, Gola G, De Leeuw F, De Smet P, Horálek J (2011b). Calculation of pseudo $PM_{2.5}$ annual mean concentrations in Europe based on annual mean PM10 concentrations and other supplementary data. ETC/ACC Technical Paper 2010/9. http://acm.eionet.europa.eu/reports/ETCACC_TP_2010_9_pseudo_PM2.5_stations

Denby B, Horálek J, de Smet P, de Leeuw F (2011c). Mapping annual mean $PM_{2.5}$ concentrations in Europe: application of pseudo $PM_{2.5}$ station data. ETC/ACM Technical Paper 2011/5. http://acm.eionet.europa.eu/reports/ETCACM_TP_2011_5_spatialPM2.5mapping

De Smet P, Horálek J, Coňková M, Kurfürst P, de Leeuw F, Denby B (2009). European air quality maps of ozone and PM_{10} for 2006 and their uncertainty analysis. ETC/ACC Technical Paper 2008/8. http://acm.eionet.europa.eu/reports/ETCACC_TP_2008_8_spatAQmaps_2006

De Smet P, Horálek J, Coňková M, Kurfürst P, de Leeuw F, Denby B (2010). European air quality maps of ozone and PM_{10} for 2007 and their uncertainty analysis. ETC/ACC Technical Paper 2009/9. http://acm.eionet.europa.eu/reports/ETCACC_TP_2009_9_spatAQmaps_2007

De Smet P, Horálek J, Coňková M, Kurfürst P, de Leeuw F, Denby B (2011). European air quality maps of ozone and PM_{10} for 2008 and their uncertainty analysis. ETC/ACC Technical Paper 2010/10. http://acm.eionet.europa.eu/reports/ETCACC_TP_2010_10_spatAQmaps_2008

De Smet P, Horálek J, Schreiberová M, Kurfürst P, de Leeuw F (2012). European air quality maps of ozone and PM_{10} for 2009 and their uncertainty analysis. ETC/ACM Technical Paper 2011/11. http://acm.eionet.europa.eu/reports/ETCACM_TP_2011_11_spatAQmaps_2009

EC (2008). Directive 2008/50/EC of the European Parliament and of the Council of 21 May 2008 on ambient air quality and cleaner air for Europe. OJ L 152, 11.06.2008, 1-44. http://eur-lex.europa.eu/LexUriServ/LexUriServ.do?uri=OJ:L:2008:152:0001:0044:EN:PDF

ECMWF: Meteorological Archival and Retrieval System (MARS). http://www.ecmwf.int/

EEA (2008). ORNL Landscan 2008 Global Population Data conversion into EEA ETRS89-LAEA5210 1km grid (eea_r_3035_1_km_landscan-eurmed_2008, by Hermann Peifer of EEA).

EEA (2011). Guide for EEA map layout. EEA operational guidelines. August 2011, version 4. http://www.eionet.europa.eu/gis/docs/GISguide_v4_EEA_Layout_for_map_production.pdf

EEA (2013b). Corine land cover 2006 (CLC2006) raster data. 100x100m gridded version 17 (12/2013) http://www.eea.europa.eu/data-and-maps/data/corine-land-cover-2006-raster-3

EEA (2013b). Corine land cover 2006 (CLC2006) raster data. 100x100m gridded version 16 (04/2012). http://www.eea.europa.eu/data-and-maps/data/corine-land-cover-2006-raster-2

EEA (2014). Air quality in Europe – 2014 report. EEA Report 5/2014. http://acm.eionet.europa.eu/reports/EEA_Rep_5_2014_AQinEurope

Eurostat (2014). Total population for European states for 2012. http://epp.eurostat.ec.europa.eu/tgm/table.do?tab=table&language=en&pcode=tps00001&tableSelection=1&footnotes=yes&labeling=labels&plugin=1

EMEP (2014). Transboundary particular matter, photo-oxidants, acidifying and eutrophying components. EMEP Report 1/2014. http://emep.int/publ/reports/2014/EMEP_Status_Report_1_2014.pdf
Gräler B, Gerharz L, Pebesma E (2012). Spatio-temporal analysis and interpolation of PM_{10} measurements in Europe. ETC/ACM Technical Paper 2011/10. http://acm.eionet.europa.eu/reports/ETCACM_TP_2011_10_spatio-temp_AQinterpolation
Gräler B, Rehr M, Gerharz L, Pebesma E (2013). Spatio-temporal analysis and interpolation of PM10 measurements in Europe for 2009. ETC/ACM Technical Paper 2012/8. http://acm.eionet.europa.eu/reports/ETCACM_2012_8_spatio-temp_PM10analyses
Horálek J, Kurfürst P, Denby B, de Smet P, de Leeuw F, Brabec M, Fiala J (2005). Interpolation and assimilation methods for European scale air quality assessment and mapping. Part II: Development and testing new methodologies. ETC/ACC Technical paper 2005/8. http://acm.eionet.europa.eu/docs/ETCACC_TechnPaper_2005_8_SpatAQ_Part_II.pdf
Horálek J, Denby B, de Smet P, de Leeuw F, Kurfürst P, Swart R, van Noije T (2007). Spatial mapping of air quality for European scale assessment. ETC/ACC Technical paper 2006/6. http://acm.eionet.europa.eu/reports/ETCACC_TechnPaper_2006_6_Spat_AQ
Horálek J, de Smet P, de Leeuw F, Denby B, Kurfürst P, Swart R (2008). European air quality maps for 2005 including uncertainty analysis. ETC/ACC Technical paper 2007/7. http://acm.eionet.europa.eu/reports/ETCACC_TP_2007_7_spatAQmaps_ann_interpol
Horálek J, de Smet P, de Leeuw F, Coňková M, Denby B, Kurfürst P (2010). Methodological improvements on interpolating European air quality maps. ETC/ACC Technical Paper 2009/16. http://acm.eionet.europa.eu/reports/ETCACC_TP_2009_16_Improv_SpatAQmapping
Horálek J, de Smet P, Corbet L, Kurfürst P, de Leeuw F (2013). European air quality maps of PM and ozone for 2010 and their uncertainty. ETC/ACM Technical Paper 2012/12. http://acm.eionet.europa.eu/reports/ETCACM_TP_2012_12_spatAQmaps_2010
Horálek J, de Smet P, Kurfürst P, de Leeuw F, Benešová N (2014a). European air quality maps of PM and ozone for 2011 and their uncertainty. ETC/ACM Technical Paper 2013/13. http://acm.eionet.europa.eu/reports/ETCACM_TP_2013_13_spatAQmaps_2011
Horálek J, Tarrasón L, de Smet P, Malherbe L, Schneider P, Ung A, Corbet L, Denby B (2014b). Evaluation of Copernicus MACC-II ensemble products in the ETC/ACM spatial air quality mapping. ETC/ACM Technical Paper 2013/9. http://acm.eionet.europa.eu/reports/ETCACM_TP_2013_9_AQmaps_with_MACCproducts
JRC (2009). Population density disaggregated with Corine land cover 2000. 100x100 m grid resolution, EEA version pop01clcv5.tif of 24 Sep 2009. http://www.eea.europa.eu/data-and-maps/data/population-density-disaggregated-with-corine-land-cover-2000-2
Malherbe L, Ung A, Colette A, Debry E (2012). Formulation and quantification of uncertainties in air quality mapping. ETC/ACM Technical Paper 2001/9. http://air-climate.eionet.europa.eu/reports/ETCACM_TP_2011_9_AQmapping_uncertainties
Mareckova K, Wankmüller R, Moosman L, Pinterits M, Tista M (2014). Inventory Review 2014. Review of emission data reported under the LRTAP Convention and NEC Directive. Stage 1 and 2 review & Status of gridded and LPS data. EEA/CEIP Technical Report 1/2014. http://www.ceip.at/fileadmin/inhalte/emep/pdf/2014/DP-143_InventoryReport_2014_forWeb.pdf
NILU (2013). EBAS, database of atmospheric chemical composition and physical properties (NILU, Norway). http://ebas.nilu.no/
ORNL (2008). ORNL LandScan high resolution global population data set. http://www.ornl.gov/sci/landscan/landscan_documentation.shtml
Schneider P, Tarrasón L, Guerreiro C, (2012), The potential of GMES satellite data for mapping nitrogen dioxide at the European scale, ETC/ACM Technical Paper 2012/9. acm.eionet.europa.eu/reports/ETCACM_TP_2012_9_GMESsatdata_NOx_Euromap
Simpson D, Benedictow A, Berge H, Bergström R, Emberson LD, Fagerli H, Hayman GD, Gauss M, Jonson JE, Jenkin ME, Nyíri A, Richter C, Semeena VS, Tsyro S, Tuovinen J-P, Valdebenito A, Wind P (2012). The EMEP MSC-W chemical transport model – technical description. Atmospheric Chemistry and Physics, 12, 7825–7865, doi:10.5194/acp-12-7825-2012.

Simpson D, Schulz M, Semeena VS, Tsyro S, Valdebenito Á, Wind P, Steensen BM (2013). EMEP model development and performance changes. Simpson D, Tsyro S, Wind P, Steensen BM (2013). EMEP model development. In: Transboundary acidification, eutrophication and ground level ozone in Europe in 2011, EMEP Report 1/2013. http://emep.int/publ/reports/2013/EMEP_status_report_1_2013.pdf

UNECE (2004). Manual on methodologies and criteria for modelling and mapping critical loads and levels and air pollution effects, risks and trends. UNECE Convention on Long-range Transboundary Air Pollution. http://www.icpmapping.org/Mapping_Manual

UN (2010). World Population Prospects – The 2010 Revision, Highlights. United Nations. Department of Economic and Social Affairs, Population Division. http://esa.un.org/unpd/wpp/index.htm

WHO (2005). WHO Air quality guidelines for particulate matters, ozone, nitrogen dioxide and sulphur dioxide. Global update 2005. http://www.who.int/phe/health_topics/outdoorair/outdoorair_aqg/en/index.html

Annex 1 Urban background maps

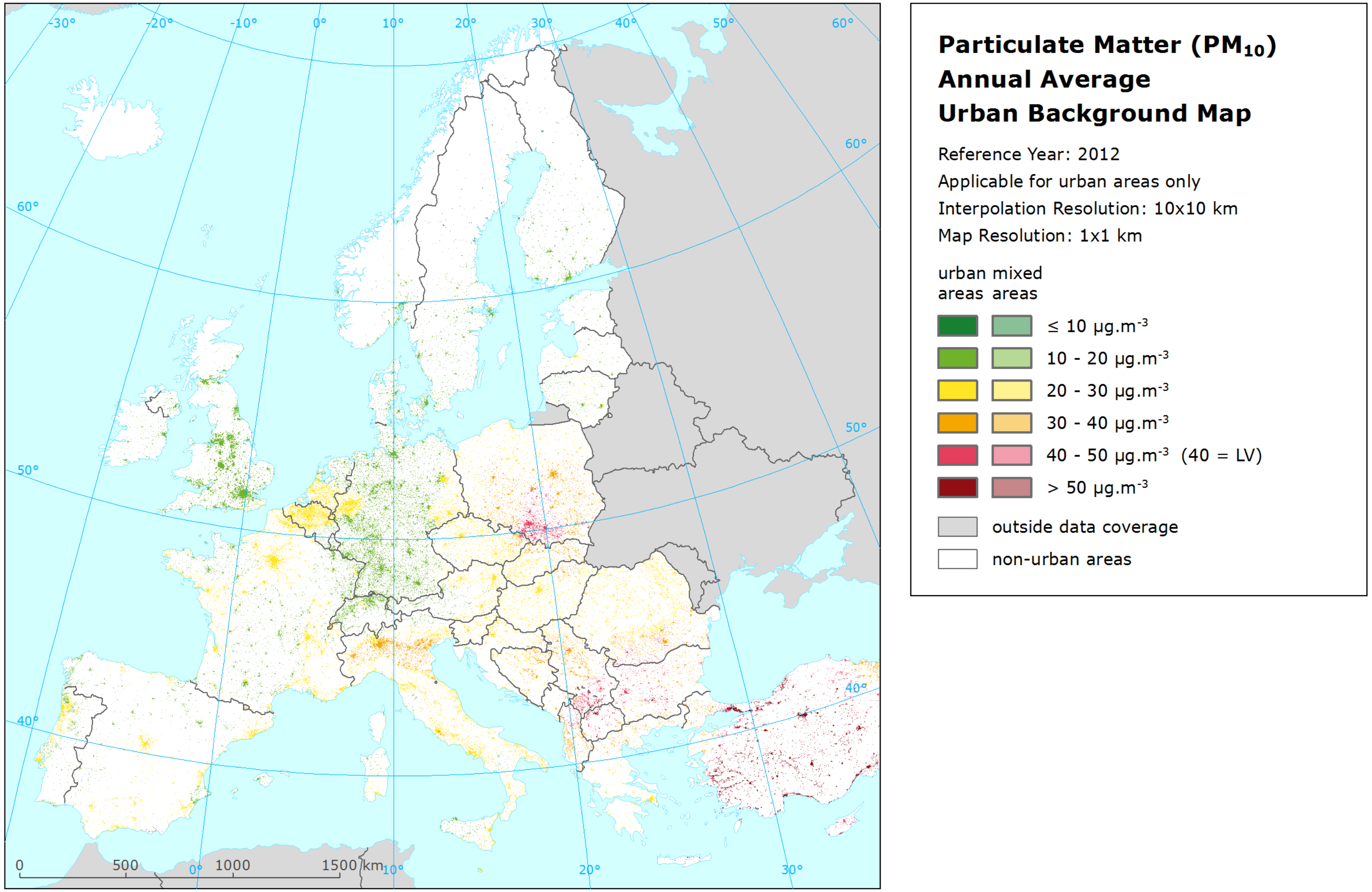

Figure A1.1 Urban background concentration map of PM_{10} – annual average, year 2012. Spatial interpolated concentration field (10x10 km grid resolution) in urban areas (1x1 km grid resolution). Units: µg.m^{-3}. Applicable for urban areas only.

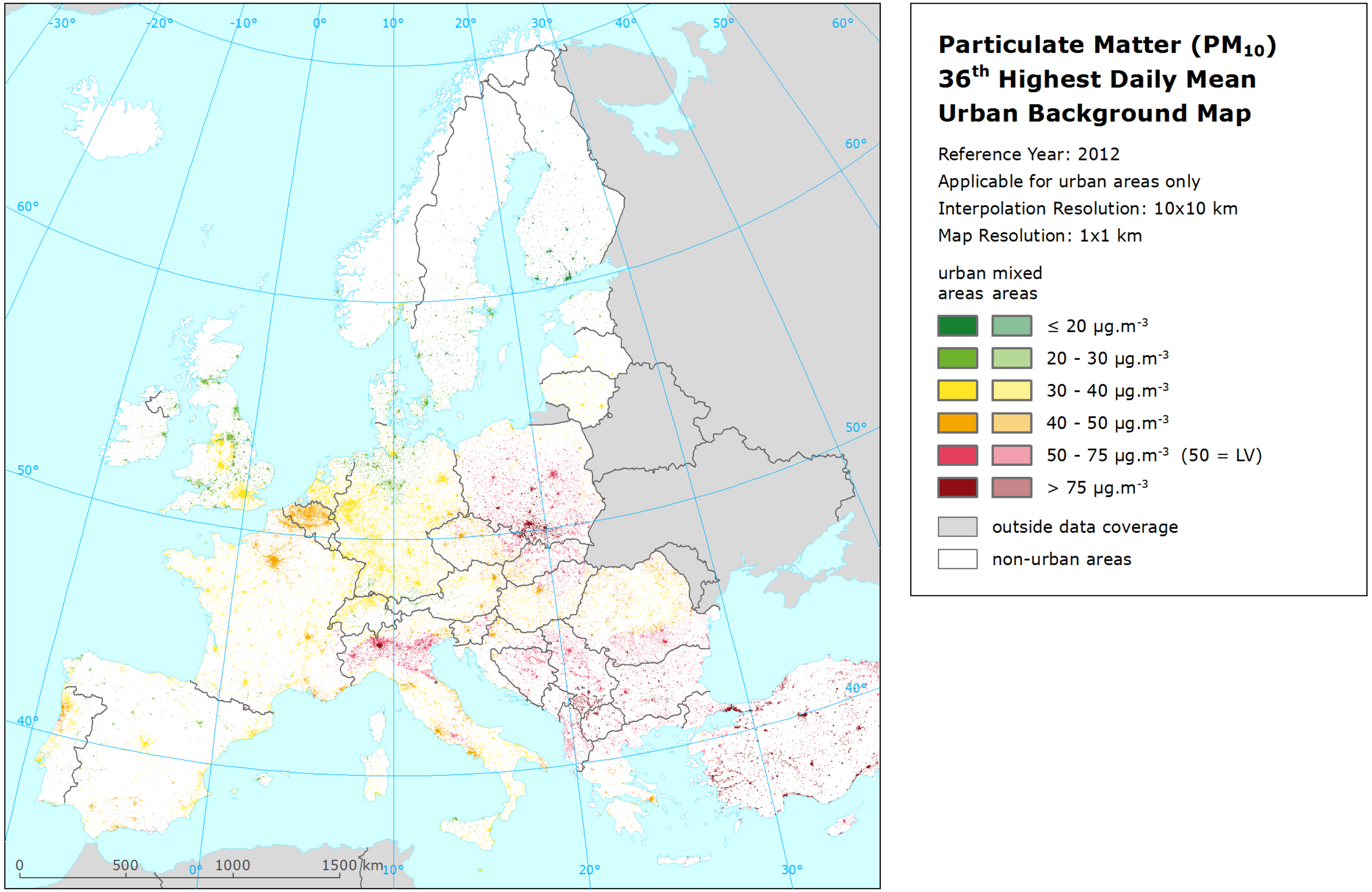

Figure A1.2 Urban background concentration map of PM_{10} – 36^{th} highest daily average value, year 2012. Spatial interpolated concentration field (10x10 km grid resolution) in urban areas (1x1 km grid resolution). Units: $\mu g.m^{-3}$. Applicable for urban areas only.

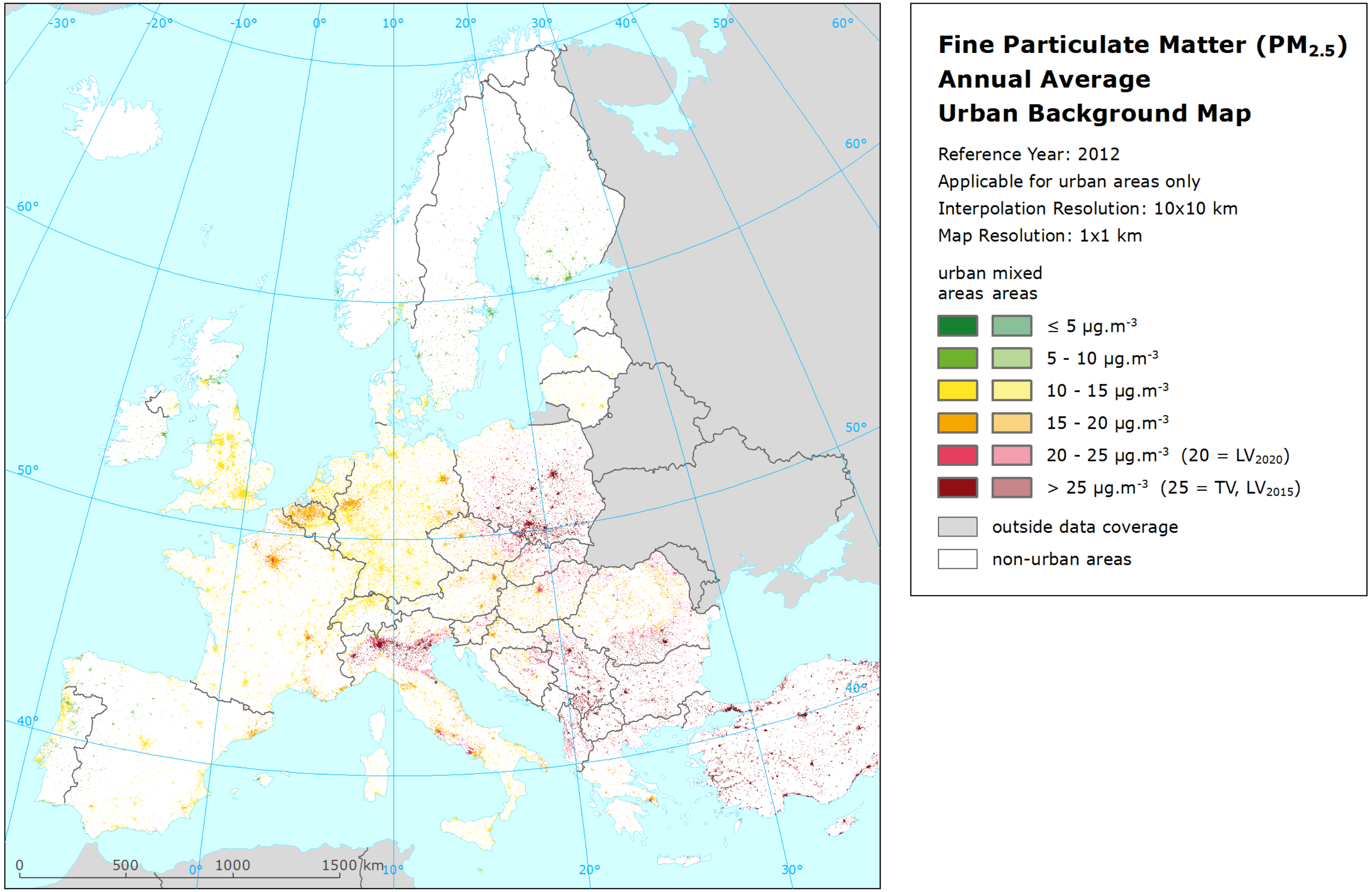

Figure A1.3 Urban background concentration map of $PM_{2.5}$ – annual average, year 2012. Spatial interpolated concentration field (10x10 km grid resolution) in urban areas (1x1 km grid resolution). Units: µg.m^{-3}. Applicable for urban areas only.

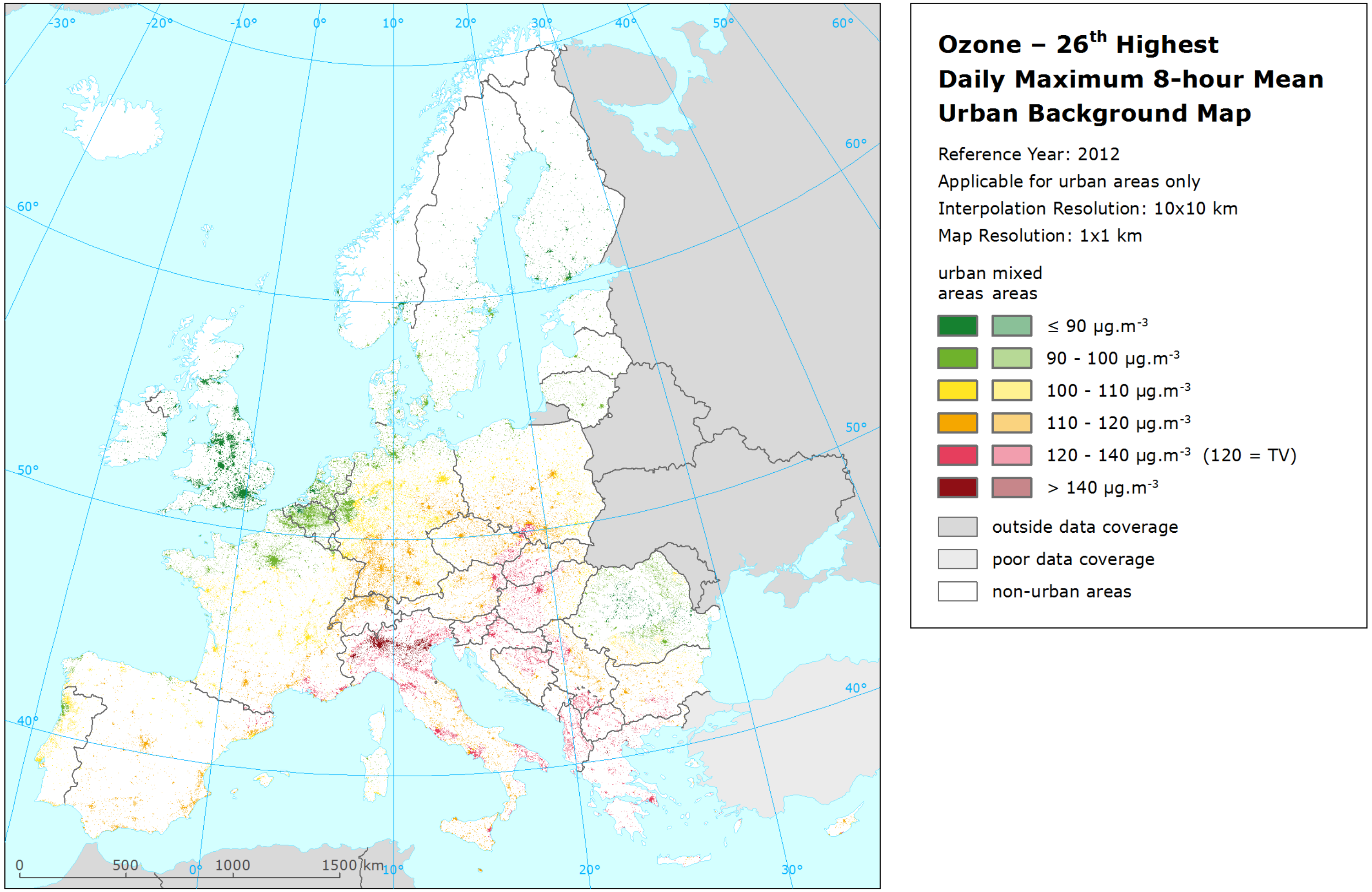

Figure A1.4 Urban background concentration map of ozone health indicator 26th highest daily maximum 8-hour value, year 2012. Spatial interpolated concentration field (10x10 km grid resolution) in urban areas (1x1 km grid resolution). Units: µg.m^{-3}. Applicable for urban areas only.

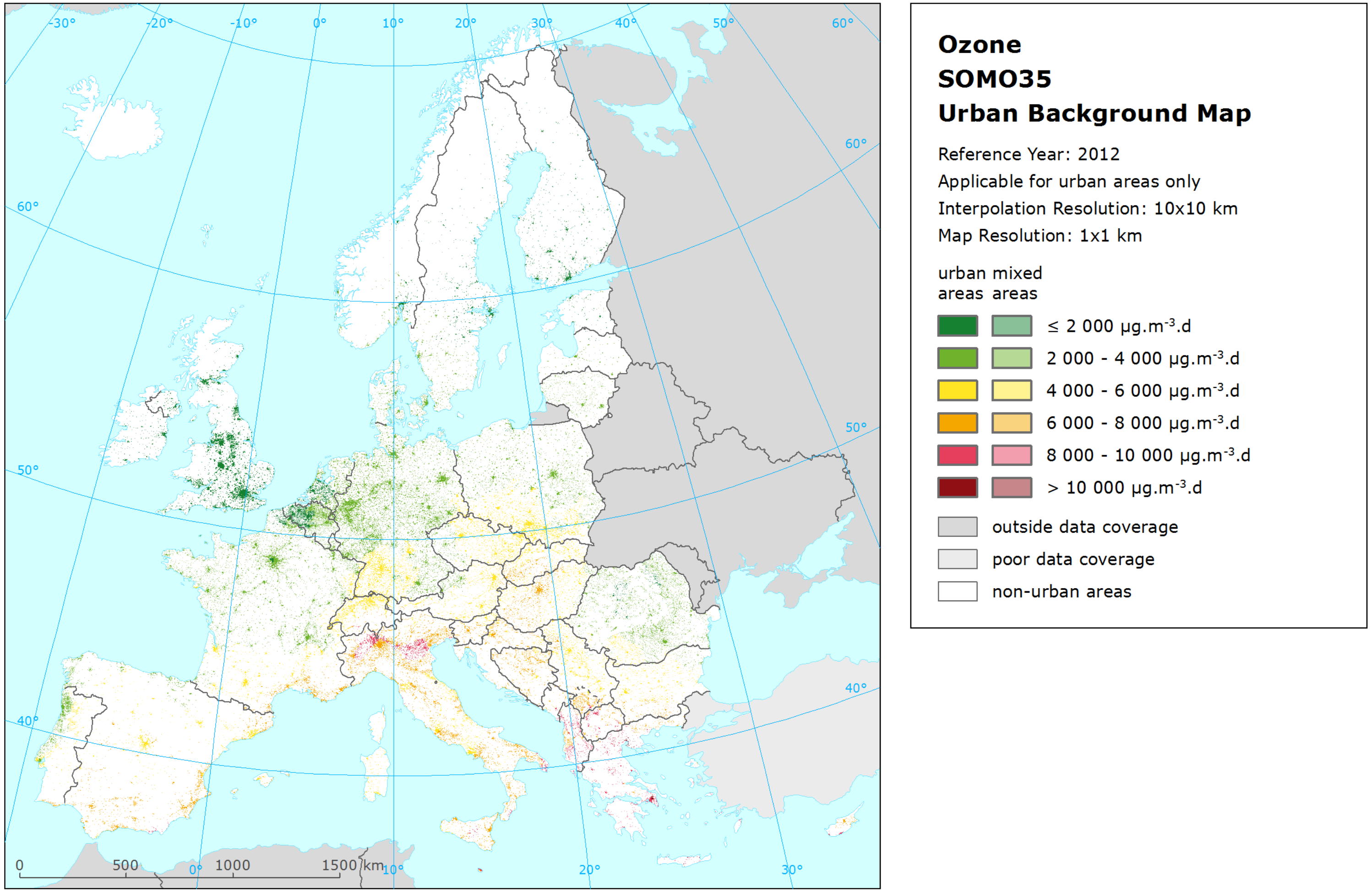

Figure A1.5 Urban background concentration map of ozone health indicator 26th highest daily maximum 8-hour value, year 2012. Spatial interpolated concentration field (10x10 km grid resolution) in urban areas (1x1 km grid resolution). Units: µg.m^{-3}.days. Applicable for urban areas only.

Annex 2 Legend classes and colour adaptations

Throughout the years, the ETC/ACM used in its map presentations its own selection of class intervals and colour schemes. The class intervals were mainly chosen to best visualise (a) the limit value (LV) or target value (TV) of the involved indicator, and (b) the numerical distribution of the interpolated concentrations over the map. The class colours were based on the habit of those used in exceedance mapping products of the EU and UNECE, such as critical deposition and concentrations threshold maps. They appeared to represent the most intuitive interpretation of maps.

As from the start of the prolonged ETC/ACM at January 1st, 2014, we intended to adapt our class intervals reflecting EU and WHO thresholds where possible and relevant, including the use colours from the EEA house style colour where appropriate.

Class intervals

The classification intervals can be used to represent and visualise, next to the LV and TV, other thresholds as well, such as the WHO guideline thresholds (AQG) and interim targets (IT), and the EU lower and upper assessment thresholds (LAT and UAT) and long term objectives (LTO). These we did include only to a limited extend in our maps, depending on the moment in time we created such indicator map for the first time. On top of that, we had the focus on having the concentration gradient best visualised in the map next to just the main threshold represented. Moreover, one should bear in mind that at the time of the initial mapping developments several thresholds were not yet defined or set in guidelines or legislation. Up to last year we stuck to our original set of intervals to avoid 'jumps' in the classification intervals every few years, making the comparison between the indicator years mapped more complex.

From this year onward, we will match the class intervals incorporating as much as possible other thresholds and those that are used by EEA. However, in a few cases we decided to deviate from EEA because of the aim for better visual and intuitive representation of gradients in the distribution of indicator concentrations in the map that prevails over the EEA classes, e.g. think of equidistant class interval symmetry and symmetry of number of classes around thresholds. Another criterion is that we wish to keep up comparability between numbers of the related exposure estimate tables from before and after the changes.

Class colours

The colours of EEA's house style provide to certain extend matching options with the colours we used so far. However, the colour schemes, i.e. the colour combinations prescribed or advised through EEA's house style, deviate quite a bit from the colour combinations we used so far. With the adapted class intervals we extensively tested a series of colour combinations in line with EEA's house style, in line with air quality maps EEA produced so far, and a series of combinations between the two, including suggestions from ourselves, colleague's and audience in general. This 'audience consisted of people used to look at and interpret such type of maps, but also people that are limited or hardly familiar with the look and feel and interpretation of such type of maps.

The main conclusion from the tests and consultation was that the maps following EEA's house style recommendations were the least appreciated and that the colour schemes matching closely with the original colour schemes we used so far, were appreciated best by a large majority.

Based on these outcomes we decided to implement the following class interval and colour scheme changes. The table gives in summary the old ETC/ACM legend and the newly implemented legend per indicator map type. It also contains a listing of legends for indicators we do not deal with in this paper, but for which we had some discussion, testing and conclusion with the goal to have a legend 'stand-by' in case its map needs to be produced.

Up to 2011-maps	*2012-maps onward*	*Motivation/remarks*
	Regular mapping products	
	PM_{10} annual mean	
leaf green ≤ 10 μg.m^{-3} solar yellow 10 - 20 μg.m^{-3} electron gold 20 - 40 μg.m^{-3} mars red 40 - 45 μg.m^{-3} (40 = LV) cattleya orchid > 45 μg.m^{-3}	green4 ≤ 10 μg.m^{-3} green3 10 - 20 μg.m^{-3} orange2 20 - 30 μg.m^{-3} orange3 30 - 40 μg.m^{-3} red3 40 - 50 μg.m^{-3} (40 = LV) red5 > 50 μg.m^{-3}	6 classes better emphasizes extremes; symmetric intervals ≤ 10: to illustrate the real lowest conc. areas 20 = WHO air quality guideline [AQG] 30 = WHO interim target 3 [IT-3]) 40 = EU LVh_{2005} (h= health) 50 = WHO interim target 2 [IT- 2]; to illustrate real highest conc. areas
	PM_{10} 36th highest daily mean	
leaf green ≤ 20 μg.m^{-3} solar yellow 20 - 30 μg.m^{-3} electron gold 30 - 50 μg.m^{-3} mars red 50 - 65 μg.m^{-3} (50 = LV) cattleya orchid > 65 μg.m^{-3}	green4 ≤ 20 μg.m^{-3} green3 20 - 30 μg.m^{-3} orange2 30 - 40 μg.m^{-3} orange3 40 - 50 μg.m^{-3} red3 50 - 75 μg.m^{-3} (50 = LV) red5 > 75 μg.m^{-3}	6 classes better emphasizes extremes; symmetric intervals 20 = EU Lower Assessment Threshold [LAT] 30 = symmetry in classes; (30 ≈ 28 = EU Upper Ass.Thr. [UAT]) 50 = EU LVh_{2005} & WHO-AQG PM10 24h-mean 75 = WHO-Interim target-3 [IT-3] PM10 24h-mean
	$PM_{2.5}$ annual mean	
leaf green ≤ 5 μg.m^{-3} solar yellow 5 - 10 μg.m^{-3} mango 10 - 15 μg.m^{-3} electron gold 15 - 25 μg.m^{-3} mars red 25 - 30 μg.m^{-3} (25 = TV) cattleya orchid > 30 μg.m^{-3}	green4 ≤ 5 μg.m^{-3} green3 5 - 10 μg.m^{-3} orange2 10 - 15 μg.m^{-3} orange3 15 - 20 μg.m^{-3} red3 20 - 25 μg.m^{-3} (20 = LV_{2020}) red5 > 25 μg.m^{-3} (25 = TV, LV_{2015})	Stick to 6 classes: better emphasizes extremes; symmetric intervals 10 = WHO-AQG 15 = WHO Interim target 3 [IT-3]) (12 = EU LAT; 17 = EU UAT) 20 = EU LVh_{2020} & EU exposure criterion obligation 2015; 25 = EU TVh_{2010} & EU LV_{2015}; WHO Interim target 2 [IT-2])
	Ozone 26th highest max. 8h running mean	
leaf green ≤ 100 μg.m^{-3} solar yellow 100 - 110 μg.m^{-3} electron gold 110 - 120 μg.m^{-3} mars red 120 - 140 μg.m^{-3} (120 = TV) cattleya orchid > 140 μg.m^{-3}	green4 ≤ 90 μg.m^{-3} green3 90 - 100 μg.m^{-3} orange2 100 - 110 μg.m^{-3} orange3 110 - 120 μg.m^{-3} red3 120 - 140 μg.m^{-3} (120 = TV) red5 > 140 μg.m^{-3}	6 classes better emphasizes extremes 100 ≈ WHO-AQG for 8h daily mean) 120 = EU TVh_{2010} (if available: 3-yr mean)
	Ozone SOMO35	
leaf green ≤ 3 000 μg.m^{-3}.d solar yellow 3 000 - 6 000 μg.m^{-3}.d electron gold 6 000 - 10 000 μg.m^{-3}.d mars red 10 000 - 15 000 μg.m^{-3}.d cattleya orchid > 15 000 μg.m^{-3}.d	green4 ≤ 2 000 μg.m^{-3}.d green3 2 000 - 4 000 μg.m^{-3}.d orange2 4 000 - 6 000 μg.m^{-3}.d orange3 6 000 - 8 000 μg.m^{-3}.d red3 8 000 - 10 000 μg.m^{-3}.d red5 > 10 000 μg.m^{-3}.d	6 classes better emphasizes extremes; symmetric intervals (No guidline or legal thresholds defined for SOMO35). 4 000: demo case: in NL corresponded earlier with O3 26th hdm 8h-mean TV (120 μg·m^{-3}·d adressed at: ETC/ACM TP 2013/13, p.53); 6 000: used throughout the years for discussion of results; > 10 000: only very occasionally values above the 15 000.

(table continues on next page)

Ozone AOT40 for crops			
< 6 000 µg.m^{-3}.h 6 000 - 12 000 µg.m^{-3}.h 12 000 - 18 000 µg.m^{-3}.h 18 000 - 27 000 µg.m^{-3}.h > TV > 27 000 µg.m^{-3}.h	≤ 6 000 µg.m^{-3}.h 6 000 - 12 000 µg.m^{-3}.h (6 000 = LTO) 12 000 - 18 000 µg.m^{-3}.h 18 000 - 27 000 µg.m^{-3}.h (18 000 = TV) > 27 000 µg.m^{-3}.h	green4 orange2 orange3 red3 red5	Threshold annotation and colour details changed slightly; 6 000 = EU LTO; EU Reporting Value (RV) 3rd DD annex III; 18 000 = EU TV_{2010} (if available: 5 years mean).
Ozone AOT40 for forests			
< 10 000 µg.m^{-3}.h 10 000 - 20 000 µg.m^{-3}.h 20 000 - 30 000 µg.m^{-3}.h 30 000 - 50 000 µg.m^{-3}.h > 50 000 µg.m^{-3}.h	≤ 10 000 µg.m^{-3}.h 10 000 - 20 000 µg.m^{-3}.h (10 000 = CL) 20 000 - 30 000 µg.m^{-3}.h (20 000 = RV) 30 000 - 50 000 µg.m^{-3}.h > 50 000 µg.m^{-3}.h	green4 orange2 orange3 red3 red5	Threshold annotation and colour details changed slightly; 10 000 = UNECE Critical Level (CL) [Mapping Manual]; 20 000 = EU RV 3rd DD annex III;

Additional maps on specific request		
NO_2 annual mean		
leaf green ≤ 10 µg.m^{-3} peridot green 10 - 20 µg.m^{-3} solar yellow 20 - 30 µg.m^{-3} electron gold 30 - 40 µg.m^{-3} mars red 40 - 46 µg.m^{-3} (40 = LV) cattleya orchid > 46 µg.m^{-3}	green4 ≤ 10 µg.m^{-3} green3 10 - 20 µg.m^{-3} orange2 20 - 30 µg.m^{-3} orange3 30 - 40 µg.m^{-3} red3 40 - 45 µg.m^{-3} (40 = LV) red5 > 45 µg.m^{-3}	6 classes better emphasizes extremes; symmetric intervals (26 = EU LAT; 32 = EU UAT) 40 = EU LVh_{2010} & WHO-AQG (46: was LV + margin of tolerance (MOT); we do not include MOT in class interval definitions.
NO_x annual mean		
leaf green ≤ 10 µg.m^{-3} solar yellow 10 - 20 µg.m^{-3} electron gold 20 - 30 µg.m^{-3} mars red 30 - 40 µg.m^{-3} (30 = CL) cattleya orchid > 40 µg.m^{-3}	green4 ≤ 10 µg.m^{-3} orange2 10 - 20 µg.m^{-3} orange3 20 - 30 µg.m^{-3} red3 30 - 40 µg.m^{-3} (30 = CL) red5 > 40 µg.m^{-3} ≤	Stick to 5 classes: all vegetation indicators have 5 classes; avoids 3 classes above CL; only very occasionally values above 50; symmetric intervals; (19.5 = EU LAT; 24 = EU UAT); 30 = EU CLv_{2010} (v= vegetation);
SO_2 annual mean/ SO_2 winter mean		
leaf green ≤ 5 µg.m^{-3} solar yellow 5 - 10 µg.m^{-3} electron gold 10 - 20 µg.m^{-3} mars red 20 - 30 µg.m^{-3} (20 = CL) cattleya orchid > 30 µg.m^{-3}	green4 ≤ 5 µg.m^{-3} green3 5 - 10 µg.m^{-3} orange2 10 - 15 µg.m^{-3} orange3 15 - 20 µg.m^{-3} red3 20 - 25 µg.m^{-3} (20 = CL) red5 > 25 µg.m^{-3}	6 classes better emphasizes extremes; symmetric intervals 20 = EU LVh/v_{2005}

(table continues on next page)

Other pollutant indicators

		CO annual mean of max 8h running mean	
<0.5 mg/m3		≤ 0.5 mg/m3	5 classes better emphasizes extremes; (Proper colour scheme yet to be determined
0.5 - 1 mg/m3		0.5 - 1.0	accounting for dealing with LV non-exceedance criterion at most classes or reconsider
1 - 2 mg/m3		1.0 - 2.0	whole class interval scheme)
> 2 mg/m3		2.0 - 2.5	
		> 2.5	10 = EU LVh_{2005}
		As annual mean	
≤ 1 ng/m^3	green4	≤ 1.0 ng/m3	6 classes better emphasizes extremes; legend symmetry among HM indicators;
1 - 3	green3	1.0 - 2.4	(Small changes to include thresholds in intervals)
3 - 6	orange2	2.4 - 3.6	2.4 = EU LAT
6 - 9	orange3	3.6 – 6.0	3.6 = EU UAT
> 9	red3	6.0 - 9.0 (6 = TV)	6.0 = EU TVh (6.6 = WHO-AQG-RV (Reference Value))
(EEA classes)	red5	> 9.0	
		Cd annual mean	
≤ 1 ng/m^3	green4	≤ 1.0 ng/m^3	6 classes better emphasizes extremes; legend symmetry among HM indicators;
1 - 2	green3	1.0 - 2.0	(Small changes to include thresholds in intervals)
2 - 5	orange2	2.0 - 3.0	2.0 = EU LAT
5 - 8	orange3	3.0 - 5.0	3.0 = EU UAT
> 8	red3	5.0 - 8.0 (5 = TV)	5.0 = EU TVh & WHO-AQG-RV
(EEA classes)	red5	> 8.0	
		Ni annual mean	
≤ 5 ng/m^3	green4	≤ 5 ng/m^3	6 classes better emphasizes extremes; legend symmetry among HM indicators;
5 - 10	green3	5 - 10	(Small changes to include thresholds in intervals)
10 - 20	orange2	10 - 14	10 = EU LAT
20 - 30	orange3	14 - 20	14 = EU UAT
> 30	red3	20 – 25 (20 = TV)	20 = EU TVh_{2005}
(EEA classes)	red5	> 25	25 = WHO-AQG--RV
		Pb annual mean	
0 - 0.1 ug/m3	green4	≤ 0.10 µg/m^3	6 classes better emphasizes extremes; legend symmetry among HM indicators;
0.1 - 0.25 ug/m3	green3	0.10 – 0.25	(Small changes to include thresholds in intervals)
0.25 - 0.5 ug/m3	orange2	0.25 – 0.35	0.25 = EU LAT
> 0.5 ug/m3	orange3	0.35 – 0.50	0.35 = EU UAT
	red3	0.50 – 1.00 (0.50 = TV)	0.50 = EU TVh_{2005} & WHO-AQG-RV
	red5	> 1.00	

(table continues on next page)

Benzene annual mean			
≤ 1.7 µg/m^3	green4	≤ 1.7 µg/m^3	6 classes for best legend symmetry with threshold and symmetric intervals; to better
1.7 – 2.0	green3	1.7 – 2.0	emphasize real highest conc. that do occur;
2.0 – 3.5	orange2	2.0 – 3.5	1.7 = WHO AQG-Reference Value (RV)
3.5 – 5.0	orange3	3.5 – 5.0	2.0 = EU LAT; 3.5 = EU UAT
> 5.0	red3	5.0 – 6.5 (5.0 = TV)	5.0 = EU TVh_{2010}
(both ETC/ACM and EEA)	red5	> 6.5	
BaP annual mean			
≤ 0.12 ng/m^3	green4	≤ 0.12 nµg/m^3	6 classes for best legend symmetry with threshold and the other indicators; to better
0.12 – 0.4	green3	0.12 – 0.4	emphasize real highest conc. that do occur;
0.4 – 0.6	orange2	0.4 – 0.6	0.12 = WHO AQG-Reference Value (RV)
0.6 – 1.0	orange3	6.0 – 1.0	0.4 = EU LAT; 0.6 = EU UAT
> 1.0	red3	1.0 – 1.5 (1.0 = TV)	1.0 = EU TVh_{2013}
(both ETC/ACM and EEA)	red5	> 1.5	

Throughout the report, the upgraded legend class intervals and colour schemes – as described in the table above – have been implemented in the concentration maps of this paper already. For better comparability with the maps presented in previous reports, being Horálek et al. (2008, 2013, 2014a) and De Smet et al. (2009, 2010, 2011, 2012), we prepared the 2012 concentration maps also with the former class intervals and colour schemes. For illustration, we include here the maps for both PM_{10} indicators, the $PM_{2.5}$ indicator and the ozone indicator SOMO35 with their former class intervals and colour schemes and their upgraded intervals and schemes. They are presented in Figures A2.1 and A2.2 and are the indicators with the main changes in visualisation. Whereas at the other ozone indicators the changes are minor only and therefore not included in this annex.

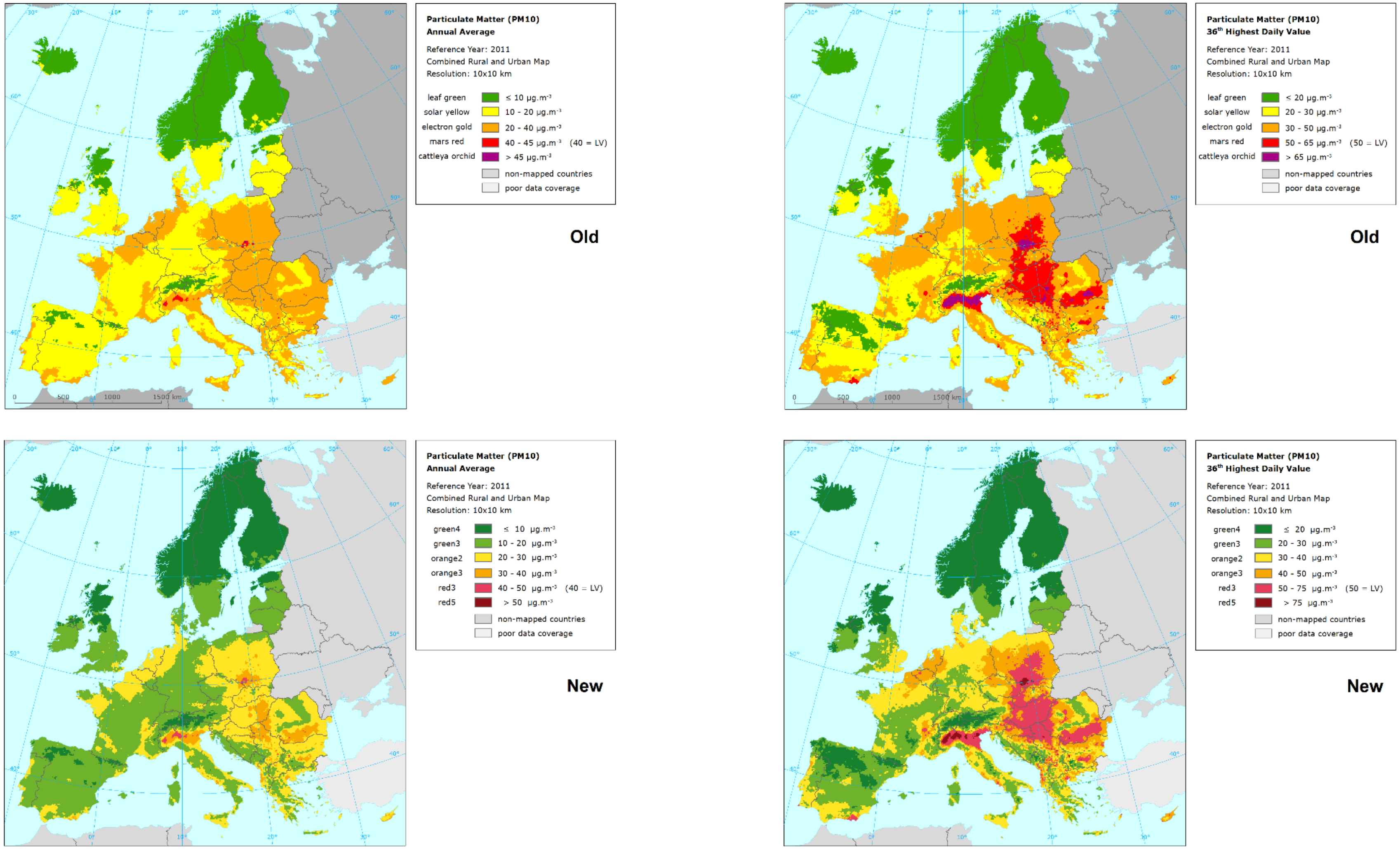

Figure A2.1 Combined rural and urban concentration maps of PM_{10} indicators annual average (left) and 36^{th} highest daily mean (right) for the year 2012. Units: $\mu g.m^{-3}$. Spatial interpolated concentration field (10x10 km grid resolution), using old (above) and new (below) legend class intervals and colour schemes.

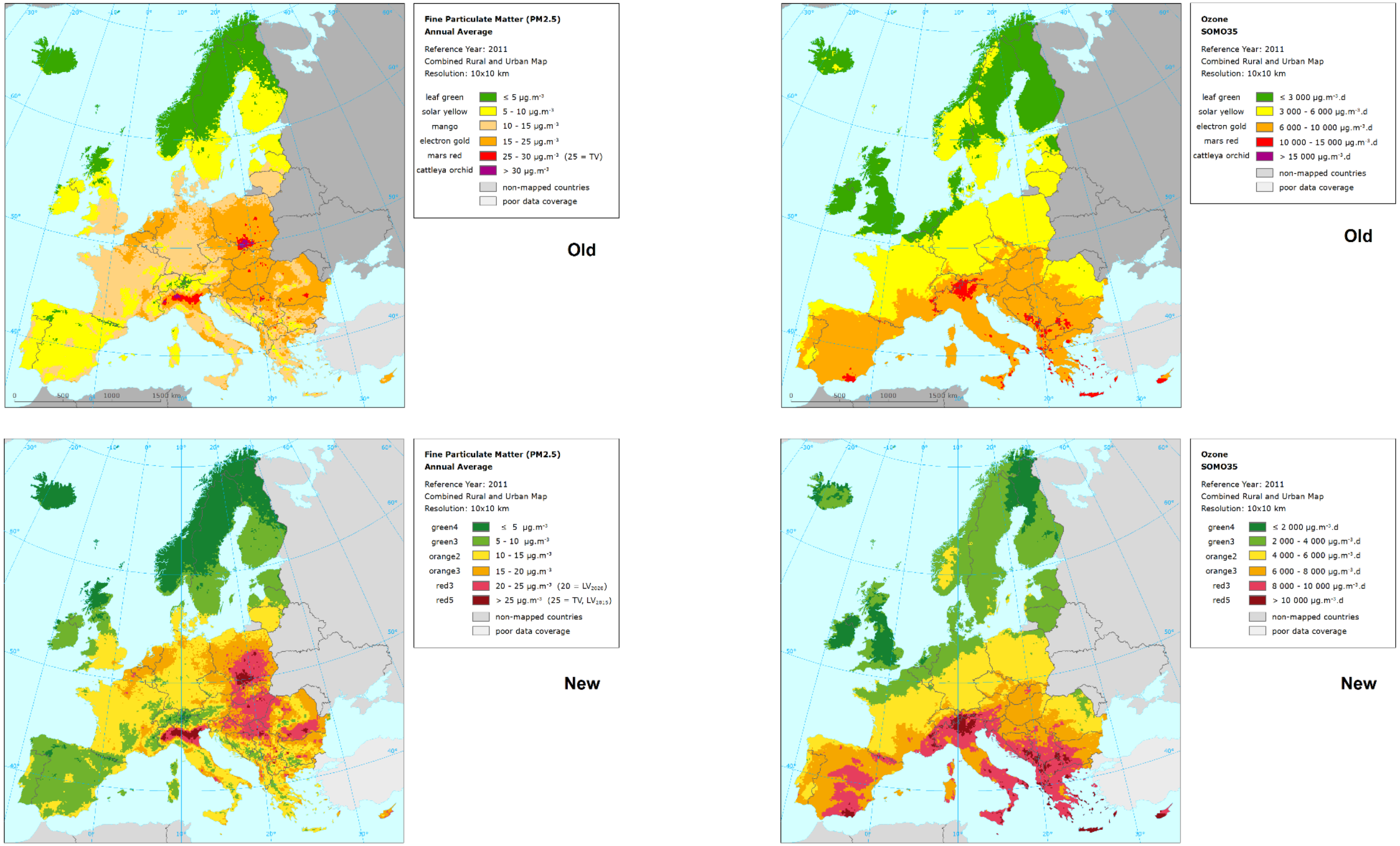

Figure A2.2 Combined rural and urban concentration maps of $PM_{2.5}$ annual average (left) and ozone indicator SOMO35 (right) for the year 2012. Units: $\mu g.m^{-3}$ (left) and $\mu g.m^{-3}$.days (right). Spatial interpolated concentration field (10x10 km grid resolution), using old (above) and new (below) legend class intervals and colour schemes.